DISSERTATION

SOIL CARBON SATURATION:
A NEW MODEL OF SOIL ORGANIC MATTER
STABILIZATION AND TURNOVER

Submitted by

Catherine E. Stewart

Graduate Degree Program in Ecology

In partial fulfillment of the requirements
for the Degree of Doctor of Philosophy
Colorado State University
Fort Collins, Colorado
Spring 2006

COLORADO STATE UNIVERSITY

March 27, 2006

WE HEREBY RECOMMEND THAT THE DISSERTATION PREPARED UNDER OUR SUPERVISION BY CATHERINE E. STEWART ENTITLED SOIL CARBON SATURATION: A NEW MODEL OF SOIL ORGANIC MATTER STABILIZATION AND TURNOVER BE ACCEPTED AS FULFILLING IN PART REQUIREMENTS FOR THE DEGREE OF DOCTOR OF PHILOSOPHY.

Committee on Graduate Work

_____
Johan Six

_____
Richard T.Conant

_____
Sally Sutton

Adviser _____
Keith Paustian

Director _____
Dan Binkley

ii

ABSTRACT OF DISSERTATION

SOIL CARBON SATURATION: A NEW MODEL OF SOIL ORGANIC MATTER STABILIZATION AND TURNOVER

The soil C saturation concept suggests an ultimate capacity of the soil to store C, dictating the rate and duration that soil may be effective in mitigating increasing atmospheric CO_2. This places a physicochemical limit on soil that is associated with textural, mineralogical and structural soil properties. This concept has been articulated in terms of four theoretical pools capable of C saturation: non-protected, physically- (microaggregate), chemically- (silt + clay), and biochemically-protected pools. My dissertation represents a multifaceted approach to examine C saturation in both whole soil and measurable soil fractions representing the four conceptual C pools. I evaluate the soil C saturation concept theoretically by modeling these relationships using published whole soil data, primary field data and through laboratory experiments.

Analyses using published long-term soil C data from agroecosystem experiments suggested that within a given site, there was little support for models including C saturation, but when all sites were combined; there was strong support for the C saturation model. In general, published data were too sparse to adequately test individual sites.

To evaluate the concept of C saturation for the four C pools, I used a three-part density, chemical, and physical fractionation scheme combined with modeling, using new data collected from eight agroecosystems in the US and Canada. I found that the chemically- and biochemically-protected pools showed strong evidence for C saturation, while the non-protected and physically-protected pools were non-saturating.

In a 2.5 year laboratory experiment, I tested C stabilization rates and limits at two C addition rate to soils differing in soil C content and physicochemical characteristics. I found C saturation dynamics were most evident in the chemically-, biochemically- and some microaggregate protected C pools. I found greater C accumulation in the non-protected pool of the high C soil, suggesting C saturation of other pools.

I conclude that SOC sequestration in many soils may be influenced by C saturation dynamics, impacting both decomposition kinetics and C stabilization. Soil C sequestration may be overestimated in models that do not account for C saturation dynamics.

Catherine E. Stewart
Graduate Degree Program in Ecology
Colorado State University
Fort Collins, Colorado 80523
Spring 2006

ACKNOWLEDGEMENTS

TABLE OF CONTENTS

CHAPTER 1

INTRODUCTION

Background

Soil organic C (SOC) constitutes roughly 1500 Gt (1m depth) or two-thirds of C in the terrestrial C pool (Post et al. 1982; Schlesinger 1997). Carbon stabilized in this pool is in a dynamic balance between C input to the soil from primary productivity and losses via heterotrophic respiration and leaching (Jenny 1941; Schlesinger 1977). Agroecosystems contain less than 1% of the vegetative C (Smil 2002), but 10% of soil C and thus contribute significantly to the global C cycle.

Broad patterns of SOC have been linked to climate factors and dominant vegetation, as well as to inherent soil properties such as texture and mineralogy (e.g. Jenny 1980). Climates with greater primary productivity and thus greater C inputs might be expected to have greater SOC accumulation, but due to increased decomposition, rarely do. The relationship between plant production, SOC and soil fertility has been recognized and used for agricultural purposes for hundreds of years (Tiessen et al. 1994; Paustian et al. 1997b).

Soil organic carbon contributes many beneficial attributes to soil quality and as a component of soil structure as well as a reservoir of essential plant nutrients. It has been correlated to aggregate structure, which contributes to overall soil structure. Soil structure is crucial, as it decreases erosion by binding mineral particles together as well as producing macropores which assist in water infiltration. As SOM decomposes, carbon bound nutrients are released and made available to plants throughout the growing season.

After cultivation of native soils, 40 - 60% of the original soil C stocks are typically lost within a few years to decades of use (Mann 1986) due to tillage exposing more soil carbon to microbial decomposition, warmer and moister soil conditions due to the absence of plants and the export of plant carbon by harvest (Janzen 2005). This resulting loss of soil structure, increased soil erosion, decreased plant productivity due to lower concentrations of soil nutrients, and decreased water infiltration all caused farmers as well as agricultural scientists to be concerned with maintaining or building soil organic carbon.

Recently, due to concerns about global climate change from the release of greenhouse gases, new interest has been spurred in soil C. As the initial conversion of agricultural land released much of the previously stored carbon through microbial respiration, it potentially contributed as much as 50 - 100 Pg of C to the atmosphere (Lal et al. 1999). The soil carbon content of agricultural land may be modified by practices that increase C inputs or decrease decomposition and it has been suggested that US agricultural lands could potentially sequester 75 - 208 Tg C yr^{-1} (Lal et al. 1999). Although not a massive amount, it could have the capability to offset rising atmospheric

CO_2 with little cost in infrastructure and could be implemented immediately, which has advantages over other proposed solutions.

Soil carbon has become more than a beneficial soil quality attribute, but a potential CO_2 mitigation strategy and has prompted intense research on questions such as: How SOC is stored? What is its composition? Can it be replaced when lost?

The C saturation concept

Over a century of work on soil carbon has revealed that soil organic matter (SOM) represents a continuum of organic molecules in varying stages of decomposition from soluble C to recalcitrant humic substances (Waksman & Cordon 1938; Baldock & Skjemstad 2000). Some organic matter decomposes rapidly, while other C is protected in aggregate structures or stabilized by association with clay structures (Christensen 2001; Six et al. 2002). Generally, it is accepted that carbon is protected from decomposition by 1) intimate association with silt and clay particles, 2) physical protection in aggregate structures, and 3) biochemical recalcitrance due to the chemical structure of the C compounds (see Baldock & Skjemstad 2000; Six et al. 2002; Krull et al. 2003 for reviews).

In the process of chemical stabilization, negatively charged organic compounds may bind tightly to negatively charged clay surfaces and iron oxides with the bridging effect of positively charged cations such as Ca^{2+} (Oades 1988; Baldock & Skjemstad 2000). Carbon bound by adsorption is generally quite stable with low turnover times, due to general unavailability to the soil microorganisms.

10

In the process of physical protection, labile SOM is encapsulated by silt and clay particles (Oades 1984; Golchin 1994). This protection produces a physical barrier between soil microorganisms and organic matter (OM) preventing decomposition. Decomposition is further slowed by anaerobic conditions within aggregate structures, limiting microbial growth. Aggregates come in many sizes, the largest contain large pieces of OM that break down on the order of weeks to months, while smaller aggregates are more stable and turn over more slowly (Elliott 1986; Jastrow 1996; Six et al. 2000).

Clay-organic matter interactions form building blocks from which other, secondary structures are formed (Tisdall & Oades 1982). Small groups of organominerals may, in turn, bind together to form silt-sized aggregates that are between 2-20 μm. These silt-sized aggregates are relatively high in SOM content due to the organomineral complexes (Christensen 2001), protecting more C that the small surface area of silt alone.

Biochemical stabilization is the result of the inherent nature of chemical compounds as they are decomposed. Certain plant structural compounds such as aromatics, humified components, and wax-derived long-chain aliphatics, inherently resist decomposition due to their chemical composition and structure (Paul et al. 2001). Due to the recalcitrant nature of this carbon, it is generally 1300-1800 years older than the total soil (Paul et al. 1997; Paul et al. 2001).

Unprotected SOM is in the form of slightly decomposed residue from plants and fungi (Christensen 2001). Due to the lack of protection, this SOM is subject to rapid decomposition and is greatly influenced by management (Cambardella & Elliott 1992).

Total soil carbon is a composite of these pools and protection mechanisms. Stability of SOC is dependent on moisture, temperature, pH, and aeration of the soil as well as the chemical structure of the soil and its accessibility to microbes. Ultimately, SOC is a balance between decomposition and the C returned to the soil.

In agroecosystems, the SOC balance is influenced by management practices such as organic matter additions, tillage intensity, fertilization, irrigation, and crop rotation. Soil organic C storage may be increased directly by increasing C returns to the soil as crop residue, manure, or other organic amendments. Carbon inputs to the system also may be increased indirectly by fertilization or irrigation treatments that increase crop productivity, biomass and root production (Paustian et al. 1997b; West & Post 2002; Ogle et al. 2005).

Crop residue and manure management ultimately control the amount of C entering an agroecosystem and subsequently affects soil organic carbon (SOC) stabilization, soil fertility and structure. Conservation management practices that increase C inputs to the soil or decrease SOM oxidation (e.g., reduced tillage) have increased soil C stocks in agroecosystems (Paustian et al. 1997c; Paustian et al. 2000). Many long-term agroecosystem studies have shown that SOC content increases proportionally to increasing C inputs (Paustian et al. 1997c; Kong et al. 2005) implying that SOC accumulation is directly related to C input.

Data from many long-term agroecosystem experiments appear to support this linear relationship between C inputs and total SOC content (Rasmussen & Collins 1991; Paustian et al. 1997b; Huggins et al. 1998a; Kong et al. 2005). However, other experiments show little or no response of SOC to differences in C addition rate, typically

12

at sites with high SOC content and low decomposition rates. For example, Soon (1998) found no effect of fertilization and straw management on a Dark Grey Solod near Beaverton, Alberta after ten years. After 30 years of continuous corn at Morris, MN, neither varying rates of fertilization nor removal of crop stover had a significant effect on SOC content of the upper 20 cm of soil (Reicosky et al. 2002). At Lamberton, MN, greater residue additions in continuous corn versus corn-soybean crop rotations over ten years (Huggins et al. 1998b) and differences in N-fertilizer rates and residue inputs over 19 years (Huggins & Fuchs 1997; Huggins et al. 1998a) did not significantly affect SOC levels. A 6-year study conducted in New Zealand on a relatively high C soil found no detectable effect of straw management treatments on SOC levels (Curtin & Fraser 2003). These studies suggest that increasing C returns to high C content soils does not necessarily increase SOC content. This apparent lack of response in SOC stabilization to the driving variable of C inputs leads to the question: Is there an upper limit to the amount of C a whole soil is capable of storing? Are there diminishing returns to SOC stabilization as the amount of C added increases?

Other researchers have found limits to C stabilization in soil fractions. Limits to C stabilization by clay surfaces have been well documented in isolated pure clays, which has been attributed to adsorption and desorption mechanisms (Harter & Stotzky 1971; Marshman & Marshall 1981). Saturation behavior with respect to C has also been observed in clay fractions of whole soils under differing management systems (Diekow et al. 2005) and through soil profiles (Roscoe et al. 2001). Hassink (1997) found that silt + clay associated C compared between cultivation treatments did not differ and suggested that those soils had reached a maximum protective capacity.

Baldock and Skjemstad (2000) proposed that each mineral matrix had a unique capacity to stabilize organic C depending not only on the presence of mineral surfaces capable of adsorbing organic materials (or a protective capacity), but also the chemical nature of the soil mineral fraction, the presence of cations, and the architecture of the soil matrix. Carter (2002) also proposed a conceptual model that included a variable capacity related to C input, aggregate stability and macro-OM in addition to the silt and clay protective capacity. He related the storage capacity of the soil to specific soil fractions including the association of SOM with silt + clay particles (< 20 μm), microaggregates (20-250 μm), macroaggregates (>250 μm), and sand-sized macro-OM. As SOC concentration increased, C associated with clay and silt would reach the protective capacity of the soil, and further C accumulation would occur in aggregate structures and macro-OM as a function of soil type and C inputs (i.e. management).

The soil C saturation concept proposed by Six et al. (2002) suggests an upper limit, or C saturation level, to soil C sequestration. In contrast to SOC accumulation models that directly relate SOC accumulation to the rate of C addition, under the soil C saturation concept, SOC accumulation is asymptotic and a function of the capacity of a soil to protect C. The difference between a soil's theoretical saturation level and the current C content of the soil is defined as saturation deficit. As a soil approaches saturation, the saturation deficit decreases and stabilization of new SOC is reduced. The asymptotic relationship between C inputs and SOC content at steady-state is a key attribute to the C saturation concept. Direct corollaries of this asymptotic relationship are that 1) the further a soil is from saturation, the greater its capacity to sequester added C, and 2) as a soil approaches saturation, the rate and amount of SOC accumulation decrease

due to a smaller saturation deficit. Soil properties such as texture and mineralogy will determine the final soil C saturation level, as well as how quickly that capacity may be attained, i.e., the slope and the asymptote of the C saturation curve (Stewart et al. 2006a).

The whole soil C saturation concept proposed by Six et al. (2002) is a function of four C pools; the physically- or microaggregate-protected C pool, the chemical or silt- and clay-protected C pool, the biochemically-protected C pool and an unprotected C pool. Each pool had a unique C saturation level and C accumulation within each pool would be dependent on its saturation deficit (i.e. how far that pool was from its theoretical saturation level). In their conceptual model, SOM is stabilized by chemical association through silt and clay particles, by physical protection due to microaggregation, and biochemical recalcitrance. The chemical stabilization of SOM by silt and clay particles is limited by the amount of silt and clay particles in a soil as well as by the cation exchange capacity and specific surface area influenced by mineralogy. Physical occlusion of labile particulate organic matter by microaggregates physically protects OM as well as reduces oxygen availability, inhibiting microbial decomposition. This microaggregate-protected pool is limited physically by texture, as silt and clay content dominates aggregate dynamics. Biochemical SOM protection occurs through the biochemical recalcitrance of its structure with low biological availability. In addition, Six et al. (2002) hypothesized a fourth, non-protected C pool, limited by the steady-state balance of C inputs and decomposition dictated by climate. These conceptual pools could be isolated by a simple three-step fractionation procedure using physical, chemical, and density fraction methods. Theoretically, whole-soil C saturation comprises the cumulative behavior of these four soils C pools.

Theoretical and experimental studies of soil C saturation

The four chapters comprising my dissertation represent a multifaceted approach to evaluating the soil C saturation concept including modeling previously published data on total soil C, theoretical development and exploration of the C saturation of different SOC fractions using primary data, and an experimental approach that directly manipulates C inputs and C saturation deficit. The second chapter asks the question: is there an upper limit to SOC sequestration? I developed three alternate models of whole soil C accumulation 1) no saturation limit (i.e., linear), 2) whole-soil C saturation limit (i.e., C saturation model), and 3) soil C saturation of a stabilized C pool, but not the whole soil (i.e., mixed model). These models are then tested against published data from long-term agroecosystem experiments (Ogle et al. 2003) using information theory and small sample Akaike information criterion (AIC_c) to quantify the relative explanatory power of these three competing models of C accumulation.

In the third chapter, I explored C saturation of soil fractions by mathematically deriving the relationship between total SOC and C inputs and soil fraction C. I then used the two scenarios of SOC accumulation in soil fractions: 1) no saturation limit (i.e., linear model), 2) whole-soil C saturation limit (i.e., C saturation model) to evaluate the behavior of measurable fractions; free POM, microaggregate-associated, silt and clay associated and non-hydrolyzable C pools that correspond to the non-protected, and physically-, chemically- and biochemically-protected C pools, respectively. In this study, I used primary data collected by employing a three-part density, chemical, and physical fractionation scheme to soil sampled from eight long-term field experiments in the US

and Canada. These eight sites represent a broad range of soils, textures, and saturation deficits.

The fourth and fifth chapters pose the questions: does saturation deficit and C addition rate influence SOC stabilization of the whole soil and of the four hypothesized C pools? The fourth chapter develops a laboratory experiment to test the soil C saturation concept and outlines soil units necessary to evaluate the incubation results. I used respiration and whole soil C data from 1.5 years of incubation to lead the reader through the concept, implementation, and evaluation of the experimental setup specifically designed to test the soil C saturation concept.

The fifth chapter reports the final 2.5 year incubation results for the whole soil as well as the fractions representing the four C pools for the six sites. After 2.5 years, stabilization of residue-derived C in the whole soil was greater in the C-horizon compared to the A-horizon in the majority of our whole soils, supporting the concept of saturation deficit driven C stabilization. Greater C stabilization in the C-horizon of the whole soil generally occurred in the chemical, physical, and biochemical C pools. The non-protected pool showed little evidence for C saturation, cut greater C accumulation in the high C soil, may indicate C saturation of other fractions. Overall, this study corroborates the whole soil C saturation concept and the soil fraction C saturation. Soils far from their saturation limit (C-horizon) do accumulate C in the chemically-, and biochemically-protected pools faster than soils closer to their C saturation limit (A-horizon).

The second chapter asks the question what is the relative C storage efficiency (i.e., C stock increase per unit C added) for different soils and is there an upper limit to

the capacity for soils to store organic C? The three alternate models of whole soil C accumulation a 1) no saturation limit (i.e., linear), 2) whole-soil C saturation limit (i.e., C saturation model), and 3) soil C saturation of a stabilized C pool, but not the whole soil (i.e., mixed model) were evaluated using published data from long-term agroecosystem experiments (Ogle et al. 2003). I hypothesized that if C accumulation proceeded in accordance to C saturation concept, SOC stabilization would decrease as the soil approached its saturation limit. Although I found only one individual site that had a C-saturation best-fit model, with the combined site data from the 17 long-term agroecosystems I found a 99% probability based on Akaike weights that the two models incorporating C saturation were the best approximation of SOC and C input data. I attributed the better C saturation model fit to the influence of C saturation deficit (i.e., the difference between the actual soil C level and the C saturation level defined for that soil) on SOC accumulation.

In modeling the data at the Sanborn, MO, I found the conventional and no-tillage treatments fit two distinct curves, although according to the C saturation concept, only a single, unique C saturation level dictated by textural and mineralogical properties should have been observed. How can the same site with the same texture and mineralogy appear to be approaching two distinct C saturation levels?

A more detailed examination of the C-saturation model revealed that both C inputs (I) and the decomposition factor (k) dictate steady-state SOC content (C_t). When combined site data were expressed as SOC content over increasing C inputs, variations in k caused by disturbance (i.e. tillage) are apparent as greater SOC content over similar ranges of C inputs for NT compared to the CT at Sanborn. The management-induced soil

18

disturbance decreased the steady-state SOC content in comparison to the soil C saturation level. I proposed the concept of *effective stabilization capacity* for the asymptotic relationship between SOC content and C inputs at levels smaller than the soil C saturation level due to conditions other than the physicochemical limitations of the soil.

The theoretical distinction between effective stabilization capacity and C saturation level explains why, over similar ranges of C additions, the SOC contents of the two treatments at Sanborn can be approaching two asymptotes even though they have the same texture and mineralogy defining a single C saturation level. In contrast to effective stabilization capacity, soil C saturation level is achieved only when C input is maximized under management conditions that minimize soil disturbance, for example under C additions to native soil. If disturbance dominates SOC content such as in tilled agroecosystems, a soil cannot achieve saturation level, but could reach an effective stabilization capacity commensurate with the input rate.

I hypothesized that if saturation deficit influenced SOC accumulation, the ratio of SOC stabilization in NT versus CT treatments (i.e., NT/CT SOC stabilization ratio) should decrease as soil C content increased across sites. I found that as CT SOC content increased, the NT/CT SOC stabilization ratio decreased, supporting the concept of C saturation deficit influencing the amount of C stabilized by NT. This effect appeared to be related to mineralogy, as the tropical sites had a steeper decrease in NT/CT SOC stabilization compared to the temperate sites, suggesting a strong influence of mineralogy on C saturation deficit and SOC stabilization in these soils.

Having found some evidence for soil C saturation based on total SOC, I was interested in examining: What is the relationship between C inputs total SOC and fraction

C stabilization? Do soil C pools representing distinct C stabilization mechanisms saturate? In the third chapter, I contrasted two scenarios of SOC accumulation in soil fractions: 1) no saturation limit (i.e., linear model), 2) whole-soil C saturation limit (i.e., C saturation model). The objectives were to theoretically explore C saturation of soil fractions and to isolate free POM, microaggregate-associated, silt and clay associated and non-hydrolyzable C pools that correspond to the non-protected, and physically-, chemically- and biochemically-protected C pools, respectively. In this study, I used primary data collected by employing a three-part density, chemical, and physical fractionation scheme to soil sampled from eight long-term field experiments in the US and Canada. These eight sites represent a broad range of soils, textures, and saturation deficits.

Differing from the analysis of the first chapter, I used total SOC content, rather than C inputs as the independent variable in my analysis because it is impossible to know C inputs for individual soil fractions. Due to the differing rates of decomposition and subsequent incorporation of C input into various C pools, those with slow turnover times do not reflect influences from field level treatments over shorter time scales. If I were to examine fraction C with C inputs as the independent variable, differences in decomposition as a result of field treatments (i.e. tillage) would produce varying levels of whole SOC, confounding the relationship of fraction C and C inputs. Therefore, when examining soil fractions, it is crucial to express soil fraction C across a normalized scale. Whole-soil SOC content, as a balance between C input and decomposition would normalize across treatments and be a more appropriate measure of C accumulation.

From the mathematical derivation, fractions behaving with linear whole soil C dynamics over C inputs express linear dynamics over whole SOC content. Similarly, whole soil C-saturation dynamics are expressed as hyperbolic relationships over whole SOC content. These models represented two alternate hypotheses of C accumulation in fractions and were then used to test for fraction saturation. I fit each fraction with a linear and C-saturation model and compared fit using r^2 calculated from corrected sum of squares.

Across and within our eight sites, I found hyperbolic relationships for both individual site and combined site data in the chemically--protected pool. The microaggregate-protected pool also showed support for C saturation in the combined site data, but the individual site data were mostly best fit with the linear model in both the μagg and iPOM fractions. At the individual sites, the biochemical pool was split between C-saturation and linear model fits, but were linear when the data were combined. The non-protected pool showed primarily linear dynamics, I found these pools to be significantly related to temperature and precipitation, suggesting a climatic influence on these pools.

Soil C saturation behavior was observed in soils from a variety of taxonomies, textures and climates suggesting that the C saturation can be generalized and may influence soil C accumulation even at sites that appear to be far from their theoretical C saturation limit.

Chapters two and three suggested that C saturation dynamics could be observed over soils with varying C saturation deficits as well as over increasing C inputs. However to date, the effect of soil C saturation deficit had only been tested indirectly by

assuming SOC content as a proxy of C saturation deficit across a broad range of sites. Additionally, the effects of C inputs have been assessed using experiments investigating effects of management (i.e., tillage, fertilization, and crop rotation), on yield and/or soil C, which often do not provide a wide enough range of treatments to effectively examine the response of soil C levels to C input rate. Across sites, interpretation of C stabilization over increasing C input levels is complicated by site effects such as differences in climate, soil texture, mineralogy and type.

The fourth and fifth chapters directly test the C saturation concept through laboratory incubations. The fourth chapter presents the design of a laboratory experiment to test the soil C saturation concept and outlines soil units necessary to evaluate the incubation results. It uses respiration and whole soil C data from 1.5 years of incubation to lead the reader through the concept, implementation, and evaluation of the experimental setup specifically designed to test the soil C saturation concept.

The objectives of this study were to examine, by experimental manipulation, the effects of saturation deficit and varying C input levels on SOC stabilization over a broad range of soils differing in physiochemical characteristics. I present an experimental approach to test the soil C saturation concept and report results of C-stabilization driven by both soil C saturation deficit and C input level. I incubated soils from six agricultural sites that are close to (i.e., A-horizon) or further from (i.e., C-horizon) saturation with low and high input rates of ^{13}C-labeled wheat straw (1× and 5×, respectively) for 1.5 years. I hypothesized that 1) the proportion of C stabilized would be greater in soils with a larger compared to smaller C saturation deficit (i.e., the C- vs. A-horizon) and 2) the

22

stabilization rate of added C would be greater if the amount of C input is small compared to the saturation deficit.

After 1.5 years, soils with greater saturation deficit led to significantly greater C stabilization in both addition rates in the sandy soils. The only site that showed C accumulation in a manner inconsistent with the C saturation hypothesis had the highest silt plus clay content of all the sites. Three sites retained a greater proportion of residue-derived C between the C- and A- horizon in the high residue addition compared to the low. These results lend support to the concept of soil C saturation and suggest that soils with low C contents and degraded lands may have the greatest rate and potential to store added C because they are further from their theoretical saturation level.

In the fifth chapter, I report the results of the incubation after 2.5 years incubation and examine C accumulation in SOM fractions. Stabilization of added ^{13}C in the whole soil was greater in the C-horizon compared to the A-horizon in the majority of our soils, suggesting soil C saturation deficit influenced the stabilization of new C across a wide range of textures (clay to sandy loam).

Greater stabilization of residue-derived C in the C- compared to A-horizon in both the 1× and 5× addition treatments suggested a limit to the amount of C that could be protected in the chemically-protected C pool. These results corroborate work supporting the influence of the silt and clay and the degree to which it is filled on soil C accumulation (Hassink 1997; Carter et al. 2003).

Generally, the microaggregate-protected pool demonstrated trends consistent with the saturation hypothesis (C- > A-horizon) suggesting that saturation deficit influences physical protection mechanisms of SOC stabilization. These results contradict those of

the composite site analysis in Chapter 3, where I found that the majority of microaggregate fractions were better fit with a linear, not the C-saturation model.

The biochemical pool showed strong evidence of saturation in both the 1× and 5× additions with the C-horizon sequestering more residue-derived C than the A-horizon. These findings clarify the influence of saturation deficit on C accumulation in the biochemically-protected pool. In the third chapter, I found mixed results in this pool, with half the sites showing linear, and the other half, C saturation dynamics.

The non-protected pool showed little direct evidence for C saturation. However, the observed greater C accumulation in the unprotected pools of the A-horizons may reflect the inability of C to be stored in silt and clay fractions because of their lower saturation deficits. If the silt and clay fractions are saturated, then the accumulation of POM C increase, as there would be no room to stabilize C products. Thus, in C accumulation in non-protected fractions should be greater in soils closer to C saturation.

Within the soil, greater C stabilization in the C-horizon of the whole soil generally occurred in the chemical, physical, and biochemical C pools. Overall, this study corroborates the whole soil C saturation concept and the C saturation of C fractions. Soils far from their saturation limit (C-horizon) do accumulate more C in the chemically-, and biochemically-protected pools than soils closer to their C saturation limit (A-horizon). Soils closer to their saturation limit have greater C accumulation in the non-protected pools.

Summary

I have shown that although soil C saturation theoretically can occur in whole soils, the rate and duration of C application necessary to observe these dynamics is unlikely to occur in natural systems (Chapter 2). The only individual site showing soil C saturation dynamics (Sanborn MO, Chapter 2) had large C inputs in the form of manure and had the longest experimental duration (greater than 90 years in the case of conventional tillage). However, when site data was composited, the broader range of C inputs produced a generally curved fit to the data. Experimentally, soil C saturation deficit influenced SOC accumulation in a broad range of soil and textures, implying that the C saturation concept may be generalized and applied in a broad range of scenarios.

In this dissertation, soil fractions have been shown to saturate. The chemically- and the biochemically-protected pools showed evidence of C saturation dynamics in both the field study and the lab study. The results of the aggregate-protected pool were mixed, indicating C saturation in the incubation (Chapter 5), but linear, non saturating dynamics in the field analysis (Chapter 3). Interestingly, the non-protected pool showed no evidence of saturation in either the field study nor the incubation, indicating that this pool is indeed not influenced by C saturation deficit. Instead, I found a significant relationship between fraction C and mean annual temperature and precipitation (Chapter 3) indicating that this pool is ultimately dictated by climatic constraints.

The influence of current SOC content (i.e. saturation deficit) on the effectiveness of C stabilization by conversion of CT to NT systems has recently been observed in an analysis of C sequestration potential by GIS methodology. Tan and Lal (2005) used constant factors to calculate $0 - 20$ cm pedon C values for Ohio using STATSGO data,

and from those treatments which showed positive C accumulation by adoption of NT, found that as SOC content of CT increased, the percent SOC increase under NT decreased exponentially. They concluded that site-specific C sequestration would be related to the current SOC content of the soil and that soils with a lower SOC content would have the greatest ability to sequester C.

Soils with low C contents and degraded lands may have the fastest rate and greatest potential to store added C, because they are further from their theoretical saturation level. Conversely, those soils with greater C content, would not provide much additional C stabilization if C inputs were increased. Further, soil C saturation implied a general order to C sequestration. Some authors suggest that SOC sequestration follows an order, based on the saturation of C pools (Hassink 1997; Carter 2002). The protective capacity is related to soil texture, and thus sandier soils have a lower and clayey soils have a higher protective capacity. Carbon content of clay fractions as a function of clay content of the soil have been found to be negative (Jolivet et al. 2003; Plante et al. 2006b) suggesting that the clay in sandy soils is closer to saturation than the clays in clayey soils. This conjecture is confirmed by several studies that have examined protective capacity and, across texture, found that soils with a lower silt + clay content tended to be saturated, while those with greater clay content still had potential to store more C (Hassink 1997; Carter et al. 2003). Once the protective capacity is filled, further C accumulation occurs in the aggregate and POM fractions. Soils near or at their 'protective capacity' have been shown to be influenced by management, but not texture (Hassink 1997; Carter et al. 2003).

Soils close to their protective capacity of silt and clay will accumulate C in the aggregate and non-protected fractions. This C is inherently less stable and subject to increased decomposition due to changes in management. To maximize the benefit of soil C storage as a potential CO_2 mitigation strategy, soil C saturation dynamics of the whole soil and related fractions must be considered.

References

Baldock JA & Skjemstad JO (2000) Role of the soil matrix and minerals in protecting natural organic materials against biological attack. Organic Geochemistry 31: 697-710

Cambardella CA & Elliott ET (1992) Particulate soil organic-matter changes across a grassland cultivation sequence. Soil Sci Soc Am J 56: 777-783

Carter MR (2002) Soil quality for sustainable land management: Organic matter and aggregation interactions that maintain soil functions. Agron J 94: 38-47

Carter MR, Angers DA, Gregorich EG & Bolinder MA (2003) Characterizing organic matter retention for surface soils in eastern Canada using density and particle size fractions. Can J Soil Sci 83: 11-23

Christensen BT (2001) Physical fractionation of soil and structural and functional complexity in organic matter turnover. Eur J Soil Sci 52: 345-353

Curtin D & Fraser PM (2003) Soil organic matter as influenced by straw management practices and inclusion of grass and clover seed crops in cereal rotations. Aust J Soil Res 41: 95-106

Diekow J, Mielniczuk J, Knicker H, Bayer C, Dick DP & Kogel-Knabner I (2005) Carbon and nitrogen stocks in physical fractions of a subtropical Acrisol as influenced by long-term no-till cropping systems and N fertilisation. Plant Soil 268: 319-328

Elliott ET (1986) Aggregate structure and carbon, nitrogen, and phosphorus in native and cultivated soils. Soil Sci Soc Am J 50: 627-633

Golchin A, J.M. Oades, J.O Skejemstad, P.Clarke (1994) Soil Structure and Carbon
Cycling. Soil Biol Biochem 32: 1043-1068

Harter RD & Stotzky G (1971) Formation of Clay-Protein Complexes. Soil Science
Society of America Proceedings 35: 383-388

Hassink J (1997) The capacity of soils to preserve organic C and N by their association
with clay and silt particles. Plant Soil 191: 77-87

Huggins DR, Buyanovsky GA, Wagner GH, Brown JR, Darmody RG, Peck TR, Lesoing
GW, Vanotti MB & Bundy LG (1998a) Soil organic C in the tallgrass prairie-
derived region of the corn belt: effects of long-term crop management. Soil
Tillage Res 47: 219-234

Huggins DR, Clapp CE, Allmaras RR, Lamb JA & Layese MF (1998b) Carbon dynamics
in corn-soybean sequences as estimated from natural carbon-13 abundance. Soil
Sci Soc Am J 62: 195-203

Huggins DR & Fuchs DJ (1997) Long-term N management effects on corn yield a soil C
of an Aquic Haplustoll in Minnesota. In: Paul EA, Elliot ET, K.Paustian & Cole
CV (Eds) Soil Organic Matter in Temperate Agroecosystems: Long-term
experiments in North America pp 121-128). CRC Press, Inc, New York

Janzen HH (2005) Soil carbon: A measure of ecosystem response in a changing world?
Can J Soil Sci 85: 467-480

Jastrow JD (1996) Soil aggregate formation and the accrual of particulate and mineral-
associated organic matter. Soil Biol Biochem 28: 665-676

Jenny H (1941) Factors of soil formation. McGraw-Hill, New York, New York, USA

Jenny H (1980) The Soil Resource:Origin and Behavior. Springer-Verlag, New York

Jolivet C, Arrouays D, Leveque J, Andreux F & Chenu C (2003) Organic carbon dynamics in soil particle-size separates of sandy Spodosols when forest is cleared for maize cropping. Eur J Soil Sci 54: 257-268

Kong AYY, Six J, Bryant DC, Denison RF & van Kessel C (2005) The relationship between carbon input, aggregation, and soil organic carbon stabilization in sustainable cropping systems. Soil Sci Soc Am J 69: 1078-1085

Krull ES, Baldock JA & Skjemstad JO (2003) Importance of mechanisms and processes of the stabilisation of soil organic matter for modeling carbon turnover. Funct Plant Biol 30: 207-222

Lal R, Follett RF, Kimble J & Cole CV (1999) Managing US cropland to sequester carbon in soil. J Soil Water Conserv 54: 374-381

Mann L (1986) Changes in soil C storage after cultivation. Soil Sci 142: 279-288

Marshman NA & Marshall KC (1981) Bacterial-Growth on Proteins in the Presence of Clay-Minerals. Soil Biol Biochem 13: 127-134

Oades JM (1984) Soil Organic-Matter and Structural Stability - Mechanisms and Implications for Management. Plant Soil 76: 319-337

Oades JM (1988) The Retention of Organic-Matter in Soils. Biogeochemistry 5: 35-70

Ogle SM, Breidt FJ, Eve MD & Paustian K (2003) Uncertainty in estimating land use and management impacts on soil organic carbon storage for US agricultural lands between 1982 and 1997. Global Change Biology 9: 1521-1542

Ogle SM, Breidt FJ & Paustian K (2005) Agricultural management impacts on soil organic carbon storage under moist and dry climatic conditions of temperate and tropical regions. Biogeochemistry: 87-121

Paul EA, Collins HP & Leavitt SW (2001) Dynamics of resistant soil carbon of midwestern agricultural soils measured by naturally occurring C-14 abundance. Geoderma 104: 239-256

Paul EA, Follett RF, Leavitt SW, Halvorson A, Peterson GA & Lyon DJ (1997) Radiocarbon dating for determination of soil organic matter pool sizes and dynamics. Soil Sci Soc Am J 61: 1058-1067

Paustian K, Andren O, Janzen H, Lal R, Smith P, Tian G, Tiessen H, van Noordwijk M & Woomer P (1997a) Agricultural soil as a C sink to mitigate CO_2 emissions. Soil and Use Management 13: 230-244

Paustian K, Collins HP & Paul EA (1997b) Management controls on soil carbon. In: Paul EA, Paustian K & Cole CV (Eds) Soil Organic Matter in Temperate Agroecosystems: Long-Term Experiments in North America pp 15-49). CRC Press, New York

Paustian K, Six J, Elliot ET & Hunt HW (2000) Management options for reducing CO_2 emissions from agricultural soils. Biogeochemistry 48: 147-163

Plante AF, Conant RT, Stewart CE, Paustian K & Six J (2006) Impact of soil texture on the distribution of soil organic matter in physical and chemical fractions. Soil Sci Soc Am J 70: 287-296

Post WM, Emanuel WR, Zinke PJ & Stangenberger AG (1982) Soil Carbon Pools and World Life Zones. Nature 298: 156-159

Rasmussen PE & Collins HP (1991) Long-term impacts of tillage, fertilizer, and crop residue on soil organic matter in temperate semiarid regions. Adv Agron 45: 93-134

Reicosky DC, Evans SD, Cambardella CA, Armaras RR, Wilts AR & Huggins DR (2002) Continuous corn with moldboard tillage: Residue and fertility effects on soil carbon. J Soil Water Conserv 57: 277-284

Roscoe R, Buurman P, Velthorst EJ & Vasconcellos CA (2001) Soil organic matter dynamics in density and particle size fractions as revealed by the C-13/C-12 isotopic ratio in a Cerrado's oxisol. Geoderma 104: 185-202

Schlesinger WH (1977) Carbon Balance in Terrestrial Detritus. Annu Rev Ecol Syst 8: 51-81

Schlesinger WH (1997) Biogeochemistry, and analysis of global change. Academic Press, San Diego, CA, USA

Six J, Conant RT, Paul EA & Paustian K (2002) Stabilization mechanisms of soil organic matter: Implications for C-saturation of soils. Plant Soil 241: 155-176

Six J, Elliot ET & Paustian K (2000) Soil macroaggregate turnover and microaggregate formation: a mechanism for C sequestration under no-tillage agriculture. Soil Biol Biochem 32: 2099-2103

Smil V (2002) The earth's biosphere: evolution, dynamics, and change. MIT Press, Cambridge, MA, USA

Soon YK (1998) Crop residue and fertilizer management effects on some biological and chemical properties of a Dark Grey Solod. Can J Soil Sci 78: 707-713

Tiessen H, Cuevas E & Chacon P (1994) The Role of Soil Organic-Matter in Sustaining Soil Fertility. Nature 371: 783-785

Tisdall JM & Oades JM (1982) Organic-Matter and Water-Stable Aggregates in Soils. Journal of Soil Science 33: 141-163

Waksman SA & Cordon TC (1938) A method for studying decomposition of isolated

   lignin, and the influence of lignin on cellulose decomposition. Soil Sci 45: 199-

   206

West TO & Post WM (2002) Soil organic carbon sequestration rates by tillage and crop

   rotation: A global data analysis. Soil Sci Soc Am J 66: 1930-1946

CHAPTER 2

SOIL CARBON SATURATION: CONCEPT, EVIDENCE AND EVALUATION

Abstract

Current estimates of soil C storage potential are based on models or factors that assume first-order decomposition kinetics and hence linearity between C input rate and C stocks at steady-state. However, soil C stocks may be inherently limited by physicochemical soil characteristics such as texture and structure, which define a whole-soil C saturation limit. Direct corollaries of a whole-soil C saturation concept are that 1) the further a soil is from saturation, (i.e., the greater the saturation deficit), the greater its capacity to sequester added C and 2) as a soil approaches saturation, the specific rate of SOC accumulation decreases due to a smaller saturation deficit. Three models were tested against long-term agroecosystem data: the first assuming no soil C saturation limit (i.e., linear), the second assuming whole-soil C saturation (C saturation model), and the third assuming soil C saturation limit of one soil C pool, but not a second C pool (mixed model) to test for an effect of saturation deficit on soil C accumulation. Within a given

34

site, there was little additional support for the C- saturation or for the mixed model over the linear model due to small sample sizes and the strictness of our model selection methods. Across all sites however, the C saturation model had the best fit. We found that different tillage practices produced distinct effective stabilization capacity curves and the ratio of no-till to conventional-till SOC decreased exponentially across increasing soil C contents, suggesting that C saturation deficit influences the rate of soil C stabilization. We conclude that SOC sequestration at high C input rates may be overestimated by models with kinetics that assume linearity between C inputs and C stocks at steady-state.

Introduction

Soil organic C (SOC) constitutes a large pool of C in the global C cycle representing a dynamic balance between C inputs to the soil and losses via respiration and leaching. In agroecosystems, the SOC balance is influenced by management practices such as organic matter additions, tillage intensity, fertilization, irrigation, and crop rotation. Soil organic C storage may be increased directly by increasing C returns to the soil as crop residue, manure, or other organic amendment. Carbon inputs to the system also may be increased indirectly by fertilization or irrigation treatments that increase crop productivity, biomass and root production.

With conversion of native ecosystems to agricultural use, 40-60% of the original soil C stocks are typically lost within a few years to decades of use (Mann 1986). Interest has grown in promoting C sequestration in soils to help mitigate increasing CO_2 levels in the atmosphere because most agricultural soils have been previously depleted with respect to organic matter (CAST 2004). This interest is also coincident with the desire to increase soil C contents to improve soil sustainability (Follett & Delgado 2002). Key questions include: what is the relative C storage efficiency (i.e., C stock increase per unit C added) for different soils and is there an upper limit to the capacity for soils to store organic C?

The C contents of native ecosystems from which agroecosystems were derived are often used as a baseline in assessing soil C capacity (Paustian et al. 1998). However, some of the oldest anthropogenic soils formed through additions of manure, peat, and charcoal in the Americas (Glaser et al. 2001), Europe (Springob et al. 2001), Africa (Blackmore et al. 1990) and New Zealand (McFadgen 1980) contain up to 2.7 ± 0.5 times

more SOC than those of adjacent, non-amended, native soils (Glaser et al. 2001). Similarly, experiments in modern agricultural settings show that agricultural soils have a substantial capacity to store organic C. For example, farmyard manure applications of 35 Mg C ha^{-1} yr^{-1} at the Rothamsted plots over 140 years increased SOC approximately three times compared to the beginning of the experiment (Jenkinson 1990). After 42 years of green manure, animal manure, sewage sludge and peat additions at rates of 2 Mg C ha^{-1} yr^{-1} at Uppsala, Sweden, SOC contents increased by 0.3 to 2 times initial SOC content (Gerzabek et al. 2001). Reducing nutrient limitations of P in Australia (Ridley et al. 1990) and N in North America (Blevins et al. 1983) have also increased plant production and consequently C input to soils. In some cases this resulted in a greater SOC content than the native equivalent (Six et al. 2002). Increases in soil C stocks in agroecosystems are often linearly related to the amount of C returned to the system (Paustian et al. 1997c; Huggins et al. 1998a; Kong et al. 2005), suggesting that soil C levels may increase continuously and without limit as C inputs increase.

As our ability to increase SOC stocks through greater C inputs and improved management practices advances, it is crucial to know what, if anything, limits the amount and rate of SOC stabilization. Recent evidence suggests that SOC stabilization by silt- and clay-sized fractions may be limited by interactions between mineral surface area and organic matter (Hassink 1997; Six et al. 2002). By comparing three alternate models, Hassink and Whitmore (1997) found that a model that incorporated a finite protective capacity, as a function of soil clay content, explained the most variance (80%) in organic matter additions and losses in ten soils. The concept of a silt and clay protective capacity was expanded in a review article by Six et al. (2002), who proposed that in addition to a

silt and clay protective capacity, a "saturation limit" exists for the entire soil. In addition to the silt and clay protected pool, Six et al. (2002) hypothesized microaggregate-protected, biochemically-protected, and non-protected C pools. In their conceptual model, SOC is stabilized through chemical association with silt and clay particles, physical protection within microaggregates and biochemical complexity of the organic compounds. A fourth, non-protected C pool, limited by the steady-state balance of C inputs and decomposition dictated by climate. Theoretically, whole-soil C saturation occurs due to the cumulative behavior of these four soil C pools.

The soil C saturation concept (Six et al. 2002) suggests a C saturation level based on texture and mineralogical characteristics of the whole-soil at steady-state with C inputs. This concept implies an upper limit for C sequestration capacity for the soil, ultimately determining its effectiveness, rate, and duration. The purpose of this study was to explore simple one-component and mixed models with assumptions of C saturation and to test these models against the common first-order model using experimental field data from long-term agroecosystem experiments.

Theory

Complex SOC models, when analyzed at steady-state, can be simplified and allow for general conclusions to be made. Here, we present the simplest form of a first-order decay model which forms the basis of SOM models such as Century, Roth C, and many other (Paustian et al. 1997a) and we compare this to simple models that include C saturation. We focus on the steady-state behavior of the models to evaluate the relationship between C addition rates and soil C levels.

38

Linear model

This model assumes that the amount of C entering a C pool is independent of the pool size and that decomposition rates are directly proportional to the size of the pool.

$$\frac{dC_t}{dt} = I - kC_t \qquad (1)$$

where the rate of change in SOC at time t (dC_t/dt) is dependent on the rate of C input (I) and losses through first-order decomposition kinetics of the SOC pool (C_t), where (k) is the specific decay constant.[1] At steady-state ($dC_t/dt = 0$),

$$C_t^* = \frac{I}{k} \qquad (2)$$

where SOC content (C_t^*) becomes directly proportional to C inputs (I). If the amount of C added to the soil pool is increased, SOC will accumulate until a new steady-state level is achieved. If I is increased by a constant proportion $I=I_i\cdot n$, SOC content at steady-state will increase by the same proportion (Figure 1a), without limit (Figure 1b). Most SOC models assume first-order decomposition kinetics and hence have a linear relationship between C inputs and SOC content at steady-state (Paustian 1994; Paustian et al. 1997b). This relationship holds even for models with multiple pools (and k's) of SOC (Parton et al. 1988; Jenkinson 1990; Bolker et al. 1998) and models where the specific decomposition rates (k) is treated as a variable (Bosatta & Agren 1999) rather than a constant (Paustian et al. 1997b).

Data from many long-term agroecosystem experiments appear to support this linear relationship between C inputs and SOC content (Rasmussen & Collins 1991; Paustian et al. 1997b; Huggins et al. 1998a; Kong et al. 2005). However, other

---

[1] For simplicity, losses via respiration are included in the term k, and losses through other pathways (e.g., leaching) are assumed to be zero.

39

No Saturation
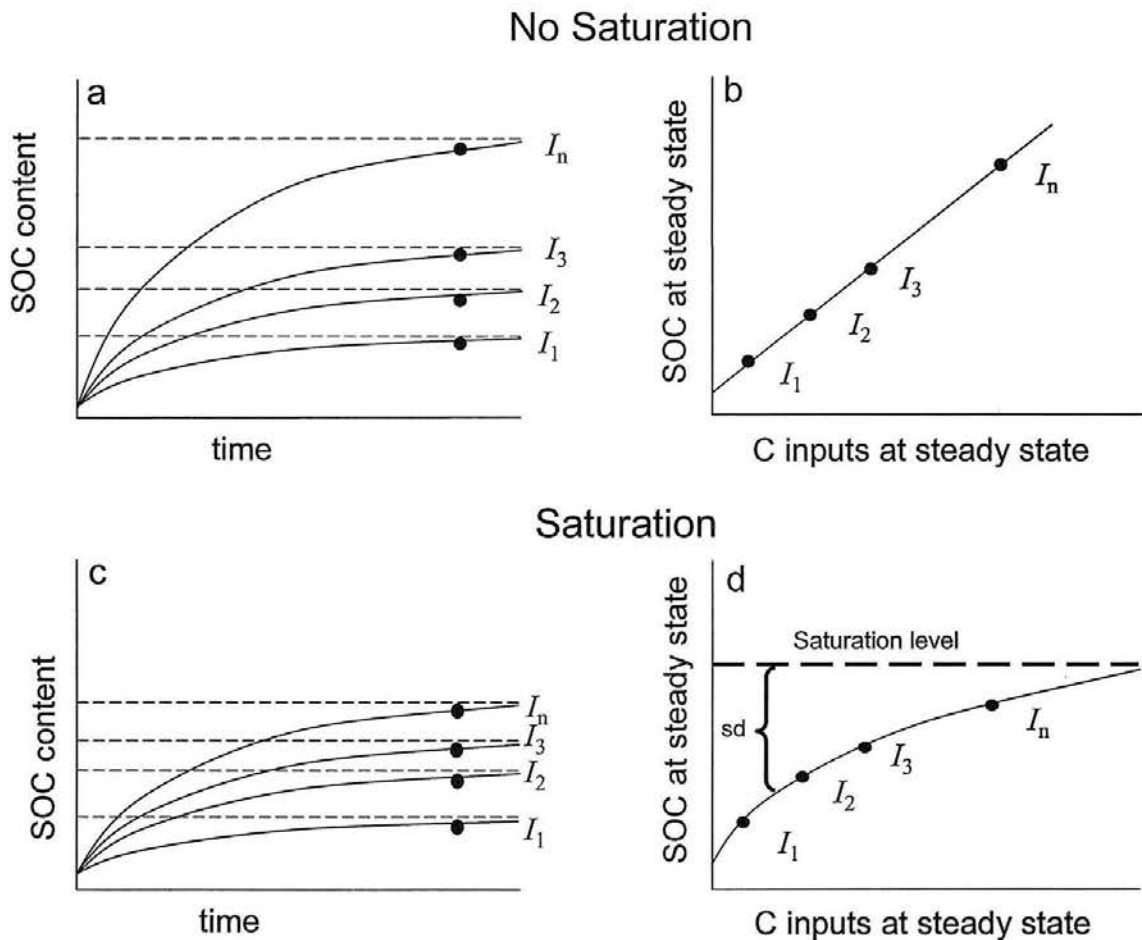
Saturation

Figure 1: Theoretical relationship between C inputs and soil organic C (SOC) contents at steady-state, with and without C saturation. Steady-state soil organic C (SOC) accumulation dynamics expressed over time (1a) produces a linear relationship when expressed over C inputs (1b) Under the conditions of C saturation, SOC stabilization with increasing input rates (at steady state) is not proportional (1c) resulting in an asymptotic relationship when expressed over C inputs (1d).

experiments show little or no response of SOC to differences in C addition rate, typically at sites with high SOC content and low decomposition rates. For example, Soon (1998) found no effect of fertilization and straw management on a Dark Grey Solod near Beaverton, Alberta after ten years. After 30 years of continuous corn at Morris, MN, neither varying rates of fertilization nor removal of crop stover had a significant effect on SOC content of the upper 20 cm of soil (Reicosky et al. 2002). At Lamberton, MN,

greater residue additions in corn versus corn-soybean crop rotations over ten years (Huggins et al. 1998b) and differences in N-fertilizer rates and residue inputs over 19 years (Huggins & Fuchs 1997; Huggins et al. 1998a) did not significantly affect SOC levels. A 6-year study conducted in New Zealand on a relatively high C soil found no detectable effect of straw management treatments on SOC levels (Curtin & Fraser 2003). These studies suggest that increasing C returns to high C content soils does not necessarily increase SOC content. This is contrary to current linear models of C stabilization but consistent with the C-saturation concept.

Carbon Saturation Model

In contrast to the linear model above, the C saturation model yields an asymptotic relationship between C inputs and SOC content at steady-state, produced by an inherent physicochemical limit to SOC protection. The soil C saturation concept may be expressed as a simple modification to the C input term in Equation 1:

$$\frac{dC_t}{dt} = I\left(1 - \frac{C_t}{C_m}\right) - kC_t \qquad (3)$$

where C_m is the maximum amount of C that can be stabilized by the soil. In this model, soil C storage is limited by a saturation deficit (*sd*) which we define as:

$$sd = 1 - \frac{C_t}{C_m} \qquad (4)$$

Solving equation 3 for steady-state C concentration (C_t^*) results in an asymptotic relationship between C inputs (*I*) and SOC (Figure 1d):

$$C_t^* = \frac{I}{k + \frac{I}{C_m}} \qquad (5)$$

41

When expressed over time, each C input level (I_i) produces a distinct steady-state SOC content (Figure 1c), similar to the linear model without saturation, however the relative SOC stabilization decreases with increasing I, rather than remaining proportional as in the linear model (Figure 1c vs. 1a). The asymptotic relationship between C inputs and SOC content at steady-state is a key attribute to the C saturation model (Figure 1b vs. Figure 1d). Direct corollaries of this asymptotic relationship are that 1) the further a soil is from saturation (i.e., the greater the saturation deficit), the greater its capacity to sequester added C, and 2) as a soil approaches saturation, the rate and amount of SOC accumulation decreases due to a smaller saturation deficit.

A few experimental studies have shown decreased SOC stabilization in high-C compared to low-C soils under the same treatments, consistent with the soil C saturation concept. After 31 years, Campbell et al. (1991b) found SOC content was not significantly different under fertilizer and wheat-fallow rotations at Melfort (C input 1.4-2.2 Mg C ha^{-1} yr^{-1}) but increased at Indian Head (C input 0.9-2.0 Mg C ha^{-1} yr^{-1}). They attributed this difference in SOC storage, at least in part, to the lesser SOC content of Indian Head (36-42 Mg C ha^{-1}) compared to Melfort (61-67 Mg C ha^{-1}, 0-15 cm). After eleven years, Nyborg et al. (1995) found less stabilization of new C in a Typic Cryoborol (Ellerslie, Alberta) with a greater C content (86.7 Mg C ha^{-1}, 0-15 cm) compared to a paired site at Breton, Alberta (Typic Cryoboralf) (33.2 Mg C ha^{-1}, 0-15 cm) under straw addition and N-fertilization treatments. This decrease in relative C stabilization as soil C content increased suggests a soil C saturation response.

Mixed Model

The C saturation model assumes that the amount of C that can be stabilized to SOM is limited and does not explicitly address the fate of residue C that is not stabilized as SOM. Hence, we can visualize a mixed C saturation model comprised of a labile residue C pool (C_1) not subject to C saturation and a second more stabilized C pool subject to saturation (C_2):

$$\frac{dC_t}{dt} = \frac{dC_1}{dt} + \frac{dC_2}{dt} \qquad (6)$$

where:

$$\frac{dC_1}{dt} = I - \alpha k_1 C_1 - (1-\alpha)k_1 \left(1 - \frac{C_2}{C_m}\right)C_1 \qquad (7)$$

and:

$$\frac{dC_2}{dt} = (1-\alpha)k_1 \left(1 - \frac{C_2}{C_m}\right)C_1 - k_2 C_2 \qquad (8)$$

with decomposition constants k_1 and k_2, respectively. The term α is a partitioning coefficient between mass loss from C_1 as respiration (α) versus non-respired decomposition products (1-α). We assign a value of 0.55 to α, similar to respiration coefficients used in other SOM models (e.g. Parton et al. 1987). Solving Equations 7 and 8 for steady-state

$$C_t^* = \frac{IC_m}{k_1(C_m - C_2 + \alpha C_2)} + \frac{(\alpha - 1)k_1 C_1 C_m}{k_1 C_1 + \alpha k_1 C_1 - k_2 C_m} \qquad (9)$$

shows the relationship between C inputs (I) and SOC (C_t). At low C inputs, this model produces nearly linear SOC accumulation dynamics, but under high C inputs, SOC accumulation is limited by the saturation term, C_m. The non-saturated pool corresponds

to a non-protected C pool and the saturated pool to mineral- and aggregate-associated C pools. The description of this curve is not asymptotic as it is for the C saturation model, but increasing curvilinear. Theoretically, SOC will increase indefinitely in this model, however at a slower rate as SOC inputs are increased. Assuming $k_1 > k_2$, the turnover rate of the total soil C increases as the recalcitrant pool approaches saturation because C is retained in the labile (unprotected) state, which is subject to a faster rate of decomposition.

The three models described above provide three scenarios of SOC accumulation: 1) no saturation limit (i.e., linear), 2) whole-soil C saturation limit (i.e., C saturation model), and 3) soil C saturation of a stabilized C pool, but not the whole soil (i.e., mixed model). By using likelihood-based methods and information theory (small sample Akaike's Information Criterion, AIC_c), we were able to quantify the relative explanatory power of these models, given the data (Anderson et al. 1998; Burnham & Anderson 2001; Burnham & Anderson 2004).Analysis Methods

We compiled the most recent SOC contents and average C inputs (as crop residues and organic amendments) from the data set that Ogle et al. (2005) compiled from long-term agricultural sites around the world. Required data included SOC stocks, soil bulk density, depth of measurement, and C inputs. We estimated rotational C inputs based on reported crop yield (and in some cases total aboveground biomass production), using regression models to estimate total C inputs from roots plus aboveground residues (Steve Williams, personal communication 2005) (Table 1) or published values from the experiment. Long-term agricultural sites were only included if the experiment was greater duration of experiment. Additionally, sites were required to have four or more C input

	Aboveground residue (AGR) (Mg dry wt ha^{-1})	Belowground residue (BGR) (Mg dry wt ha^{-1})
Alfalfa	0.325 * GDW[‡]	0.43 * (GDW[‡] + AGR)
Oat	1.09 * GDW + 0.387	0.26 * (GDW + AGR)
Soybean	1.712 * GDW + 0.795	0.24 * (GDW + AGR)
Corn	1.03 * GDW + 0.610	0.21 * (GDW + AGR)
Wheat		
winter	1.61 * GDW + 0.389	0.21 * (GDW + AGR)
spring	1.29 * GDW + 0.715	
Barley	0.95 * GDW + 0.625	0.20 * (GDW + AGR)

Table 1 Regression equations for above- and belowground C input from grain dry weight (GDW) for common crops in long-term agroecosystems experiments. Equations are based on long-term crop yield data from US agroecosystem experiments compiled by Steve Williams (personal communication 2005).‡ GDW = grain dry wt. (Mg ha^{-1}); for alfalfa GDW=aboveground biomass dry weight.

than 12 years in age (to exclude sites where soil C stocks may be far from steady-state). levels (e.g., differences in crop rotations or organic matter addition treatments) on which to base a reasonable regression line. Sites with multiple treatments (e.g., tillage and crop rotation) were split as tillage could confound the C input effect.

An additional factor in the analysis is that the long-term experiments do not, strictly speaking, represent a true steady-state condition with respect to SOM levels as a function of C input, because of the very long residence time of some recalcitrant SOC. For example, when C inputs are totally eliminated (e.g., bare fallow experiments), a substantial fraction of the SOC persists over many decades (Paustian et al. 1992; Plante et al. 2004). The true steady-state condition for all three models under the condition of zero C inputs, however, is zero SOC. An intercept term (R) was added to the linear model in

Equation 2 to account for the residual SOC that is not affected over the course of the agroecosystem experiment:

$$C_t^* = \frac{I}{k} + R \tag{10}$$

Due to the composite nature of the mixed model, there is not a unique steady-state solution in terms of C_t. To determine the sensitivity of the steady-state solution to the proportion of C in C_1 and C_2, we ran the model iteratively with fixed proportions of C_2 (0.1 to 0.9). We found that the parameter estimates varied only slightly across all proportions of C_2 and produced less than nine percent variation in AIC_c value.

Traditional statistics lack a formal method of incorporating the uncertainty of the data into the model. However, information-theory integrates model-selection uncertainty by penalizing models with poor predictor choice, errors in structure, or poor explanation of the given data. Information theory also allows a set of competing models to be tested and a "best" model or models (if there is high uncertainty) to be determined based on the data (Anderson et al. 1998). We used small sample Akaike information criterion (AIC_c) for model selection, i.e.,

$$AIC_c = AIC + \frac{2K * (K+1)}{n - K - 1} \tag{11}$$

where K is the number of estimable parameters, n is the sample size and

$$AIC = -2 \log L[(\theta_i \mid Y)] + 2K \tag{12}$$

with $L(\theta_i \mid Y)$ as the maximized likelihood, a function of the unknown parameters θ_i, given the data Y and the model. To compare models, AIC_c values were rescaled as differences (Δ_i) between the AIC_c of model i and the best approximating model (Δ_i

46

=AIC$_{ci}$ - AIC$_{c\ min}$).   The relative likelihood of a model, given the data and the set of models, or its 'probability', is expressed by weights.

$$w_i = \frac{e^{-1/2\Delta_i}}{\sum_i e^{-1/2\Delta_i}} \qquad (13)$$

We used this method to test the likelihood of the linear (Equation 10), C saturation (Equation 5), and mixed (Equation 9) models given the C input and SOC data. All models were fit using PROC NLMIXED in SAS/STAT (SAS Institute, Cary NC) to normalize for the treatment of variance in model fits, and to obtain AIC and AIC$_c$ values. A model was considered to be best fit if differences in $\Delta_i > 2$.

Results & Discussion

We found 17 sites that matched our criteria from a variety of temperate agroecosystems in the U.S. and Canada (Table 2). They varied in SOC contents from 7.7 to 121.9 Mg C ha^{-1} and C inputs from 0.17 to 7.42 Mg C ha^{-1} yr^{-1}. Ranking the models by $\Delta_i > 2$, only five sites had a clear best-fit model; the linear model for Lancaster 2, Pendleton, Sanborn CT, and Sterling, and the C saturation model for Sanborn NT. The linear and C saturation models were indistinguishable at 11 sites, but both had better fits than the mixed model.   There was no evidence in the Morrow corn-soybean rotation data to distinguish between any of the models (Table 3).

Both tillage treatments at Sanborn appear to have curvilinear dynamics over increasing C inputs (Figure 2). Using AIC$_c$ as a model selection criterion, only NT has substantial support for the C saturation model. The penalty of adding parameters to the model is illustrated by the good fit of the mixed model and in the AIC values of both

47

tillage treatments, but lack of substantiation when compared by AIC_c to the linear and C saturation models.

The lack of model differentiation within a site is, in part due, to the small sample size within a site (*n* of four input levels in six sites). The Akaike value, especially for small sample sizes (AIC_c), greatly penalizes models with both small sample size and a larger number of parameters. Without this correction (AIC), four of five best model fits were either the C-saturation or mixed model (Table 3). The penalty of adding another parameter in the mixed compared to the linear and C saturation models, explains why none of the sites show a best-fit mixed model fit with AIC_c as a selection criterion

In addition to small sample size, lack of model differentiation may be due to a small range of C inputs within a site. Differences between the highest and lowest input levels were < 2 Mg C ha^{-1} at eight sites. According to the C saturation concept, an asymptotic relationship would better fit the data than the linear model, but if C input levels are low, the asymptotic trend in SOC accumulation may not be evident. Smaller sections of an asymptotic curve can appear linear in the range being observed. Within each site, a small range of C inputs will not necessarily capture the full range of linear to asymptotic behaviors expected from a soil subject to C saturation. The conjecture that C input range was too small to exhibit C saturation dynamics within a given site is supported by three of the four linear best-fit models (Lancaster, Pendleton, and Sterling), where inputs were less than 3.5 Mg C ha^{-1}. Two of these sites, (Lancaster, Pendleton) also had only four C inputs values.

To overcome the small sample size within sites, we also fit our three models against the combined site data. Combining site data could confound the C saturation

analysis if C inputs (I) co-varied with decomposition rate (k), resulting in an apparent saturation response of less SOC accumulation at high input rates because of faster decomposition rates due to optimal temperature and moisture conditions. We found no significant relationship, however, between decomposition (k calculated using the linear

Site	Treatment duration (years)	Treatments	Reference
Breton, AB	51	Crop rotation N fertilizer addition Manure addition	(Izaurralde et al. 2001)
Indianhead, SK	30	Crop rotation	(Campbell & Zentner 1997)
Lamberton, MN	22	N fertilizer	(Darmody & Peck 1997)
Lancaster2, PA	14	Tillage	(Karlen et al. 1994)
Lancaster1, PA	14	Residue management	(Vanotti et al. 1997)
Mandan, ND	12	Tillage N fertilizer	(Halvorson et al. 2002)
Melfort, SK	30	Crop rotation	(Campbell et al. 1991c)
Morrow, IL	27	Crop rotation	Darmody & Peck 1997
Pendleton, OR	17	Tillage	(Rasmussen & Albrecht 1997)
Sanborn, MO	CT 96 NT 25	Tillage Manure addition	(Grant et al. 2001)
Sterling, CO	12	Crop rotation Topographic location	(Sherrod et al. 2003)
Stratton, CO	12	Crop rotation Topographic location	(Sherrod et al. 2003)
Swift Current, SK	13	Crop rotation N & P fertilizer	(Campbell et al. 1999)
Walsh, CO	12	Crop rotation Topographic location	(Sherrod et al. 2003)

Table 2: Long-term agroecosystem sites selected for use in comparative model analyses.

Table 3: Linear, C saturation and mixed model fit statistics. AIC = Akaike Information Criterion, AICc = Akaike Information Criterion corrected for small sample size, Δ_i = AICc$_i$-AICc$_{min}$, and w_i is the relative weight given each model based on AICc.

Site	n	AIC			AICc			Δ_i			w_i		
		linear	CSAT	Mixed	linear	CSAT	Mixed	linear	CSAT	Mixed	linear	CSAT	Mixed
Breton, AB	6	31.3	32.8	33.7	43.3	44.8	93.7	0.0	1.5	50.4	0.7	0.3	0.0
Indianhead, SK	7	29.2	30.2	29.9	37.2	38.2	89.9	0.0	1.0	52.7	0.6	0.4	0.0
Lamberton, MN	4	23.6	23.4	27.4	47.6	47.4	87.4	0.1	0.0	40.0	0.5	0.5	0.0
Lancaster2, PA	4	26.6	29.5	30.0	50.6	53.5	90.0	0.0	2.9	39.4	0.8	0.2	0.0
Lancaster1, PA	5	34.0	34.3	38.3	58.0	58.3	98.3	0.0	0.3	40.3	0.5	0.5	0.0
Mandan, NE	17	74.7	75.5	78.2	76.5	77.4	83.7	0.0	0.8	7.2	0.6	0.4	0.0
Melfort, SK	8	37.2	37.2	41.1	43.2	43.2	71.1	0.0	0.0	28.0	0.5	0.5	0.0
Morrow, IL													
corn	4	28.0	29.0	31.2	52.0	53.0	91.2	0.0	1.0	39.2	0.6	0.4	0.0
corn-soybean	4	27.3	29.1	13.2	51.3	53.1	73.2	0.2	1.9	21.8	0.7	0.3	0.0
corn-oat-hay	4	26.1	27.5	27.5	50.1	51.5	87.5	0.0	1.46	37.4	0.7	0.3	0.0
Pendleton, OR	4	9.4	15.5	7.5	33.4	39.5	67.3	0.0	6.1	33.8	1.0	0.1	0.0

Table 3: cont'd

Site	n	AIC			AICc			Δ_i			w_i		
		linear	CSAT	Mixed	linear	CSAT	Mixed	linear	CSAT	Mixed	linear	CSAT	Mixed
Sanborn, MO													
conventional-till	6	34.8	38.8	33.8	46.8	50.8	93.8	0.0	3.9	46.9	0.9	0.1	0.0
no-till	5	32.7	29.6	22.7	56.7	53.6	82.7	3.1	0.0	29.2	0.2	0.8	0.0
Sterling, CO	12	60.3	62.8	62.1	63.3	65.8	72.05	0.0	2.6	8.76	0.8	0.2	0.0
Stratton, CO	12	66.6	65.0	69.0	69.6	68.0	79.0	1.5	0.0	11.0	0.3	0.7	0.0
Swift Current, SK	7	33.6	34.4	36.2	41.6	42.4	96.2	0.0	0.8	54.6	0.6	0.4	0.0
Walsh, CO	10	59.8	60.5	64.5	63.8	64.5	79.5	0.0	0.7	15.8	0.6	0.4	0.0
Combined Sites	**119**	**1057.3**	**1048.5**	**1052.5**	**1057.5**	**1048.7**	**1053.0**	**8.8**	**0.0**	**4.3**	**0.0**	**0.9**	**0.1**
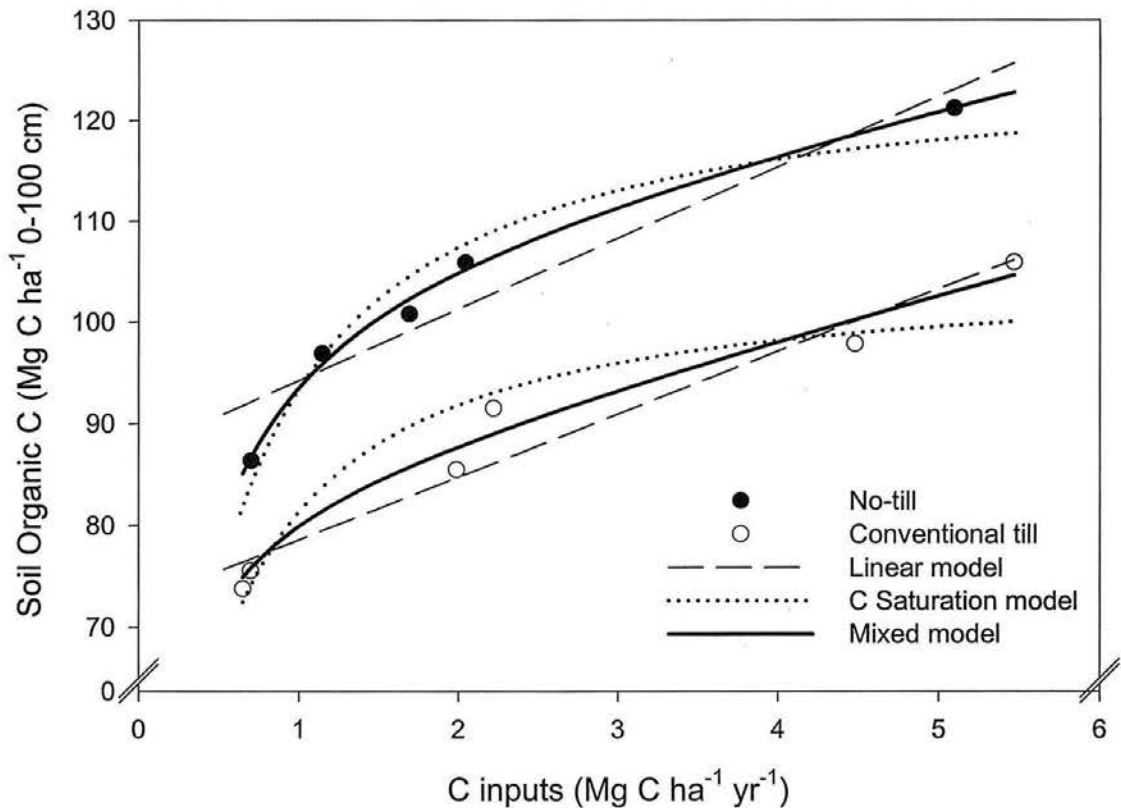
Figure 2: Linear, C saturation, and mixed model fits of soil organic C content (Mg C ha^{-1}) as a function of C inputs (Mg C ha^{-1} yr^{-1}) in the manure plots at Sanborn in no- and conventional-tillage treatments (25 and 96 years, respectively).

model fit) and C inputs (I) (data not shown). Although there is great variability in the data, when the three models were tested against all the sites combined, the C saturation model had greater support ($\Delta_i = 0$) in the data than either the linear ($\Delta_i = 8.78$) or the mixed model ($\Delta_i = 2.33$) (Figure 3 and Table 3). This result supports the concept of an asymptotic or C saturation model valid for all sites combined. Combining Akaike weights (w_i) as an estimation of probability, that there is a 99% probability either the C saturation or mixed model is the best approximation of this data. In conclusion, C saturation dynamics were evident in the combined site data, but were not always apparent within
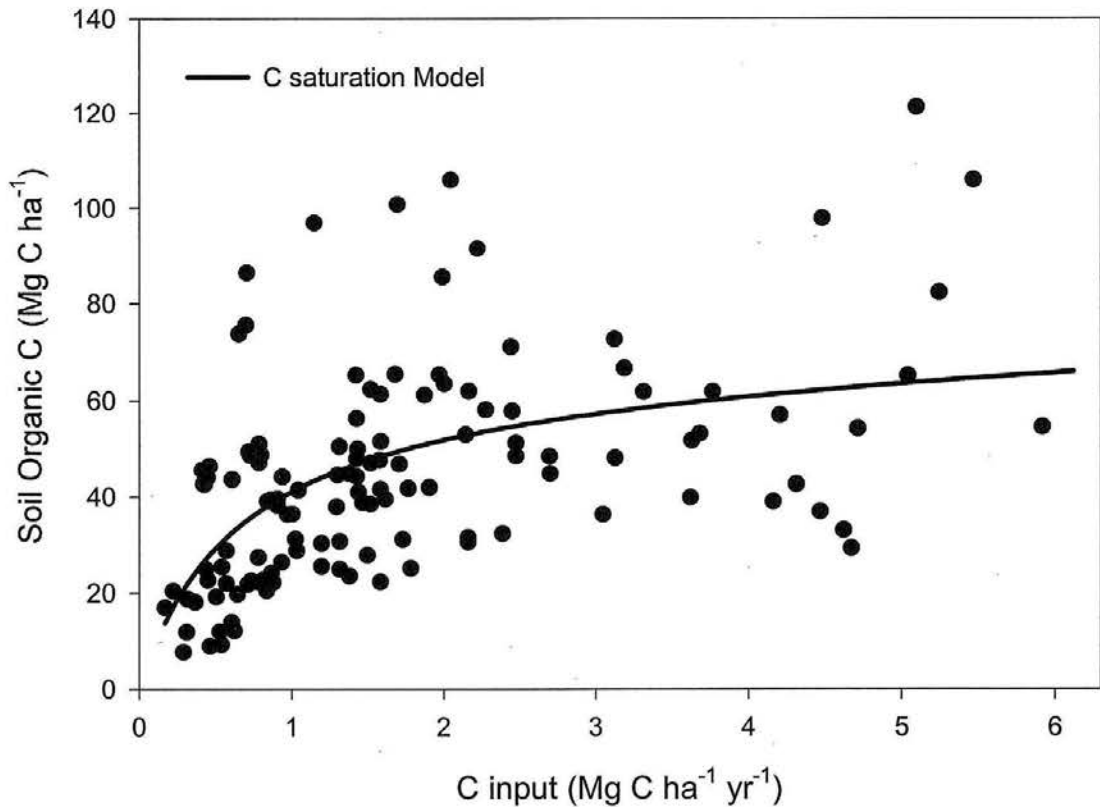
Figure 3 Soil organic C content (Mg C ha^{-1}) expressed as a function of C inputs (Mg C ha^{-1} yr^{-1}) for the 17 long-term agroecosystem experiments reported in Table 1.

individual sites, likely because of small sample sizes and small ranges of C input within sites

Soil C saturation and tillage

Evidence of C saturation has been suggested in some long-term agroecosystem experiments that show little response in SOC accumulation to increasing C inputs (e.g.,Campbell et al. 1991a; Solberg et al. 1997). However, data from the Sanborn

experiment appears to contradict the C saturation concept (Figure 2). According to the C saturation concept, each soil will have a unique C saturation level dictated by textural and mineralogical properties. If evaluated over increasing C inputs, SOC content will approach an asymptote (Figure 1). The conventional and no-tillage treatments imposed at Sanborn fit two distinct curves. How can the same site with the same texture and mineralogy appear to be approaching two distinct C saturation levels? One might also ask if the asymptote would be greater under no-tillage at sites such as Melfort where only conventional tillage treatments exist.

The C saturation model in Equation 5 shows that the SOC content (C_t) is dependent on both C inputs (I) and k. The parameter k may be thought of as a decomposition factor describing variation both across and within sites. Climatic factors such as mean annual temperature, precipitation, potential evapotranspiration dominate decomposition dynamics across sites, and subsequently alter k. Within a site, k is influenced by disturbance factors such as tillage. Decomposition dynamics, through k, alter the slope and intercept of the SOC and C input relationship in the models. Factors that influence decomposition rate thus also influence SOC storage and its relationship to C inputs at steady-state.

A soil under a management regime with increased decomposition (e.g., conventional tillage) with differing rates of C additions may therefore show an asymptotic SOC response at steady-state (CT curve in Figure 4). At the greater addition rates, the soil may appear to be approaching SOC saturation due to little or no SOC accumulation as C inputs are increased further (Figure 4).

However, a change in management (e.g., reduction or elimination of tillage) can decrease decomposition and thereby increase steady-state SOC content over the same range of C inputs. We propose the term "effective stabilization capacity" for these asymptotic relationships between SOC content and C inputs at levels smaller than the soil C saturation level due to conditions other than the physicochemical limitations of the soil. In the case of the Sanborn plots, the management-induced soil disturbance decreased the steady-state SOC content in comparison to the soil C saturation level. In contrast, soil C saturation level is achieved only when C input is maximized under management conditions that minimize soil disturbance, for example under manure additions to native soil. If disturbance dominates SOC content such as in tilled agroecosystems, a soil cannot achieve an absolute saturation level, but could reach an effective stabilization capacity commensurate with the input rate. Although these soils are not approaching C saturation level, the asymptotic relationship between C inputs and SOC content in these soils is indicative of C saturation dynamics.

The theoretical distinction between effective stabilization capacity and C saturation level explains why, over similar ranges of C additions, the treatments at Sanborn can be approaching two asymptotes even though they have the same texture and mineralogy defining a single C saturation level. This also implies none of the soils used in this analysis are approaching their absolute saturation level, but rather are approaching their effective stabilization capacity because of tillage-induced disturbances.

In addition to an upper limit for C stabilization, the C saturation concept has the corollary that the greater the saturation deficit, or the further a soil is from saturation, the greater its capacity to sequester added C. That is, a greater proportion of added C will be
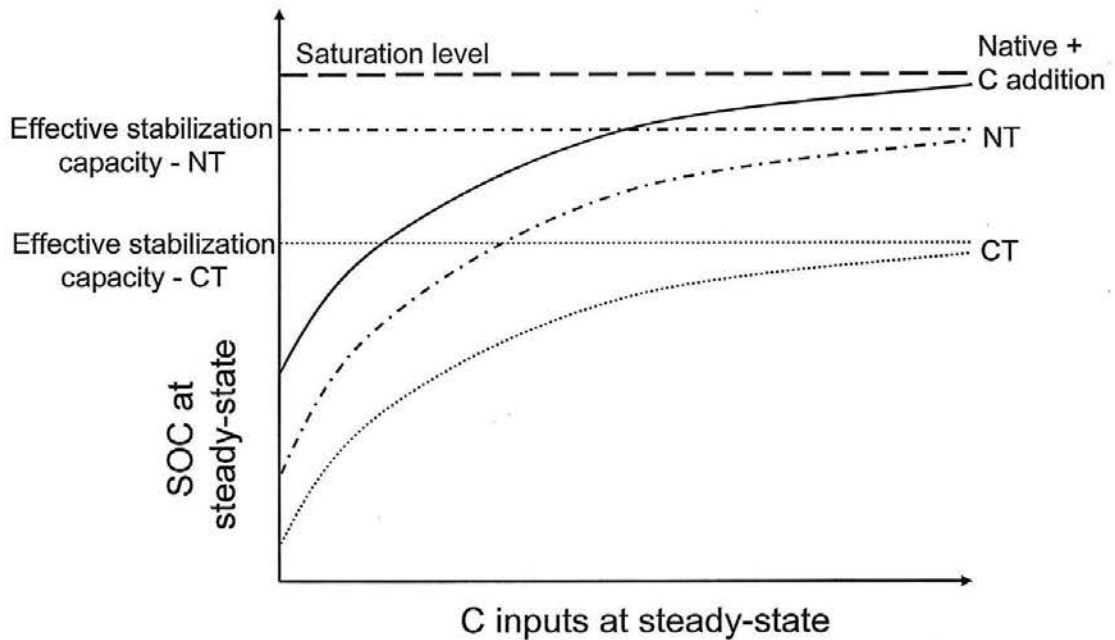
Figure 4: Soil C accumulation dynamics under theoretical decomposition regimes produced by management scenarios. Since no-tillage has less decomposition than conventional tillage, steady-state SOC content will be greater under the same C inputs level. Effective stabilization capacity is the upper limit to C storage due to intense decomposition (CT). These systems may appear to illustrate soil C saturation, but are not considered saturated due to C decomposition conditions dominating C stabilization. Soil C saturation is imposed by physical and chemical properties of a soil under conditions when C inputs are maximized and disturbance minimized.

stabilized in a soil with a greater C saturation deficit. Evidence suggests that SOC storage in NT soils is greater than in CT soils because of the physical protection of labile C in aggregate structures as well as increases in labile particulate organic matter. The amount of additional C stored in the NT treatment should theoretically decrease relative to that of the CT treatment as soil C content increases because a large saturation deficit (CT) will result in the stabilization of a greater proportion of any added C compared to a soil with a smaller deficit (NT).

Using a sub-set of global agroecosystem data compiled by Ogle et al. (2005) from a variety of depths, we compared the relative stabilization of C in NT to CT systems as a function of CT SOC content. As SOC content increases, the ratio should decrease because of a decreased capacity of the soil to store C (i.e., a decreased C saturation deficit.) We found that as SOC content increased, the ratio of SOC stabilization in NT versus CT treatments (NT/CT SOC stabilization ratio) decreased exponentially (Figure 5), a result consistent with the C saturation concept. In addition, the curvilinear relationship over increasing SOC content suggests that the saturation deficit influences the amount of C that can be stored in NT soils. The decrease in slope of the NT/CT ratio as SOC content increased was much also steeper in tropical compared to temperate sites (Figure 5).

This is probably because of the lesser stabilization capacity inherent to tropical soils due to a dominance of 1:1 clay minerals with a less surface area than 2:1 minerals comprising the temperate soils. Six et al. (2002) demonstrated a lower saturation level for the silt and clay protected C pool in (sub)tropical soils with 1:1 clay minerals than in temperate soils with a 2:1 mineralogy. Generally faster SOC cycling under tropical climates probably also influences the observed steeper relationship.

In summary, we found that the ratio of SOC storage between NT and CT treatments decreased as SOC content increased. We suggest that this decrease in C accumulation of NT relative to CT is consistent with C saturation. This trend was evident in both temperate and tropical soils; with the steeper decline in the tropical sites.
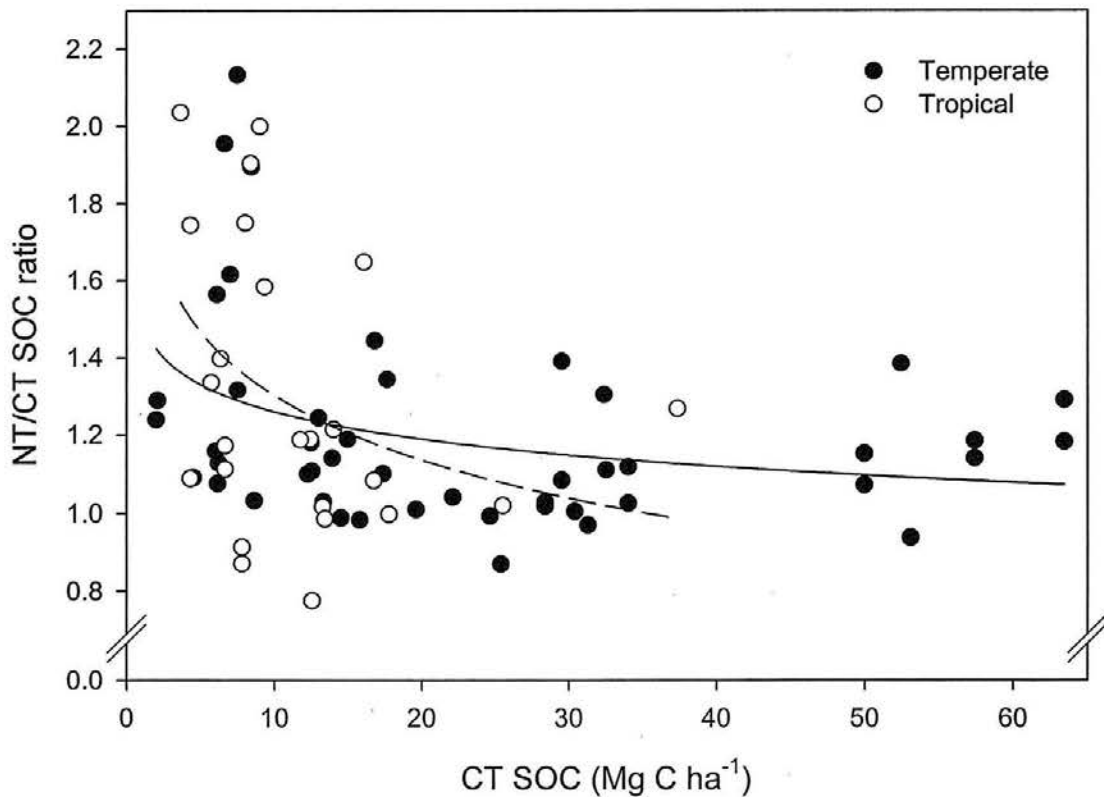
Figure 5 Relative soil organic C concentrations of paired no-till relative to conventional tillage treatments (NT/CT SOC ratio) as a function of soil organic C concentration (Mg C ha⁻¹) from 24 long-term temperate and tropical agro-ecosystem experiments (Ogle et al. 2005).

Summary

Three models were tested against agroecosystem data: the first assuming no soil C saturation limit (i.e., linear), the second assuming whole-soil C saturation (C saturation model), and the third assuming soil C saturation limit of one soil C pool, but not a second C pool (mixed model). We found the C saturation model to be the preferred model for data pooled across all sites. Given our data, there was less than 1% "probability" that the linear model was appropriate. This suggests that across these sites, SOC accumulation is

asymptotic with respect to C inputs. Within individual sites, only Sanborn showed a C saturation best-fit. Four sites had good support for the linear model, and all other sites had too few C input levels or too small a range of C inputs to detect a best-fit model.

We suggest, based on data from Sanborn, that agroecosystems may never approach C a true C saturation level where tillage disturbance accelerates SOC decomposition. However, within tillage treatments, asymptotic SOC dynamics are possible. We propose the term effective stabilization capacity to describe the maximum C sequestration possible with increasing C input under a particular management scenario.

We also tested the effect of C saturation deficit on the relative ratio of SOC stabilization of NT compared to CT systems. We found greater relative C accumulation in NT compared to CT at sites with small compared to large SOC contents, supporting the concept that saturation deficit influences the amount of C sequestered.

The true soil C saturation level may be of small practical importance, as large organic C inputs must be maintained over long time periods to sequester large quantities of C. Of more practical interest is the behavior of soils as they approach their effective stabilization capacity as well as the influence of C saturation deficit on SOC accumulation in non-saturated soils. Although current simulation models are fairly successful in explaining SOC accumulation in degraded agricultural soils, the validity of these models need to be further examined under scenarios of increasing C inputs and increasing SOC contents, where saturation effects may be manifested. However, additional research is needed to firmly establish the validity of the saturation concept and better quantify the controls on SOC kinetics for C-rich soils.

References

Anderson D.R., Burnham K.P. and White G.C. 1998. Comparison of Akaike information criterion and consistent Akaike information criterion for model selection and statistical inference from capture-recapture studies. J. Appl. Statist. 25: 263-282.

Blackmore A.C., Mentis M.T. and Scholes R.J. 1990. The origin and extent of nutrient-enriched patches within a nutrient-poor savanna in South-Africa. J. Biogeogr. 17: 463-470.

Blevins R.L., Thomas G.W., Smith M.S., Frye W.W. and Cornelius P.L. 1983. Changes in soil properties after 10 years continuous non-tilled and conventionally tilled corn. Soil Tillage Res.: 135-146.

Bolker B.M., Pacala S.W. and Parton W.J. 1998. Linear analysis of soil decomposition: Insights from the century model. Ecol. Appl. 8: 425-439.

Bosatta E. and Agren G. 1999. Soil organic matter quality interpreted thermodynamically. Soil Biol. Biochem. 31: 1889-1891.

Burnham K.P. and Anderson D.R. 2001. Kullback-Leibler information as a basis for strong inference in ecological studies. Wildl. Res. 28: 111-119.

Burnham K.P. and Anderson D.R. 2004. Multimodel inference - understanding AIC and BIC in model selection. Sociol. Method. Res. 33: 261-304.

Campbell C.A., Biederbeck V.O., McConkey B.G., Curtin D. and Zentner R.P. 1999. Soil quality-effect of tillage and fallow frequency. Soil Organic Matter Quality as Influenced by Tillage and Fallow Frequency in a Silt Loam in Southwestern Saskatchewan. Soil Biol. Biochem. 31: 1-7.

Campbell C.A., Biederbeck V.O., Zentner R.P. and Lafond G.P. 1991a. Effect of crop
rotations and cultural-practices on soil organic-matter, microbial biomass and
respiration in a Thin Black Chernozem. Can. J. Soil Sci. 71: 363-376.

Campbell C.A., Lafond G.P., Zentner R.P. and Biederbeck V.O. 1991b. Influence of
fertilizer and straw baling on soil organic matter in a Thin Black Chernozem in
western Canada. Soil Biol. Biochem. 23: 443-446.

Campbell C.A. and Zentner R.P. 1997 Crop production and soil organic matter in long-
term crop rotations in the semi-arid northern Great Plains of Canada. In: Paul
E.A., Paustian K., Elliot E.T. and Cole C.V. (eds), Soil Organic Matter in
Temperate Agroecosystems: Long-Term Experiments in North America. CRC
Press, New York pp. 317-334.

Campbell G.A., Browren K.E., Schnitzer M., R.P. Zentner and Townley-Smith L. 1991c.
Effect of crop rotations and fertilization on soil organic matter and some
biochemical properties of a thick black Chernozem. Can. J. Soil Sci. 71: 377-387.

CAST. 2004. Climate change and greenhouse gas mitigation: Challenges and
opportunities for agriculture. Council for Agriculture Science and Technology,
Ames, IA p 120.

Curtin D. and Fraser P.M. 2003. Soil organic matter as influenced by straw management
practices and inclusion of grass and clover seed crops in cereal rotations. Aust. J.
Soil Res. 41: 95-106.

Darmody R.G. and Peck T.R. 1997 Soil organic carbon changes through time at the
University of Illinois Morrow Plots. In: Paul E.A., Paustian K., Elliot E.T. and

Cole C.V. (eds), Soil Organic Matter in Temperate Agroecosystems: Long-Term Experiments in North America. CRC Press, New York pp. 161-169.

Follett R.F. and Delgado J.A. 2002. Nitrogen fate and transport in agricultural systems. J. Soil Water Conserv. 57: 402-408.

Gerzabek M.H., Haberhauer G. and Kirchmann H. 2001. Soil organic matter pools and carbon-13 natural abundances in particle-size fractions of a long-term agricultural field experiment receiving organic amendments. Soil Sci. Soc. Am. J. 65: 352-358.

Glaser B., Guggenberger G., Haumaier L. and Zech W. 2001 Persistence of soil organic matter in archaeological soils (Terra Preta) of the Brazilian Amazon region. In: Rees R.M. (ed) Sustainable management of soil organic matter. CABI Pub., New York pp. 190-195.

Grant R.F., Juma N.G., Robertson J.A., Izaurralde R.C. and McGill W.B. 2001. Long-term changes in soil carbon under different fertilizer, manure, and rotation: Testing the mathematical model ecosys with data from the Breton plots (vol 65, pg 205, 2001). Soil Sci. Soc. Am. J. 65: 1872-1872.

Halvorson A.D., Wienhold B.J. and Black A.L. 2002. Tillage, nitrogen, and cropping system effects on soil carbon sequestration. Soil Sci. Soc. Am. J. 66: 906-912.

Hassink J. 1997. The capacity of soils to preserve organic C and N by their association with clay and silt particles. Plant Soil 191: 77-87.

Hassink J. and Whitmore A.P. 1997. A model of the physical protection of organic matter in soils. Soil Sci. Soc. Am. J. 61: 131-139.

Huggins D.R., Buyanovsky G.A., Wagner G.H., Brown J.R., Darmody R.G., Peck T.R., Lesoing G.W., Vanotti M.B. and Bundy L.G. 1998a. Soil organic C in the tallgrass prairie-derived region of the corn belt: effects of long-term crop management. Soil Tillage Res. 47: 219-234.

Huggins D.R., Clapp C.E., Allmaras R.R., Lamb J.A. and Layese M.F. 1998b. Carbon dynamics in corn-soybean sequences as estimated from natural carbon-13 abundance. Soil Sci. Soc. Am. J. 62: 195-203.

Huggins D.R. and Fuchs D.J. 1997 Long-term N management effects on corn yield a soil C of an Aquic Haplustoll in Minnesota. In: Paul E.A., Elliot E.T., K.Paustian and Cole C.V. (eds), Soil Organic Matter in Temperate Agroecosystems: Long-term experiments in North America. CRC Press, Inc, New York pp. 121-128.

Izaurralde R.C., McGill W.B., Robertson J.A., Juma N.G. and Thurston J.J. 2001. Carbon balance of the Breton Classical Plots over half a century. Soil Sci. Soc. Am. J. 65: 431-441.

Jenkinson D.S. 1990. The turnover of organic carbon and nitrogen in soil. Philosophical Transactions of the Royal Society of London Series Biological Sciences 329: 361-368.

Karlen D.L., Wollenhaupt N.C., Erbach D.C., Berry E.C., Swan J.B., Eash N.S. and Jordahl J.L. 1994. Long-Term Tillage Effects on Soil Quality. Soil Tillage Res. 32: 313-327.

Kong A.Y.Y., Six J., Bryant D.C., Denison R.F. and van Kessel C. 2005. The relationship between carbon input, aggregation, and soil organic carbon stabilization in sustainable cropping systems. Soil Sci. Soc. Am. J. 69: 1078-1085.

Mann L. 1986. Changes in soil C storage after cultivation. Soil Sci. 142: 279-288.

McFadgen B.G. 1980. Maori Plaggen soils in New-Zealand, Their origin and properties. J. R. Soc. N. Z. 10: 3-18.

Nyborg M., Solberg E.D., Malhi S.S. and Izaurralde R.C. 1995 Fertilizer N, crop residue, and tillage alter soil C and N content in a decade. In: Lal R., Kimble J., Levine E. and Stewart B.A. (eds), Advances in soil science: Soil Management and Greenhouse Effect. CRC Press Inc., Boca Ration, FL pp. 93-100.

Ogle S.M., Breidt F.J. and Paustian K. 2005. Agricultural management impacts on soil organic carbon storage under moist and dry climatic conditions of temperate and tropical regions. Biogeochemistry: 87-121.

Parton W.J., Schimel D.S., Cole C.V. and Ojima D.S. 1987. Analysis of factors controlling soil organic matter levels in Great Plains grasslands. Soil Sci. Soc. Am. J. 51: 1173-1179.

Parton W.J., Stewart J.W.B. and Cole C.V. 1988. Dynamics of C, N, P and S in grassland soils - a model. Biogeochemistry 5: 109-131.

Paustian K. 1994 Soil biota: management in sustainable farming systems. In: Pankhurst C.E., Doube D.M., Gupta V.V.S.R. and Grace P.R. (eds), Modeling Soil Biology and Biochemical Processes for Sustainable Agriculture Research. CSIRO, Australia pp. 182-193.

Paustian K., Ågren G. and Bosatta E. 1997a Modeling litter quality effects on decomposition and soil organic matter dynamics. In: Giller K. (ed) Driven by Nature: Plant Litter Quality and Decomposition. CAB International, UK pp. 313-336.

Paustian K., Andren O., Janzen H., Lal R., Smith P., Tian G., Tiessen H., van Noordwijk M. and Woomer P. 1997b. Agricultural soil as a C sink to mitigate CO_2 emissions. Soil and Use Management 13: 230-244.

Paustian K., Cole C.V., Sauerbeck D. and Sampson N. 1998. CO_2 mitigation by agriculture: An overview. Clim. Change 40: 135-162.

Paustian K., Collins H.P. and Paul E.A. 1997c Management controls on soil carbon. In: Cole C.V. (ed) Soil Organic Matter in Temperate Agroecosystems: Long-Term Experiments in North America. CRC Press, New York pp. 15-49.

Paustian K., Parton W.J. and Persson J. 1992. Modeling soil organic-matter in organic-amended and nitrogen-fertilized long-term plots. Soil Sci. Soc. Am. J. 56: 476-488.

Plante A.F., Chenu C., Balabane M., Mariotti A. and Right D. 2004. Peroxide oxidation of clay-associated organic matter in a cultivation chronosequence. Eur. J. Soil Sci. 55: 471-478.

Rasmussen P.E. and Albrecht S.L. 1997 Crop management effects on organic carbon in semi-arid Pacific northwest soils. In: Lal R., Kimble J.M., Follett R.F. and Stewart B.A. (eds), Advances in Soil Science: Management of carbon sequestration in soil. CRC Press, Boca Raton, FL pp. 209-219.

Rasmussen P.E. and Collins H.P. 1991. Long-term impacts of tillage, fertilizer, and crop residue on soil organic matter in temperate semiarid regions. Adv. Agron. 45: 93-134.

Reicosky D.C., Evans S.D., Cambardella C.A., Armaras R.R., Wilts A.R. and Huggins D.R. 2002. Continuous corn with moldboard tillage: Residue and fertility effects on soil carbon. J. Soil Water Conserv. 57: 277-284.

Ridley A.M., Helyar K.R. and Slattery W.J. 1990. Soil acidification under subterranean clover (Trifolium-subterraneum L) pastures in North-Eastern Victoria. Aust. J. Exp. Agric. 30: 195-201.

Sherrod L.A., Peterson G.A., Westfall D.G. and Ahuja L.R. 2003. Cropping intensity enhances soil organic carbon and nitrogen in a no-till agroecosystem. Soil Sci. Soc. Am. J. 67: 1533-1543.

Six J., Conant R.T., Paul E.A. and Paustian K. 2002. Stabilization mechanisms of soil organic matter: Implications for C-saturation of soils. Plant Soil 241: 155-176.

Solberg E.D., Nyborg M., Izaurralde R.C., Mahli S.S., Janzen H.H. and Molina-Ayala M. 1997 Carbon storage in soils under continuous cereal grain cropping: N fertilizer and straw. In: Stewart B.A. (ed) Management of carbon sequestration in soil. CRC Press, Boca Raton, FL pp. 235-213.

Soon Y.K. 1998. Crop residue and fertilizer management effects on some biological and chemical properties of a Dark Grey Solod. Can. J. Soil Sci. 78: 707-713.

Springob G., Brinkmann S., Engel N., Kirchmann H. and Bottcher J. 2001. Organic C levels of Ap horizons in North German Pleistocene sands as influenced by climate, texture, and history of land-use. J. Plant Nutr. Soil Sci. 164: 681-690.

Vanotti M.B., Bundy L.G. and Peterson A.E. 1997 Nitrogen fertilizer and legume-cereal rotation effects on soil productivity an organic matter dynamics in Wisconsin. In: Paul E.A., Paustian K., Elliot E.T. and Cole C.V. (eds), Soil Organic Matter in

Temperate Agroecosystems: Long-Term Experiments in North America. CRC

Press, New York pp. 105-119.

CHAPTER 3

SOIL CARBON SATURATION: LINKING CONCEPT AND MEASURABLE CARBON POOLS

Abstract

The soil C saturation concept suggests a limit to C accumulation with increasing steady-state C inputs determined by inherent physicochemical characteristics such as textural, mineralogical, and structural characteristics of the soil. This concept implies an ultimate soil C stabilization capacity comprised of four pools potentially capable of C saturation: non-protected, physically-protected, chemically-protected, and biochemically-protected. Whole soil C saturation has been evaluated and corroborated by experimental data and model analysis of total C in whole soil. However, the behavior of individual C pools has not been examined. We contrasted two scenarios of SOC accumulation in soil fractions: 1) no saturation limit (i.e., linear model), 2) whole-soil C saturation limit (i.e., C saturation model). Our objectives were to theoretically explore C saturation of soil fractions, namely, free POM, microaggregate-associated C, silt and clay associated C and non-hydrolyzable C pools that correspond to the non-protected, physically-, chemically- and biochemically-protected C pools, respectively. We used soils from long-term agroecosystem experiments across the US and Canada. We also assessed the

mechanisms by which C is stabilized in these soils and determined values of fraction C saturation capacity (C_{maxf}) when appropriate. We found support for C saturation in the chemically-protected pool for most sites and in the biochemically-protected pools for some sites. The microaggregate and non-protected C pools exhibited non-saturation, linear dynamics. Soil C saturation behavior was observed in soils from a variety of taxonomies, textures and climates suggesting that the C saturation concept can be generalized and may influence soil C accumulation even at sites that appear to be far from their theoretical C saturation limit.

Introduction

Soil carbon stabilization has been linked to physical soil properties, specifically the amount, reactivity and surface area of clay minerals. Adsorption to silt- and clay-sized particles protect soil organic carbon (SOC) from decomposition and is controlled by the availability of active clay adsorption sites. Studies of pure clays have found a limit to the stabilization of added organic material (Harter & Stotzky 1971; Marshman & Marshall 1981) implying an upper limit to the capacity of soil to protect C by clay adsorption.

Adsorption mechanisms have also been used to describe silt + clay SOC protection within the whole soil. Hassink and Whitmore (1997) explored the influence of soil texture on SOC accumulation by comparing three alternate models of physical protection. Compared to models that incorporated SOC stabilization as a linear function of texture, or microbial efficiency, they found that a model incorporating a finite protective capacity explained the most variance in organic matter additions and losses as

a function of soil clay content. This led them to suggest that C accumulation did not necessarily depend only on the protective capacity (i.e. texture) of the soil, but the degree to which the protective capacity was already occupied by organic matter.

According to Hassink and Whitmore (1997), the capacity of a whole soil to protect C was based solely on the silt + clay protective capacity and that SOC accumulation in excess of the silt + clay protective capacity would be subject to higher rates of decomposition. Hassink et al. (1997) found that the silt + clay fraction of the 0-10 cm layer of their sandy grassland soils contained the same amount of C as their arable counterparts, leading them to conclude that their soils had reached a maximum amount of C associated with the silt and clay fractions. When the protective capacity of the soil had been exceeded, further C additions were not stabilized by the silt + clay fraction and thus C accumulated in the light and intermediate macroorganic matter fractions (> 20 μm) (Hassink et al. 1997). Similar to Hassink and Whitmore (1997), Carter et al. (2003) found that sites near or at silt + clay C capacity level, accumulated C only in the POM fraction.

However, several researchers have proposed that the capacity of the soil to sequester C is based on more than physical protection by silt and clay, being attributable to aggregate protection and biochemical recalcitrance as well. Baldock and Skjemstad (2000) proposed that each mineral matrix had a unique capacity to stabilize organic C depending not only on the presence of mineral surfaces capable of adsorbing organic materials (or a protective capacity), but also the chemical nature of the soil mineral fraction, the presence of cations, and the architecture of the soil matrix. They further suggested that the dispersion technique used by Hassink et al. (1997) destroyed C

protection by aggregate structures and that redistribution of C from POM to silt and clay soil particles would be likely. They could not exclude the possibility that the constant C content of the silt + clay fraction might be an effect of the dispersion methodology rather than saturation of adsorption sites and stressed the importance of linking fractionations that isolated both chemical and architectural properties.

Carter (2002) also proposed a conceptual model that included a variable capacity related to C input, aggregate stability and macro-OM in addition to the silt and clay protective capacity. He related the storage capacity of the soil to specific soil fractions including the association of SOM with silt + clay particles (< 20 µm), microaggregates (20-250 µm), macroaggregates (>250 µm), and sand-sized macro-OM. As SOC concentration increased, C associated with clay and silt would reach the protective capacity of the soil, but further C accumulation would occur in aggregate structures and macro-OM as a function of soil type and C inputs (i.e. management).

The whole soil C saturation concept proposed by Six et al. (2002) included not only a silt + clay protected pool (Hassink and Whitmore 1997, Carter 2002), but a microaggregate protected pool and a biochemically-protected pool and a non-protected pool (Figure 1). Biochemical SOM protection occurs through the biochemical recalcitrance of its structure has low biological availability. The fourth, non-protected C pool, limited by the steady-state balance of C inputs and decomposition dictated by climate. Although they suggest that this fraction is saturatable, they postulate no mechanism behind this occurrence. Each of the conceptual pools could be isolated by a simple three-step fractionation procedure using physical, chemical, and density fraction methods.
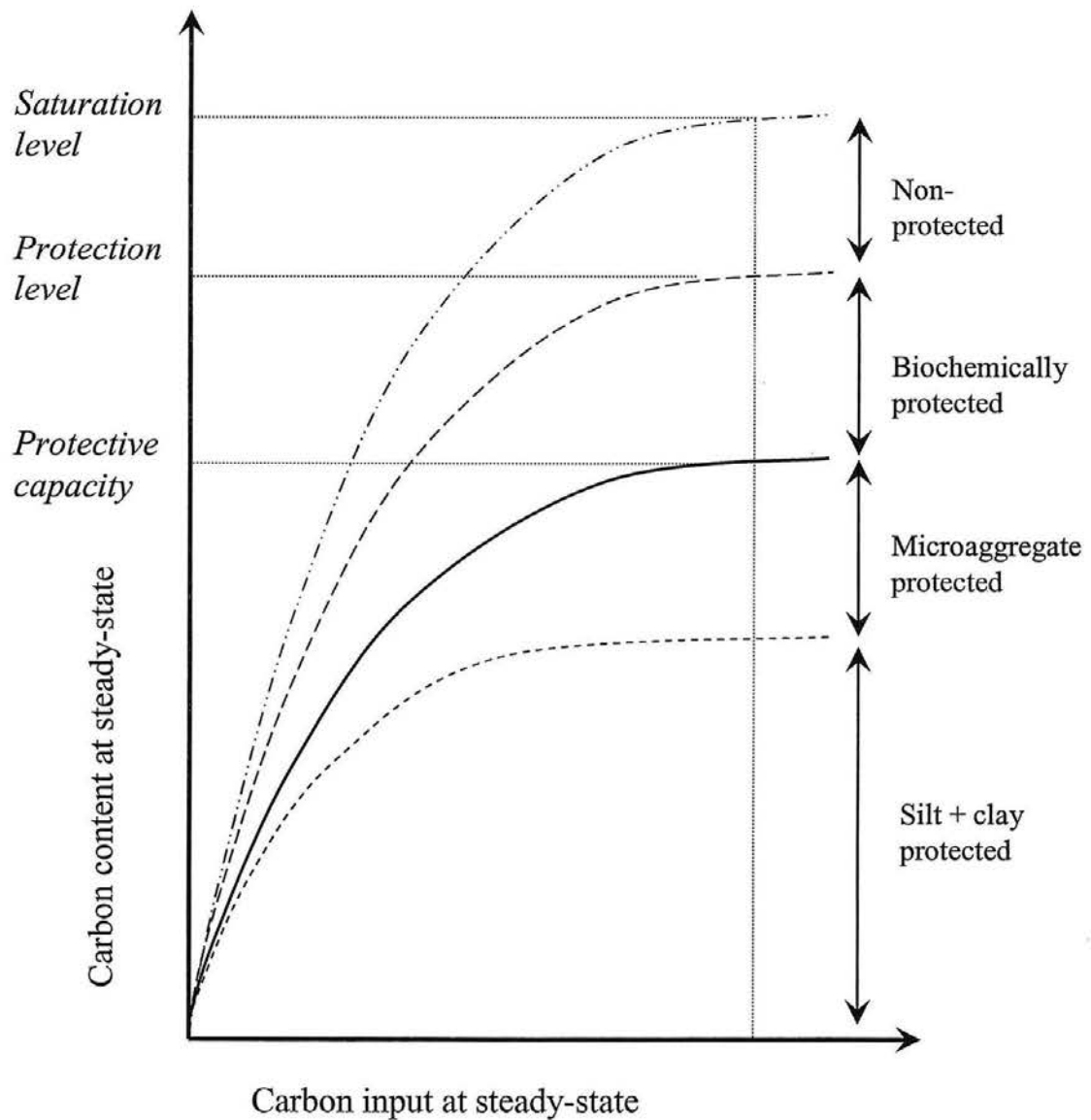
Figure 1: Soil C saturation concept for the whole soil comprised of four conceptual C pools. Modified from Six et al. 2002.

Theoretically, whole-soil C saturation is comprised of the cumulative behavior by each of the four soils C pools.

Although there is some evidence of C saturation behavior in whole soil (Six et al 2002, Chapter 2), more robust generalizations are difficult, due to the lack of experimental data and potentially confounding factors in combined site analyses. Examination of isolated soil fractions for C saturation behavior has yielded evidence for a

silt + clay protective capacity (e.g. Hassink 1997; Carter et al. 2003). Others mechanisms of soil C saturation including aggregation and biochemical protection have yet to be examined (Baldock & Skjemstad 2000). Our objectives were to: 1) to isolate soil fractions which correspond to the non-protected, and physically-, chemically- and biochemically-protected C pools proposed by Six et al. (2002) from soils of long-term agroecosystem experiments across the US and Canada, and 2) to quantify the relative explanatory power of a linear versus C saturation model, given our data. We also assess the mechanisms by which C is stabilized in these soils and determine values of C saturation capacity (C_{maxf}) when appropriate. We hypothesized that the chemically-protected pool, the aggregate-protected pool, and the biochemically-protected pool would exhibit C saturation dynamics due to physicochemical limitations. Carbon saturation dynamics should also occur in the non-protected pool, not as a function of physical limitation, but rather because of the balance between C inputs and decomposition.

Materials & Methods

Field sampling

Soils were sampled between 2002 and 2004 from several long-term agroecosystem experiments comparing conventional tillage to no-till treatments (Table 1). Some of the long-term experiments included crop rotation treatments too. Samples were also taken from adjacent "native" soil at each site that had never been in agricultural production. Surface cores (0-20 cm) were taken and separated into 0-5 cm and 5-20 cm depth increments in the field. Soils were packaged to remain cool and

73

Table 1 Site characteristics of the eight sites we sampled for this analysis. Treatment abbreviations: No tillage (NT), conventional-tillage (CT), native grassland (NG), no straw (NS)

Site	Location	Soil Type	Treatments	% Sand	% Silt	% Clay	Whole SOC† Range
Akron, CO	40° 09' N, 103° 09' W	Aridic Paleustoll	NG NT wheat-fallow CT wheat-fallow NT soybean	32	41	27	0.60-2.40
Lexington, KY	38° 07' N, 84° 29' W	Typic Paleudalf	NG, NT, CT	5	68	27	1.10-3.32
Hoytville, OH	41° 00' N, 84° 00' W	Mollic Ochraqualf	Native forest NT soybean CT soybean NT oats CT oats	19	39	42	1.67-7.45
Breton, AB, Canada	53° 07' N, 114° 28' W	Typic Cryoboralf	Native forest NT NS No Nitrogen CT NS No Nitrogen NT Straw Nitrogen CT Straw Nitrogen	31	39	30	0.60-7.22
Swift Current, SK, Canada	50° 17' N, 107° 48' W	Aridic Haploboroll	NG, NT, CT	26	47	27	1.16-4.24
Scott, SK, Canada	52° 22' N, 108° 50' W	Typic Borroll	NG, NT, CT	28	44	28	1.50-9.26
Stewart Valley, SK, Canada	50° 17' N, 107° 48' W	Aridic Haploboroll	NG, NT, CT	20	35	45	1.20-4.26
Watkinsville, GA	33° 54' N, 83° 24' W	Typic Kanhapludult	NG, NT, CT	69	12	19	0.48-3.24

† Units expressed as g C 100 g^{-1} whole soil.

uncompacted during transport to the laboratory. In the laboratory, large rocks, recognizable surface litter, and root material were removed as samples were gently broken by hand and passed through an 8-mm sieve. Soil cores were then composited by field replicate, air-dried, passed through a 2-mm sieve, and stored at room temperature until further analysis.

Soil texture was determined using a modified version of the standard hydrometer method without removal of carbonates or organic matter (Gee & Bauder 1986) on a 30 g subsample dispersed by shaking the soil for 18 hours in 100 mL of 5g L^{-1} sodium-hexametaphosphate solution. Total sand contents were determined by sieving (53 μm) and clay contents were measured by the two hour hydrometer method. Silt contents were determined by difference.

Soil fractionation

Separation of the various C pools was accomplished by a combination of physical and chemical fractionation techniques in a simple, three-step process (Figure 2) detailed by Plante et al. (2006b). The first step was the partial dispersion and physical fractionation of the soil to obtain three size fractions: > 250 μm (coarse non-protected particulate organic matter, **cPOM**), 53-250 μm (microaggregate fraction, **μagg**), and < 53 μm (easily dispersed silt and clay, **dSilt** and **dClay**). Physical fractionation was accomplished by fractionating air-dried 2 mm sieved soil in the microaggregate isolator described by Six et al. (2000). The microaggregate isolator dispersed the > 2 mm soil with 50 glass beads in running water over a 250 μm sieve so that microaggregates and finer particles are flushed through the 250 μm mesh screen. Material > 250 μm (cPOM)

plus sand, remained on the sieve. Microaggregates were collected on a 53 μm sieve that is subsequently wet sieved by hand for 50 strokes in 2 minutes (Elliott 1986) to separate the easily dispersed silt- and clay-sized fractions from the water-stable microaggregates. The resulting suspension was centrifuged to separate the easily dispersed silt- and clay-sized fractions. Fractions were oven-dried (60°C) and weighed.
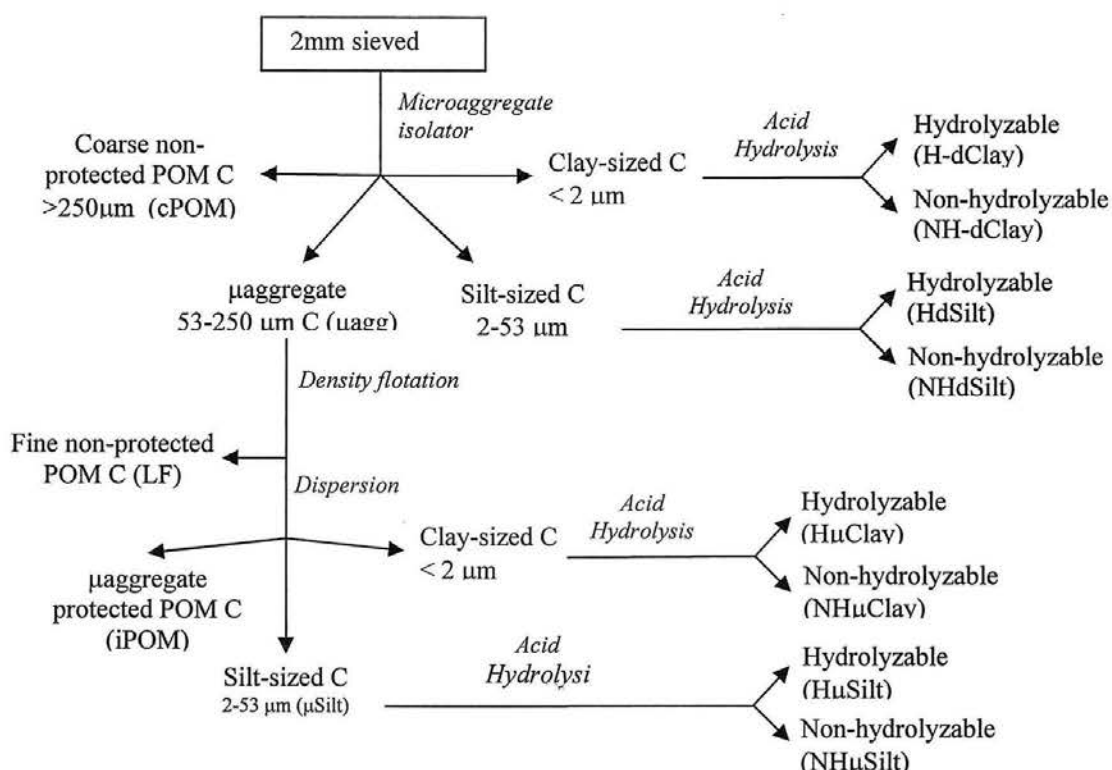
Figure 2: A three-step soil fraction scheme to isolate the C pools based on physical, chemical and biochemical protection mechanisms. Modified from Six et al. (2002).

The second step involved further fractionation of the microaggregate fraction isolated in the first step (Six et al. 2001, Plante et al 2006b). Density flotation using 1.85 g cm^{-3} sodium polytungstate (SPT) was used to isolate fine non-protected POM (**LF**). After removing the fine non-protected POM, the heavy fraction was dispersed overnight by shaking with 12 glass beads and passed through a 53 μm sieve, separating the

microaggregate protected POM (>53 μm in size, **iPOM**) and the microaggregate derived silt- and clay-sized fractions (**μSilt** and **μClay**).

The third step involved the acid hydrolysis of each of the isolated silt- and clay-sized fractions. The silt- and clay-fractions from both the density floatation (μSilt and μClay) and the initial dispersion and physical fractionation (dSilt and dClay) were subjected to acid hydrolysis as described in Plante et al. (2006a). Acid hydrolysis consisted of refluxing at 95°C for 16 h in 25 ml of 6 M HCl. After refluxing, the suspension was filtered and washed with deionized water over a glass-fiber filter. Residues were oven-dried at 60°C, weighed and analyzed for organic C content. These represented the non-hydrolyzable C fractions (**NH-dSilt, NH-dClay, NH-μSilt** and **NH-μClay**). The hydrolyzable C fractions (**H-dSilt, H-dClay, H-μSilt** and **H-μClay**) were determined by difference between the total organic C content of the fractions and the C contents of the non-hydrolyzable fractions.

This three-step process isolates a total of sixteen fractions of C, some of which are composites of others (e.g., μagg is composed of LF, iPOM, μSilt and μClay, and the latter two are each composed of hydrolyzable and non-hydrolyzable portions). This fractionation scheme is based on the assumed link between the isolated fractions and the protection mechanisms involved in the stabilization of organic C within that pool and is described in detail by Six et al. (2002). The non-protected C pool consists of the coarse particulate organic matter fraction (cPOM) isolated during the first dispersion step, and the fine non-protected POM fraction (LF) isolated during the second fractionation step. The physically-protected C pool consists of the microaggregate (μagg) fraction as a whole and the particulate organic matter occluded within it (iPOM). The chemically-

protected pool corresponds to the hydrolyzable portion of the silt- and clay-sized fractions isolated during the initial dispersion (H-dSilt and H-dClay). Carbon is stabilized in these fractions through mineral-organic matter bindings, dictated by both texture and mineralogy of the soil. The biochemically-protected pool corresponds to the non-hydrolyzable C remaining in the silt and clay fractions after acid hydrolysis (NH-dSilt and NH-dClay).

Due to the step-wise fractionation procedure, some isolated fractions represent more than a single C protection mechanism, or C pool. The microaggregate-derived non-hydrolyzable fractions (NH-μSilt and NH-μClay) represent both the biochemical and physical protection mechanisms. Similarly, the hydrolyzable microaggregate-derived silt and clay fractions (H-μSilt and H-μClay) capture both the chemical and physical protection mechanisms. The μSilt and μClay fractions represent a composite of the physical, biochemical and chemical protection mechanisms.

Carbon Analyses

Carbon contents for all fractions except fine non-protected POM were measured using a LECO CHN-1000 analyzer (Leco Corp., St. Joseph, MI). Fine non-protected POM was measured on a Carlo Erba NA 1500 CN analyzer due to smaller sample size. Soil carbonates were determined by a modified pressure transducer method described by Sherrod et al. (2002).

Theory underlying models

In Chapter 2, I modeled the relationship between whole soil C and C inputs using three simple models of SOC accumulation: 1) a single pool model that assuming no C saturation limit (i.e., a linear response of steady-state SOC as a function of C inputs); (2) a single pool model assuming whole-soil C saturation (i.e., asymptotic steady-state SOC as a function of C inputs), and a model with two pools representative of each of the previous models (i.e., a mixed model with both linear and asymptotic dynamics). We apply and there describe only the steady-state solution of first two models here.

The linear model assumed that residue C transformed into SOC was independent of pool size and that decomposition rates are directly proportional to the pool size. At steady-state,

$$C_t^* = \frac{I^*}{k} + R \tag{1}$$

SOC content (C_t^*) is directly proportional to C inputs (I^*) where (k) is the specific decay constant. An intercept term (R) was added to the linear model in Equation 1 to account for the residual SOC that is not affected over the course of an agroecosystem experiment.

In the C saturation model, soil organic C accumulation was limited by saturation deficit (sd), or how far from C saturation (C_m) a soil is:

$$sd = 1 - \frac{C_t^*}{C_m} \tag{2}$$

Consequently, at steady-state, the SOC concentration (C_t^*), an asymptotic relationship between C inputs (I^*) and SOC is observed:

$$C_t^* = \frac{I^*}{k + \frac{I^*}{C_m}} \tag{3}$$

Direct corollaries of this asymptotic relationship are that 1) the further a soil is from saturation (i.e., the greater the saturation deficit), the greater its capacity to stabilize added C, and 2) as a soil approaches whole soil saturation (C_m), the rate and amount of SOC accumulation decreases due to a smaller saturation deficit.

We could not use C inputs as the independent variable in an analysis of fraction C because it is impossible to know C inputs for individual soil fractions. Due to the differing rates of decomposition and subsequent incorporation of C input into various C pools, those with slow turnover times do not reflect influences from field level treatments over shorter time scales. If we were to examine fraction C with C inputs as the independent variable, differences in decomposition as a result of field treatments (i.e. tillage) would produce varying levels of whole SOC, confounding the relationship of fraction C and C inputs. Therefore, when examining soil fractions, it is crucial to express soil fraction C across a normalized scale. Whole-soil SOC content, as a balance between C input and decomposition would normalize across treatments and be a more appropriate measure of C accumulation. We demonstrate with the following derivation that the principles of C saturation may be observed using SOC as an analog for C input.

To verify that the C saturation concept may be expressed for individual C fractions using total SOC as the independent variable, we constructed two hypothetical model scenarios in which the whole soil is comprised of two pools (e.g. active and passive) which either have 1) linear C accumulation as a function of C inputs or 2) asymptotic C accumulation as a function of C inputs in accordance with the C saturation concept. Using these two hypothetical cases, we explore the relationship of the first

carbon pool and total SOC content to see whether C saturation can be expressed with total SOC as the independent variable.

In the linear case, we assumed a model comprised of two fractions (C_1 and C_2) with steady-state solutions of;

$$C_1^* = \frac{I^* * p_1}{k_1} \tag{5}$$

$$C_2^* = \frac{I^* * p_2}{k_2} \tag{6}$$

$$C_t^* = C_1^* + C_2^* \tag{7}$$

where p_1 and p_2 are the proportion of C input partitioned to pools C_1^* and C_2^*, and k_1 and k_2 are the decomposition rates of each pool, respectively. We then isolated I^* in equation 5; substituted the right hand side of equation 6 for C_2^* in equation 7; and then substituted the solution of I^*. We then solved equation 7 in terms of C_1^* and obtained

$$C_1^* = C_t^* \frac{p_1 k_2}{p_1 k_2 + p_2 k_1} \tag{8}$$

where fraction C in C_1 is a linear function of whole SOC content.

In the C-saturation case, the total SOC (C_t^*) was comprised of two fractions (C_1^* and C_2^*) each with hyperbolic steady-state C-saturation dynamics in the form of eq. 3 above. The two pools were:

$$C_1^* = \frac{I^* p_1}{k_1 + \frac{I^*}{C_{m1}}} \tag{9}$$

$$C_2^* = \frac{I^* p_2}{k_2 + \frac{I^*}{C_{m2}}} \tag{10}$$

81

where p_1 and p_2 are the proportion of C input partitioned to pools $C_1{}^*$ and $C_2{}^*$, and k_1 and k_2 are the decomposition rates of each pool, and C_{m1} and C_{m2} their saturation limits, respectively. We then isolated I^* in equation 5; substituted the right hand side of equation 6 for $C_2{}^*$ in equation 7; and then substituted the solution of I^*. We then solved equation 7 in terms of $C_1{}^*$ and obtained

$$C_1^* = \frac{C_t(k_2 p_1 Cm_2 - k_1 p_1 Cm_2) + (k_2 p_1 Cm_1 Cm_2 + k_1 p_2 Cm_1 Cm_2) \pm \sqrt{\begin{array}{l} C_t^2(k_2 p_1 Cm_2 - k_1 p_1 Cm_2)^2 - 2C_t(k_2^2 p_1^2 Cm_1 Cm_2^2 \\ - k_2 p_1 Cm_2^2 k_1 p_2 Cm_1 - k_1 p_2 Cm_1^2 k_2 p_1 Cm_2 + k_1^2 Cm_1^2 p_2^2 Cm_2) \\ + (k_2 p_1 Cm_1 Cm_2 + k_1 p_2 Cm_1 Cm_2)^2 \end{array}}}{2(k_2 p_1 Cm_2 - k_1 p_1 Cm_2)} \tag{11}$$

which, by grouping constants (represented by α, β, and δ) may be simplified to:

$$C_1^* = \frac{\alpha C_t + \beta \pm \sqrt{\alpha^2 C_t^2 - \delta C_t + \beta^2}}{2\alpha} \tag{12}$$

There are two solutions to this equation, one negative and one positive. The negative root produces an asymptote for $C_1{}^*$, $\dfrac{\beta - \dfrac{\delta}{2}}{\alpha}$ as $C_t{}^*$ goes to infinity or

$$\frac{\left(\begin{array}{l} (k_2 f_1 Cm_1 Cm_2 + k_1 f_2 Cm_1 Cm_2) - k_2^2 f_1^2 Cm_1 Cm_2^2 + k_2 f_1 Cm_2^2 k_1 f_2 Cm_1 \\ + k_1 f_2 Cm_1^2 k_2 f_1 Cm_2 - k_1^2 Cm_1^2 f_2^2 Cm_2 \end{array} \right)}{(k_2 f_1 Cm_2 - k_1 f_1 Cm_2)}$$

Although the solution is complex, a simple two-pool model following C saturation dynamics of the whole-soil demonstrates asymptotic behavior when expressed as fraction of C content over whole SOC content.

In this theoretical exercise, we have demonstrated that simple two pool models exhibiting either linear or C saturation dynamics as a function of C inputs in the whole soil produce either linear or asymptotic behavior when expressed as a function of fraction

C content over increasing whole SOC content. Therefore a measured soil fraction exhibiting linear dynamics is not influenced by C saturation, while a fraction exhibiting curvilinear or asymptotic dynamics is influenced by C saturation when expressed over whole SOC content.

Having derived the theoretical relationship between fraction C and whole SOC content, our next objective was to evaluate the fractions at our sites for either linear or C saturation dynamics. Due to the complexity in the linear and the C-saturation solutions in terms of C_l, it would be impossible to use equation 12 to evaluate fraction C as a function of whole SOC content because there are too many parameters with unknown values. However, simple linear and hyperbolic equations may be substituted instead to obtain general fit of the data.

The two simple models we use to describe fraction behavior over increasing SOC content are the linear case:

$$C_f^* = aC_t^* + b \tag{13}$$

and the C saturation case:

$$C_f^* = \frac{C_t^*}{k_f + \frac{C_t^*}{C_{\text{max}f}}} \tag{14}$$

where C_f^* is the C content of the fraction as a function of the whole SOC content (C_t^*) at steady-state. In the linear case (Equation 13), a and b control the slope and intercept. In the saturated case (Equation 14), $C_{\text{max}f}$ is the C saturation limit of the fraction and k_f controls the rate at which saturation is achieved. Additionally, the simple hyperbolic equation allows an explicit estimate of $C_{\text{max}f}$, or fraction C saturation limit.

83

The linear and C-saturation models were fit using PROC REG and PROC NLIN in SAS/STAT (SAS Institute, Cary NC). The criterion for model fit was r^2 values calculated for both using corrected sum of squares. Parameter estimates for C_{maxf} were compared using confidence limits of the estimates from PROC NLIN, as multiple model fits for each site were unavailable. Differences between C_{maxf} were considered significantly different if their confidence limit did not overlap.

Results

Individual Sites

Generally, our sites had a small range of SOC contents (Table 1). Differences between the highest and lowest SOC levels were less than 4 g C 100 g^{-1} soil at five sites. The site that had the broadest range of whole SOC content (Scott, SK, 1.5 – 9.26 g C 100 g^{-1} soil) fit the majority of fractions with the C saturation model. We used Scott, SK, to test C saturation dynamics without confounding factors such as texture and mineralogy, as well as compare estimates of SOC storage capacity (C_{maxf}) between fractions.

The fraction data comprising the chemically-protected pool (H-dSilt and H-dClay fractions) were mainly fit with the C saturation model (Table 2). The H-dSilt fraction data was best fit with the C saturation model at seven sites. At five sites, the H-dClay data was best fit with the C saturation model and three sites with the linear model. At Scott, SK, both the H-dSilt and H-dClay fraction data were best fit with the C saturation model (Table 3, Figure 3). The estimate of saturation level (C_{maxf}) at Scott, SK was significantly greater for the H-dClay compared to the H-dSilt fraction (i.e. 4.87 versus

84

2.11 g fraction C 100 g^{-1} whole soil C).

The results for the biochemical pool (NH-dSilt and NH-dClay fractions) were mixed. Four sites demonstrated best fits with the C saturation model for both the NH-dSilt and NH-dClay fractions and the other four sites in both fractions were best fit with the linear model. At the Scott, SK site specifically, the NH-dSilt and NH-dClay fraction data were best fit with the C saturation model (Table 3 and Figure 4), and as in the chemically protected pool, the C_{maxf} estimate was significantly greater for NH-dClay than that of the NH-dSilt (i.e. 6.00 versus 3.35 g fraction C 100 g^{-1} whole soil C).
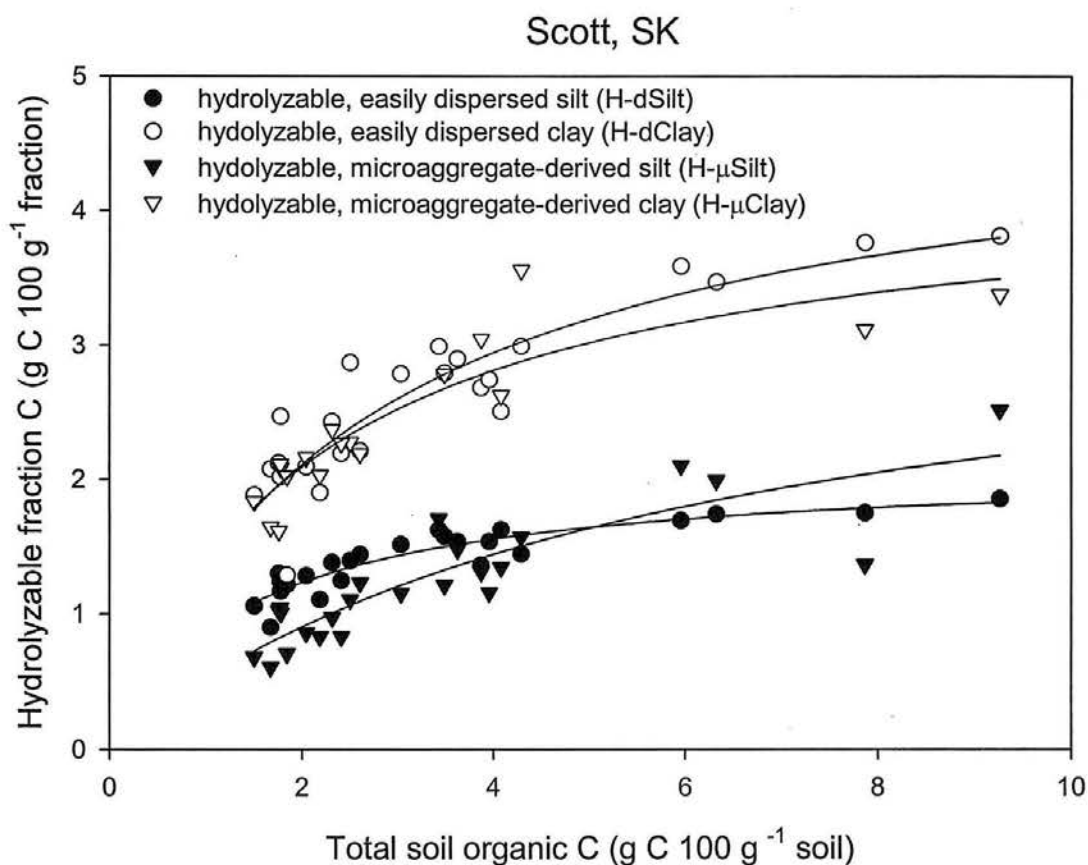
Figure 3: Organic C content of the chemically protected pools isolated from the easily dispersed (H-dSilt, H-dClay) and microaggregate derived (H-µSilt, H-µClay) fractions from Scott, SK samples. Lines represent the best fit C saturation model for each fraction.

Table 2: Number of sites out of eight for which the relationship between whole-soil OC and fraction OC concentrations are best fit by the linear or C saturation models based on r^2.

SOC Pool	Isolated fraction	Linear model best fit	C saturation model best fit
Non-protected	cPOM	8	0
	LF	6	2
Physical	µagg	7	1
	iPOM	8	0
Chemical	H-dSilt	1	7
	H-dClay	3	5
Biochemical	NH-dSilt	4	4
	NH-dClay	4	4
Chemical × biochemical	dSilt	3	5
	dClay	3	5
Physical × biochemical	NH-µSilt	4	4
	NH-µClay	5	3
Physical × chemical	H-µSilt	3	5
	H-µClay	4	4
Physical × chemical × biochemical	µSilt	5	3
	µClay	5	3

Table 3: Best fitting model for the relationship between whole-soil OC and fraction OC concentrations for each isolated fraction from the Scott, SK samples based on r^2 value. Differences between estimates of C_{maxf} were considered significantly different if their confidence limit did not overlap. Linear models have no estimate of C_{maxf}.

SOC Pool	Isolated fraction	Best fitting model	C_{maxf} estimate $\pm$ standard error[†]
Non-protected	cPOM	Linear	n/a
	LF	Linear	n/a
Physical	µagg	Linear	n/a
	iPOM	Linear	n/a
Chemical	H-dSilt	C saturation	2.11 ± 0.09
	H-dClay	C saturation	4.87 ± 0.38
Biochemical	NH-dSilt	C saturation	3.35 ± 0.44
	NH-dClay	C saturation	6.00 ± 0.59
Chemical × biochemical	dSilt	C saturation	5.34 ± 0.35
	dClay	C saturation	10.89 ± 0.51
Physical × biochemical	NH-µSilt	C saturation	5.52 ± 0.72
	NH-µClay	C saturation	4.53 ± 0.62
Physical × chemical	H-µSilt	C saturation	3.56 ± 0.64
	H-µClay	C saturation	4.29 ± 0.32
Physical × chemical × biochemical	µSilt	C saturation	9.04 ± 1.03
	µClay	C saturation	9.15 ± 0.78

† Units expressed as g fraction C 100 g^{-1} whole soil C.

Figure 4: Organic C content of the biochemically-protected pools isolated from easily dispersed (NH-dSilt, NH-dClay) and microaggregate-derived (NH-μSilt, NH-μClay) fractions from Scott, SK samples. Lines represent the best fit C saturation model for each fraction.

Scott, SK

Legend:
- ● non-hydrolyzable, easily dispersed silt (NH-dSilt)
- ○ non-hydolyzable, easily dispersed clay (NH-dClay)
- ▼ non-hydolyzable, microaggregate-derived silt (NH-μClay)
- ▽ non-hydolyzable, microaggregate-derived clay (NH-μClay)

y-axis: Non-hydrolyzable fraction C (g C 100 g^{-1} fraction)
x-axis: Total soil organic C (g C 100 g^{-1} soil)
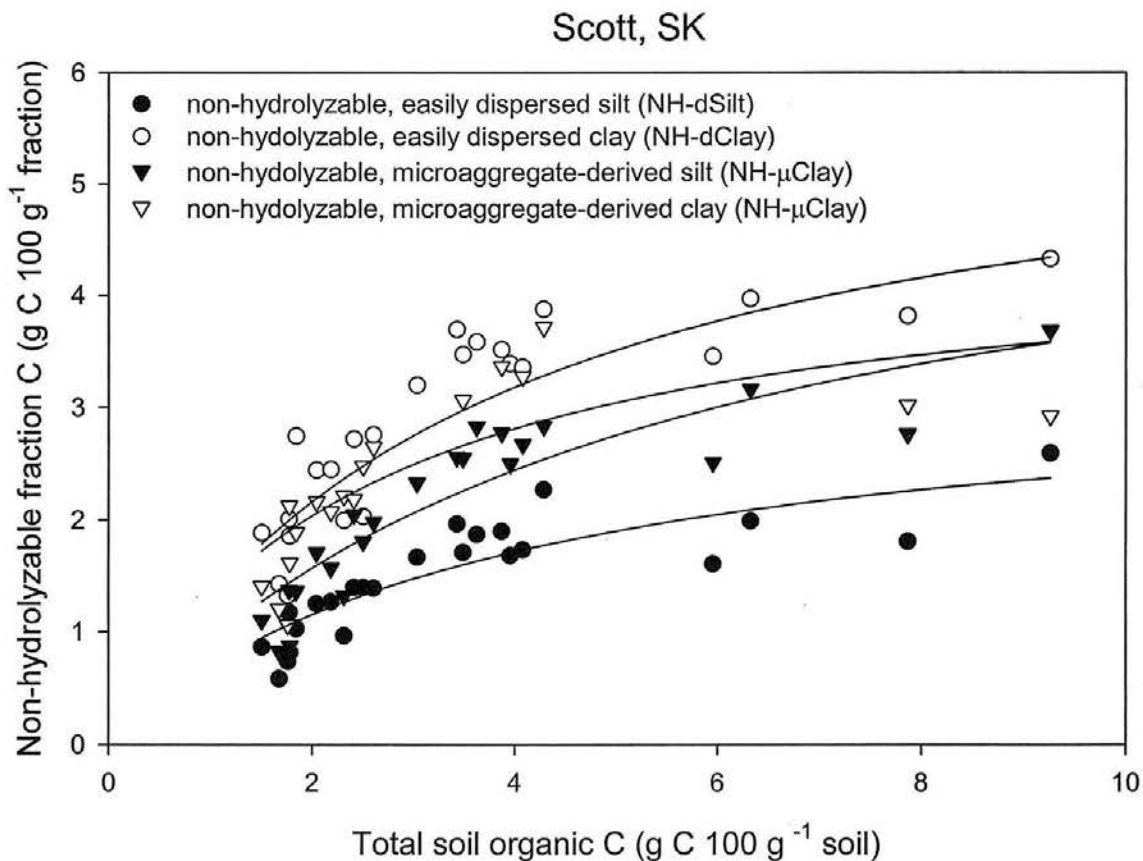
In contrast to the results of the chemical and biochemical pools, the model fits for the physically-protected pool (μagg and iPOM fractions) were mostly linear (Table 2). Seven sites demonstrated linear model fits for the μagg fraction data and the other site was fit with the C saturation model. Although the majority of the fractions were fit by the linear model, the differences between the linear and C-saturation models were small (< 1.3 × r^2, Appendix 1) and the parameter estimates for this fraction unrealistically large (Appendix 2). The iPOM fraction data were fit by the linear model for each site (Table

88

2). At Scott, SK, both the µagg and iPOM fraction data were best fit with the linear model (Table 3 and Figure 5c).

Similar to the physically-protected pool, the fraction data comprising the non-protected pool (cPOM and LF fractions) were best fit primarily with linear models (Table 2). The cPOM fraction data from all eight sites were best fit with the linear model, while the LF data from six sites were best fit with the linear model and two sites with the C saturation model. The LF data from the two sites fit with the C saturation model had negative values for k, producing a decreasing relationship rather than an increasing hyperbolic curve. The linear dynamics of the non-protected pool are exemplified by the Scott, SK site (Figure 5a and 5b).

The model fits of the chemical × biochemical pool (dSilt and dClay fractions) were similar to the results of the individual pools themselves, with the majority of best fit models being with the C saturation model (Table 2). In both the dSilt and dClay fraction data, five sites, including Scott, SK (Table 3) were fit with the C saturation model, while three sites had a linear model fit. Estimates of C_{maxf} at Scott, SK for the dClay fraction were significantly greater than that of the dSilt fraction (i.e. 10.89 versus 5.34 g fraction C 100 g^{-1} whole soil C).

The results for the physical × biochemical pool (NH-µSilt and NH-µClay fractions) were mixed. The NH–µSilt was evenly split with four sites fit with C saturation model and the other four with the linear model. Five sites in the NH-µClay fraction were fit with the linear model and three with the C saturation model. Data for the two fractions from the Scott, SK site were fit with the C saturation models (Table 3), and estimates of C_{maxf} for NH-µSilt and NH-µClay did not significantly differ.

89

Figure 5: Organic C content of the non-protected (cPOM, LF) and physically-protected (iPOM) pools isolated from Scott, SK samples. Lines represent the best fit linear model for each fraction.
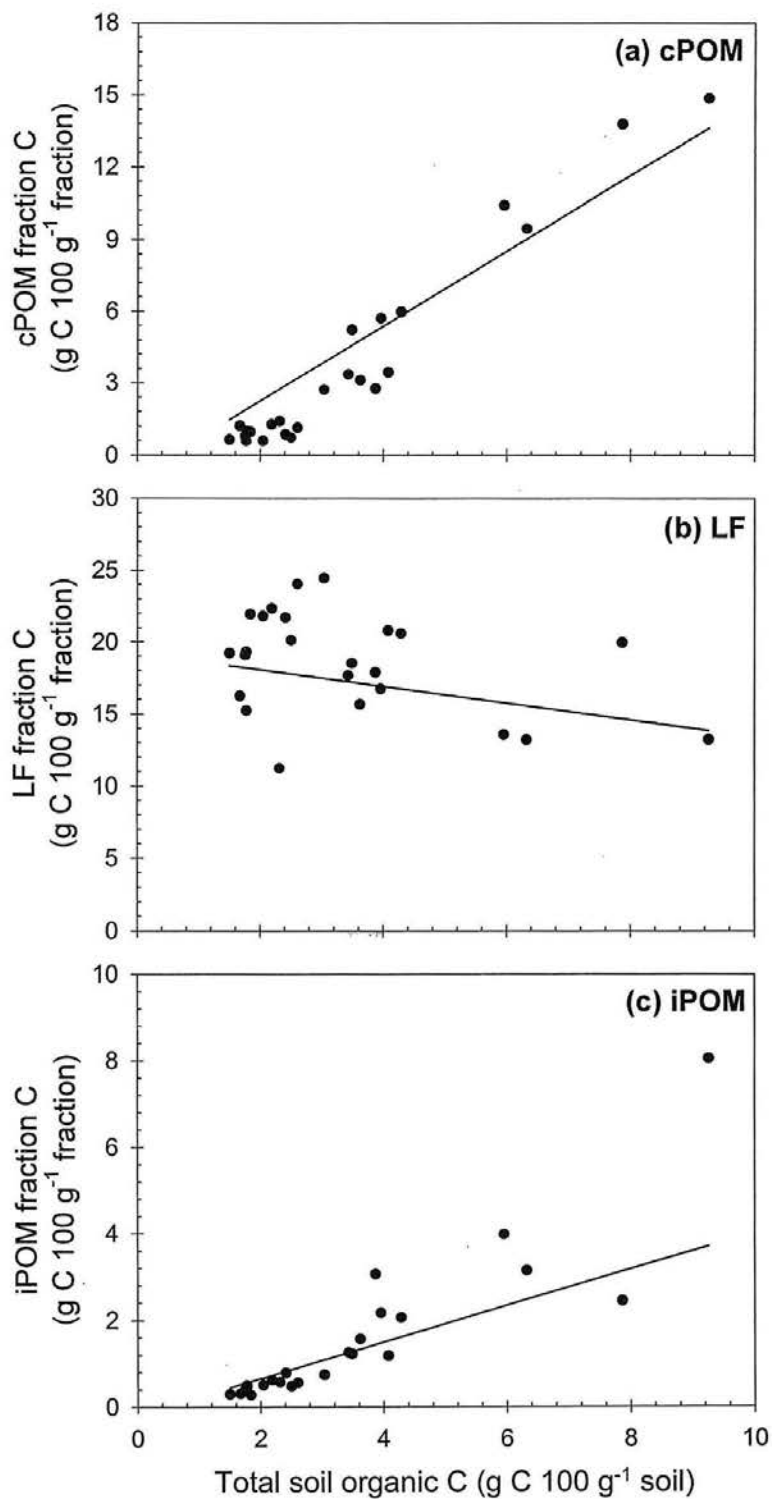
The physical × chemical pool (H-μSilt and H-μClay fractions) results were also mixed. Five sites' H-μSilt fraction was fit with the C saturation model while the other three were linear. In the H-μClay fraction, four sites were fit with the C saturation model and four with the linear model. At the Scott, SK site, H-μSilt and H-μClay fraction data were best fit with the C saturation model (Table 3), and estimates of saturation level (C_m) for H-μSilt and H-μClay did not significantly differ.

In the physical × chemical × biochemical pool (μSilt and μClay fractions), just over half the sites' fraction data were fit with the C saturation model. The other three were fit with the linear model. Similar to the results for the individual fractions at Scott, SK, both the μSilt and μClay fractions were fit with the C saturation model. However, the estimates of C_{maxf} for μClay and μSilt did not differ.

Finally, we compared the effect of aggregation on estimates of C_{maxf} for the silt and clay- sized particles at Scott, SK. Physical protection did not influence C_{maxf} of the clay-size particles (H-dClay vs. H-μClay) but the C_{maxf} of H-μSilt was significantly greater than H-dSilt (Figure 4). The NH-μSilt fraction had a significantly greater C_{maxf} than the NH-dSilt, but there was no significant difference between estimated C_{maxf}s between the NH-μClay and NH-dClay fractions (Figure 5).

All site data combined

Overall, six fractions of the combined site data were best fit with the linear model and ten were best fit by the C saturation model (Table 4). The chemically-protected pool and interactions with other pools (chemical × biochemical, physical × chemical, and physical × chemical × biochemical pools) were best fit by the C saturation model. This is

consistent with the majority of model fits at individual sites. The estimate of C_{maxf} was significantly greater in the H-dClay and dClay compared to the H-dSilt and dSilt fractions, respectively. However, the H-μSilt and μSilt fractions had a greater estimate of C_{maxf} than the H-μClay and μClay fractions, although not significant.

The non-protected, biochemical and the physical × biochemical pools were all fit with the linear model. The linear fit of the NH-dSilt fraction was contrary to the results from Scott, SK where the data were fit by the C saturation model, but mirrored the mixed results of the individual site analysis, where the model fits were split between linear and C saturation (Table 4).

Discussion

We have shown that the whole soil C saturation relationship between C input and SOC may be expressed mathematically yielding linear and hyperbolic relationships when expressed as soil fraction C as a function of whole SOC. Soil fractions expressing linear dynamics of C accumulation as whole SOC increases are not subject to C saturation, while those that express a curvilinear or asymptotic relationship to increasing whole SOC do express C saturation dynamics. This mathematical relationship explicitly links the theory of C saturation to measurable C pools as a function of whole SOC content.

Additionally, the expression of individual fraction C concentration as a function of increasing whole SOC concentration accounts for differences in both C input as well as differing rates of decomposition in management treatments and allows us to examine the stabilization of C within fractions as whole SOC increases. We acknowledge the limitations to this analysis imposed by using soils from different environments and with

92

Table 4: Best fitting models for the relationship between whole-soil OC and fraction OC concentrations for each isolated fraction with all site data combined. Linear models have no estimate of C_{maxf}.

SOC Pool	Isolated fraction	Best fitting model	C_{maxf} estimate ± standard error[†]
Non-protected	cPOM	Linear	n/a
	LF	n/a[*]	n/a
Physical	μagg	C saturation	45.87 ± 11.69
	iPOM	C saturation	8.45 ± 3.84
Chemical	H-dSilt	C saturation	3.30 ± 0.30
	H-dClay	C saturation	5.21 ± 0.43
Biochemical	NH-dSilt	Linear	n/a
	NH-dClay	Linear	n/a
Chemical × biochemical	dSilt	C saturation	10.46 ± 1.15
	dClay	C saturation	14.09 ± 1.37
Physical × biochemical	NH-μSilt	Linear	n/a
	NH-μClay	Linear	n/a
Physical × chemical	H-μSilt	C saturation	4.17 ± 0.60
	H-μClay	C saturation	3.86 ± 0.46
Physical × chemical × biochemical	μSilt	C saturation	17.34 ± 2.20
	μClay	C saturation	14.80 ± 2.03

* Due to the significant relationship between decomposition constant (k) (estimated from the linear model fit) and average SOC content (C_t), we do not report the model fit for the LF due to possible confounding factors of the analysis. † Units expressed as g fraction C 100 g^{-1} whole soil C.

different experimental durations, which will vary in their approximation of steady-state conditions. However, this expression of fraction C capacity was suggested by Carter (2002) for a Charlottetown fine sandy loam and we believe it to be the best way to examine C saturation dynamics within soil fractions.

Chemically-protected pool

The C saturation best fit models in the majority of the chemically-protected fractions (H-dClay and H-dSilt) in both individual and combined site data sets supports the concept of an ultimate limit to C storage associated with these fractions. These results support previous work on the limits to the silt + clay protective capacity for soil C sequestration (Hassink 1997; Six et al. 2002; Carter et al. 2003; Jolivet et al. 2003), but also illustrate distinct C saturation dynamics for the silt-sized versus clay-sized fractions.

Our estimates of clay saturation from the best fit models at individual sites range from 28.5 to 690.9 g C kg^{-1} clay and overlap to greatly exceed other estimates from tropical systems of 48.8 g C kg^{-1} clay (Diekow et al. 2005) and 32.5g C g kg^{-1} clay (Roscoe et al. 2001). It is important to note, however, that the properties and behavior of clay-sized fractions differ because of their method of isolation. To compare estimates made by Diekow et al. (2005) and Roscoe et al. (2001) using complete dispersion of the soil by sonification, we use only our easily-dispersed clay fraction (dClay), which excludes clay C retained as silt-sized and microaggregate fractions and it also includes both chemical and biochemical protection mechanisms. Despite these differences, greater estimates of clay saturation in our study are likely due to 2:1 dominated

mineralogy of our temperate soils compared to the tropical 1:1 kaolinitic and iron oxide dominated soils of Diekow et al. (2005) and Roscoe et al. (2001).

Although Hassink et al. (1997) found no differences in silt + clay SOC protection due to mineralogy, Six et al. (2002) found that silt and clay associated C of 1:1 dominated soils was significantly less than that of 2:1 soils and attributed the difference in C stabilization mainly to clay type. Minerals with a 2:1 configuration have a greater surface charge, which accounts for greater SOC storage in the mineral fraction of these soils.

We also observed C saturation dynamics of the chemically-protected H-dSilt fraction data of all the individual and combined site data. This contrasts the work of Diekow et al. (2005) who found their silt fraction to be linearly related to whole C content. Diekow et al. (2005) attributed the linear relationship to the composite nature of the silt-sized fraction which also contained silt-sized plant debris, and fungal hyphae. Sanitation may break up and cause a redistribution of C throughout the fractions, causing the silt + clay fractions to contain greater amounts of C than may otherwise be the case. Due to our step-wise fractionation, POM was removed, and our silt-sized fraction is likely dominated by mineral-organic matter interactions rather than POM. However, it is important to note that our silt-sized fraction likely contains clay-sized particles, due to incomplete dispersion (Plante et al. 2006b).

The C saturation limit to the chemically-protected pool is dictated by texture and mineralogy. Greater SOM protection in finer textured soils is correlated to greater C content in the silt + clay fractions for soils with greatly differing mineralogies (Carter et al. 1997; Hassink 1997; Six et al. 2002). This linear fit was significantly different for

cultivated, grassland, and forest silt + clay fractions (0-53 µm) (Six et al. 2002) and was likely due to differences in disturbance and C input. Hassink & Whitmore (1997) found that estimates of protective capacity were linearly related to clay particles. We also found that estimates of C saturation of both the silt and the clay fractions (C_{maxf}) to be linearly related to the silt + clay content of the soil, suggesting a direct relationship between silt and clay content and C sequestration capacity.

Biochemical protection

Half the individual site's fraction data was best fit with the C saturation model in the biochemically-protected pool (Table 2), but the composite data fit with a linear model (Table 4). These results support the hypothesis that biochemically-protected fractions would be influenced by C saturation, but only at some sites.

Biochemical protection is acquired through condensation or complexation reactions or the inherent complex chemical nature of the plant material and is defined as biochemically resistant to decomposition (Six et al. 2002). Biochemically-protected C does associate with silt and clay particles, and therefore would be expected to reach saturation level. However, C that is biochemically recalcitrant (i.e. charcoal) may not interact with clay or silt particles and would therefore be independent of the C saturation mechanisms. Our sites appear to be dominated by biochemically recalcitrant plant-derived material, as our biochemically protected fractions show some evidence of C saturation.

This mechanism of biochemical protection is independent of silt and clay associated C protection mechanisms, but has been related to textural properties (Plante et

al. 2006b). Plante et al. (2006b) found that texture did not influence the proportion of NHC within their silt- and clay-sized fractions. However, they did note a greater susceptibility of the clay- compared to the silt-sized fraction to hydrolyze which they attributed to differences in biochemical composition between the two fractions. Carbohydrate concentration of clays is greater than that of the silt-sized fractions (Guggenberger et al. 1994; Amelung et al. 1999; Kiem & Kogel-Knabner 2003) and could account for differences in hydrolyzability between the two fractions.

Physically-protected pool

Most of the microaggregate fractions at individual sites and combined were best fit by the linear model. However, generally small differences in r^2 values between the linear and C-saturation model fits may be due to the composite nature of this fraction and the linear C accumulation in the iPOM fraction. Our μagg fraction is comprised of 12-30% iPOM C, and 60-75% μSilt and μClay C. Although microaggregate protection has been proposed as the main process of POM C stabilization by limiting microbial access to the substrate as well as decreasing oxygen diffusion and microbial activity within aggregates (Six et al. 2002), the physical protection of POM appears to be less important in μagg C stabilization than the chemical stabilization by silt and clay binding (Denef et al. 2004). The change of the μagg fraction C over increasing C contents suggest that although iPOM comprised a small proportion of total μagg C, it contributed greatly to C accumulation dynamics in the μagg fraction, producing the linear relationship rather than the curved, C-saturation relationship of the μSilt and μClay fractions. This suggests that microaggregate silt- and clay- associated C will saturate before iPOM.

The combined site data for the µagg fraction, however, was best fit with the C saturation model. Again, this could be due to the behavior of the iPOM fraction, which was also best fit with the C saturation model for the combined sites. It is possible that even though we had large range of whole SOC contents, the capacity of this fraction was only beginning to be approached. Stewart et al. (2006a) found that C saturation dynamics required a broad range of C inputs to elicit C saturation dynamics and C accumulation appeared to be linear over shorter segments of a C saturation curve.

The theoretical limit to the µagg protected pool was based on the clay content of the soil as well as the type of clay available to protect POM (Six et al. 2002). This relationship is supported by the work of Kolbl & Kögel-Knabner (2004), who found a log-normal relationship between clay content and occluded POM C. We found that the total mass of microaggregates does appear to reach a maximum level as clay content increases, suggesting that C accumulation in this fraction is indeed limited by soil texture.

Non-protected pool

Over the range of C contents we examined, the linear results of the non-protected pool both with the combined and individual site data was contrary to our hypothesis of C saturation in this pool. The majority of cPOM fractions at individual sites as well as combined fit with the linear model indicates little support for C saturation dynamics in this fraction. Our data support those of Diekow et al. (2005) who also found no finite capacity of the total POM fraction to store C. They found an increasing exponential relationship between whole SOC and POM C stock in the 0 - 2.5 cm depth (Mg ha^{-1}), and a linear relationship for the 2.5 - 7.5 cm depth.

In the LF portion of this pool, the negative relationship between whole SOC and fraction C content was unexpected, but may reflect incorporation of LF into aggregate structures or mineral association at greater C concentrations. This finding is also contrary to the lack of significant relationship between C input and LF that Six et al. (2002) found for Melfort using data from Janzen et al. (1992) and Campbell et al. (1991a). Saturation dynamics of the LF were also suggested by Solberg et al. (1997), as C stabilization in the LF decreased despite increased yields over increasing N fertilizer applications (25, 50 and 75 kg ha^{-1}).

The non-protected pool proposed by Six et al. (2002) consists of plant residues, fungal hyphae and spores, and in some cases charcoal. The plant-derived nature of this pool has been verified visually, as well as through biochemical characterization (e.g. low carbohydrate and high lignin concentration). The hypothetical saturation behavior of the non-protected C pool is independent of the other protection mechanisms and is determined by the balance between C input through plant production and the specific decomposition rate of the components C in the pool. Thus, controls on microbial activity such as soil temperature, moisture, substrate biodegradability and N availability would influence C storage in this pool. Across our sites, cPOM C content was significantly related to MAT×MAP, suggesting that the non-protected C pool is indeed constrained by climatically controlled variables such as temperature and moisture.

Conclusions

The analysis of C saturation may be expanded from whole soil analyses to individual soil fractions evaluated over whole SOC content. From the mathematical

99

derivation, we found that fractions behaving with linear whole soil C dynamics over C inputs express linear dynamics over whole SOC content. Similarly, we found that whole soil C-saturation dynamics are expressed as hyperbolic relationships over whole SOC content. These simple relationships may be used to evaluate fraction dynamics across a range of treatments.

Across and within our eight sites, we found hyperbolic relationships for both individual site and combined site data in the chemically protected pool. The microaggregate protected pool also showed support for C saturation in the combined site data, but the individual site data were mostly fit with the linear model in both the μagg and iPOM fractions. At the individual sites, the biochemical pool was split between C-saturation and linear model fits, but linear when the data were combined. The non-protected pool showed primarily linear dynamics in the cPOM fraction, and negative linear dynamics in the LF. Although the non-protected pool showed little evidence of saturation, we found these pools to be significantly related to temperature and precipitation, suggesting a climatic influence on these pools.

Carbon saturation dynamics were observed in soil fractions from a variety of taxonomies, textures and climates suggesting that C saturation is a general property across climates. These data suggest that the chemical as well as the biochemically-protected pool is influenced by C saturation dynamics. These relationships suggest individual fractions, particularly the chemically-protected pool, are capable of C saturation, even though the whole soils may not be saturated with respect to C. If the chemically-protected pool is filled, further accumulation of C will likely occur in aggregate and non-protected fractions. This C is inherently less stable and subject to

increased decomposition due to changes in management, questioning the stability and practicality of soils as a means of CO_2 mitigation.

References

Denef, K., Six, J., Merckx, R., Paustian, K., 2004. Carbon sequestration in microaggregates of no-tillage soils with different clay mineralogy. Soil Science Society of America Journal 68, 1935-1944.

Gee, G.W., Bauder, J.W., 1986. Particle size analysis. In: Klute, A. (Ed.), Methods of Soil Analysis, Part I. Physical and Mineralogical Methods, 2nd ed. American Society of Agronomy, Madison, WI, pp. 383-411.

Harris, D., Horwath, W.R., van Kessel, C., 2001. Acid fumigation of soils to remove carbonates prior to total organic carbon or carbon-13 isotopic analysis. Soil Science Society of America Journal 65, 1853-1856.

Kong, A.Y.Y., Six, J., Bryant, D.C., Denison, R.F., van Kessel, C., 2005. The relationship between carbon input, aggregation, and soil organic carbon stabilization in sustainable cropping systems. Soil Science Society of America Journal 69, 1078-1085.

Paustian, K., Collins, H.P., Paul, E.A., 1997. Management controls on soil carbon. In: Paul, E.A., Paustian, K., Cole, C.V. (Eds.), Soil Organic Matter in Temperate Agroecosystems: Long-Term Experiments in North America. CRC Press, New York, pp. 15-49.

Paustian, K., Six, J., Elliot, E.T., Hunt, H.W., 2000. Management options for reducing CO_2 emissions from agricultural soils. Biogeochemistry 48, 147-163.

Plante, A.F., Conant, R.T., Stewart, C.E., Paustian, K., Six, J., 2005. Impact of soil texture on the distribution of soil organic matter in physical and chemical fractions. Canadian Journal of Soil Science.

SAS Institute, 2003 SAS Institute, SAS/STAT Language Guide for Personal Computers. Release 8.2, SAS Institute, Cary, NC.

Sherrod, L.A., Dunn, G., Peterson, G.A., Kolberg, R.L., 2002. Inorganic carbon analysis by modified pressure-calcimeter method. Soil Science Society of America Journal 66, 299-305.

Six, J., Elliot, E.T., Paustian, K., 2000. Soil macroaggregate turnover and microaggregate formation: a mechanism for C sequestration under no-tillage agriculture. Soil Biology and Biochemistry 32, 2099-2103.

Six, J., Conant, R.T., Paul, E.A., Paustian, K., 2002. Stabilization mechanisms of soil organic matter: Implications for C-saturation of soils. Plant and Soil 241, 155-176.

Stewart, C.E., Paustian, K., Conant, R.T., Plante, A.F., Six, J., 2006. Soil C saturation I: Concept, evidence, and evaluation. Biogeochemistry.

Sumner, M.E., Miller, W.P., 1996. Cation exchange capacity and exchange coefficients. In: Sparks, D.L. (Ed.), Methods of Soil Analysis. Part 3. Chemical Methods. Soil Science Society of America, Inc., Madison, Wisconsin, pp. 1201-1229.

CHAPTER 4

SOIL CARBON SATURATION: EVALUATION AND

CORROBORATION BY LONG-TERM INCUBATIONS

Abstract

Although current estimates of soil organic C (SOC) sequestration potential are made without any explicit limit to soil C storage, it has been hypothesized that the SOC pool has an upper, or saturation limit. This study experimentally tests whether limits to soil C stabilization capacity exist, by examining C stabilization rates after the addition of two different C input levels to a broad range of soils differing in soil C content and physicochemical characteristics. We incubated soils from six agricultural sites that are close to (i.e., A-horizon) or further from (i.e., C-horizon) saturation with low and high input rates of ^{13}C-labeled wheat straw for 1.5 years. We hypothesized that 1) the proportion of C stabilized would be greater in soils with a larger compared to smaller C saturation deficit (i.e., the C- vs. A-horizon) and 2) the stabilization rate of added C would be greater if the amount of C input is small compared to the saturation deficit. Four sites had significantly more C accumulation in the C- compared to the A-horizon within at least one addition level. Greater saturation deficit led to significantly greater C

stabilization in both addition rates in the sandy soils. The only site that showed C accumulation in a manner inconsistent with the C saturation hypothesis had the highest silt plus clay content of all the sites. Three sites retained a greater proportion of residue-derived C between the C- and A- horizon in the high residue addition compared to the low. These results lend support the concept of soil C saturation and suggest that soils with low C contents and degraded lands may have the greatest rate and potential to store added C because they are further from their theoretical saturation level.

Introduction

Crop residue and manure management ultimately controls the amount of C entering an agroecosystem and subsequently effects soil organic carbon (SOC) stabilization, soil fertility and structure. Conservation management practices that increase C inputs to the soil or decrease soil organic matter oxidation (e.g., reduced tillage) have increased soil C stocks in agroecosystems (Paustian et al. 1997c; Paustian et al. 2000). Many long-term agroecosystem studies have shown that SOC content increases proportionally to increasing C inputs (Paustian et al. 1997c; Kong et al. 2005) implying that SOC accumulation is directly related to C input. However, several agricultural sites with high initial SOC contents have shown little or no increase in SOC content as C inputs increase (for reviews see Six et al. 2002; Stewart et al. 2006) suggesting that SOC accumulation was influenced by the amount of soil C already present in the soil (i.e., a non-linear increase in SOC as C inputs increase).

To explain these apparent observations of non-linear SOC accumulation, Six et al. (2002) proposed a model of C stabilization with an upper limit to SOC accumulation, or

soil C saturation level. Reviewing previous work on C stabilization in soil fractions, they suggested that physiochemical characteristics of a soil define the soil C saturation level and this in turn limits further SOC accumulation. Soil C saturation level for the entire soil is a composite of C pools and is defined as the theoretical maximum amount of C a soil is capable of containing over non-limiting C inputs. Soil properties such as texture and mineralogy will determine the final soil C saturation level, as well as how quickly that capacity may be attained, i.e., the slope and the asymptote of the C saturation curve (see Figure 1) (Six et al. 2002). The difference between a soil's theoretical saturation level and the current C content of the soil is defined as saturation deficit. As a soil approaches saturation, the saturation deficit decreases and new SOC stabilization is reduced.
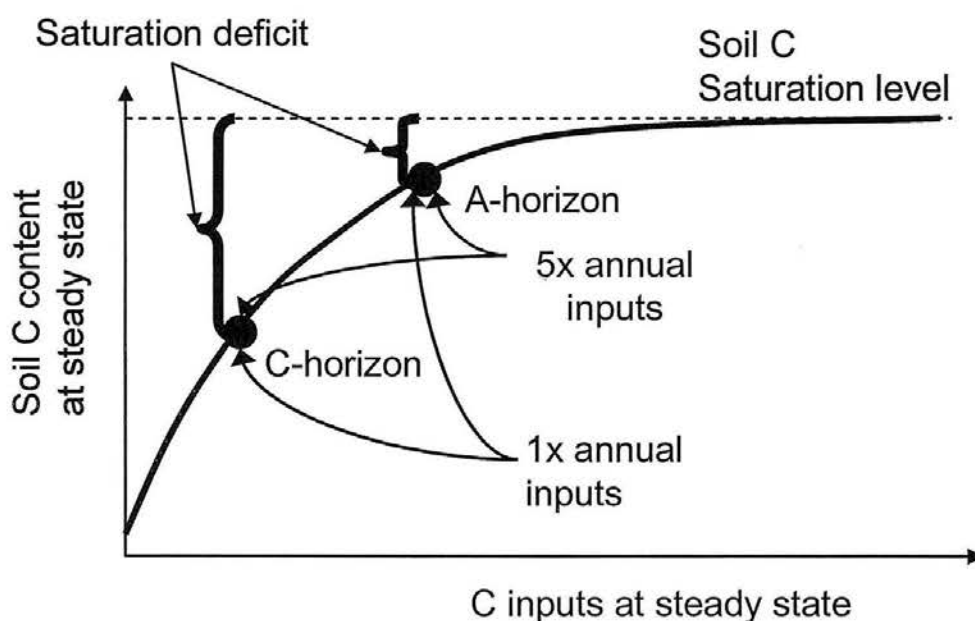
Figure 1: Illustration of the C saturation concept expressed over increasing C inputs at steady state. Saturation level is the maximum amount of C a soil is capable of holding at steady-state with C inputs also at steady state, and saturation deficit is the difference between a soil's current SOC content and its theoretical saturation level.

The whole-soil C saturation concept presented by Six et al. (2002) was further explored by Stewart et al. (2006a) who compared the linear model (i.e., a non-saturated model) to two mathematical models incorporating soil C saturation concept, a whole-soil C saturation limit (1-pool model), and a soil C saturation limit to one of two soil C pools (2-pool model). Across 17 agroecosystem sites, they found a 99% probability based on Akaike weights that the saturation models were the best approximation of the data; and suggested that C saturation deficit influenced the rate of C accumulation.

Additionally, they tested the effect of C saturation deficit on SOC stabilization by using long-term paired CT-NT treatments. In many experiments, NT treatments have sequestered more SOC than CT treatments due to increased aggregation and particulate organic matter stabilization (Six et al. 2000; Denef et al. 2004). Stewart et al. (2006) hypothesized that if saturation deficit influenced SOC accumulation, the ratio of SOC stabilization in NT versus CT treatments (i.e., NT/CT SOC stabilization ratio) should decrease as soil C content increased across sites. They found that as SOC content increased, the NT/CT SOC stabilization ratio decreased lognormally, supporting the concept of C saturation deficit influencing the amount of C stabilized by NT. This effect appeared to be related to mineralogy, as the tropical sites had a steeper decrease in NT/CT SOC stabilization compared to the temperate sites, suggesting a strong influence of mineralogy on C saturation deficit and SOC stabilization in these soils.

This work suggested that C saturation dynamics could be observed over soils with varying C saturation deficits as well as over increasing C inputs. However to date, the effect of soil C saturation deficit has only been tested indirectly by assuming SOC content as a proxy of C saturation deficit across a broad range of sites (Stewart et al.

107

2006a). Additionally, the effects of C inputs have been assessed using experiments investigating effects of management (i.e., tillage, fertilization, and crop rotation), on yield and/or soil C, which often do not provide a wide enough range of treatments to effectively examine the response of soil C levels to C input rate. Across sites, interpretation of C stabilization over increasing C input levels is complicated by site effects such as differences in climate, soil texture, mineralogy and type.

The objectives of this study were to examine, by experimental manipulation, the effects of saturation deficit and varying C input levels on SOC stabilization over a broad range of soils differing in physiochemical characteristics. We present an experimental approach to test the soil C saturation concept and report results of C-stabilization driven by both soil C saturation deficit and C input level.

Materials and Methods

Rationale for experimental approach to test C saturation concept

To examine the influence of soil C saturation deficit on SOC accumulation, we needed a broad range of soils that varied in texture and saturation deficit, but where other factors affecting C dynamics (e.g. temperature and moisture) were similar. However, the controlling variables that produce the soil characteristics of interest also confound a field-based experiment to test the soil C saturation concept. Paramount is that field soil C contents balance C inputs (i.e., crop productivity) and decomposition, both processes mediated by climate. Over the duration of a field study, the soil C saturation deficit is confounded by climatic variation across sites. Hence, field-level experiments have too many confounding variables to directly test the effect of C saturation deficit. Therefore,

we chose to directly test the influence of saturation deficit and increasing C inputs on C stabilization by using laboratory incubations, where both residue addition and decomposition factors could be controlled.

We chose six long-term agricultural research sites that were all cultivated under continuous corn for at least the last 15 years to minimize any effects of differing crop rotations (Table 1). We assumed the C content of the soils reflected steady-state C levels. Since we cannot compare C saturation deficits across sites due to confounding texture effects, we obtained low and high organic matter soils by sampling the A- and C- genetic horizons at each site. The A- and C- horizons of our soils were similar in most major properties (e.g. clay content, pH, CEC) except for SOC content (Table 2). The sites we chose varied up to an order of magnitude in SOC content between the A- and C- horizon. We hypothesized that the C-horizon, due to its larger saturation deficit, would retain a greater proportion of added C compared to the A-horizon. We also hypothesized that the C-horizon would sequester C faster than the A-horizon when the rate of added C was small compared to the saturation deficit. To test these two hypotheses, we added different amounts (i.e., 1× and 5× average annual C addition under field conditions) of ^{13}C-labelled wheat straw to both the A- and the C- horizons and were then able to trace the fate of added C within each soil. If, there was an upper limit to C stabilization, then at lower input rates (1× addition) the soil would retain a greater proportion of added C compared to the high input rate (5×). This can be evaluated by a ratio, (5C-5A)/(1C-1A) that indicates the relative effect of residue addition rate on SOC stabilization, correcting for the fact that between sites, saturation deficit differs (estimated by the difference between A- and C- horizon SOC content). A SOC stabilization ratio less than one

109

indicated greater C stabilization in the 1× compared to the 5× addition, and supported the soil C saturation concept. Greater amounts of C input, afforded less protection by the soil, would thus be available for decomposition and not stabilized.

Table 1: Site characteristics of incubation soils.

Site	Latitude Longitude	MAT °C †	MAP mm ‡	Soil classification	Textural class
Forest ecosystems					
Wauseon, OH	41.5° N, 84.1° W	10.6	541	Oxyaquic Hapludalf	Sandy loam
Kellogg Biological Station, MI	42°24'N, 85°24'W	9.7	890	Typic Hapludalf	Loam
Saginaw, MI	42.5° N 85.5° W	8.5	788	Aeric Haplaquept	Clay
Grassland ecosystems					
Sioux City, IA	42° 24' N, 96° 23' W	8.9	660	Mollic Udifluvent	Sandy loam
Lamberton, MN	44.2° N, 95.2° W	6.2	632	Aquic Haplustoll	Clay loam
Mead, NE	41.1° N, 96.2° W	9.7	887	Typic Argiudoll	Silty clay loam

† MAT, mean annual temperature

‡ MAP, mean annual precipitation

Table 2 Basic soil characteristics of the A and C horizon of six agricultural sites.

Site		Texture (g 100g soil⁻¹)			pH	Total Organic C†	$\delta^{13}C$	Total N†	CEC ‡
		Sand	Clay	Silt					
Wauson, OH									
	A	85	7	8	5.7	1.1	-19.2	0.10	9.5
	C	90	7	3	6.4	0.1	-24.77	0.01	10.9
Kellogg Biological Station, MI	A	12	30	58	6.6	0.9	-23.32	0.10	23.5
	C	4	31	65	6.4	0.8	-22.22	0.07	23.1
Saginaw, MI									
	A	12	69	19	8.2	1.5	-21.64	0.18	36.6
	C	19	67	14	8.4	0.2	-24.22	0.05	37.7
Sioux City, IA									
	A	69	10	22	7.3	1.1	-19.25	0.10	15.4
	C	62	10	28	8.1	0.6	-24.01	0.04	17.2
Lamberton, MN									
	A	40	32	28	6.3	1.9	-15.98	0.19	28.6
	C	36	32	32	8.6	0.2	-23.57	0.03	37.3
Mead, NE									
	A	8	38	55	6.3	1.8	-14.57	0.20	25.6
	C	9	31	60	7.3	0.2	-20.76	0.04	28.7

† (g 100g soil⁻¹)

‡ CEC, Cation exchange capacity (Meq 100 g⁻¹)

Soil Sampling

We sampled A- (0-20 cm) and C- genetic horizons (variable depths) were in spring 2001 from six long-term agricultural field experiments (Table 1). These sites included three grassland-derived soils (Mead, NE; Wauseon, OH; and Lamberton, MN) and three forest-derived soils (Sioux City, IA; East Lansing, MI; and W.K. Kellogg Biological Station, MI) arrayed across temperature gradients. Samples were taken from soil pits dug to corresponding horizon depth. Soils were packaged to remain cool and uncompacted during transport to the laboratory. In the laboratory, large rocks,

recognizable surface litter, and root material were removed, as samples were gently broken by hand and passed through an 8-mm sieve. Soils were then air-dried, passed through a 2-mm sieve, and stored at room temperature.

Soil Analyses

All soils were analyzed for pH, texture, carbonates, field capacity, total C and N content, and base saturation (base saturation was done only on the A-horizon samples). Soil pH was determined in 2:1 water: soil ratio using a digital pH meter (Radiometer, Copenhagen). Soil texture was determined using a modified version of the standard hydrometer method without removal of carbonates or organic matter (Gee & Bauder 1986) on a 30 g subsample dispersed with 100 ml of five percent sodium-hexametaphosphate solution for 18 hours. Total sand content was determined by sieving (53 µm) and clay content was measured by the two hour hydrometer method. Silt was determined by difference. Soil carbonates were determined by a modified pressure transducer method described by Sherrod et al. (2002).

Field capacity was determined on three replicates from a 50 g subsample of two-mm sieved soil, wet slowly with eight ml of deionized water in glass test tubes, covered with perforated parafilm, and allowed to equilibrate overnight. A subsample from the middle of the column was then weighed, dried overnight in a 105°C oven and weighed again. Field capacity was calculated using the equation:

Field Capacity (FC) = (wet weight – dry weight)/(dry weight)*100

Cation exchange capacity (for both horizons) and base saturation (for the A-horizons) were determined by the Plant, Soil and Water Testing Laboratory, Colorado

State University, Fort Collins, Colorado using the ammonium acetate method at a pH of seven (Sumner & Miller 1996).

^{13}C Wheat Labeling

Spring wheat (Triticum aestivum, AC Teal, var awnless) was continuously labeled with ^{13}C in a 1.22 m x 1.37 m x 3.90 m airtight Plexiglas chamber. Air was mixed with two fans (2.83 m^3 displacement) and humidity was maintained between 70% and 90% with a Frigidaire dehumidifier operated by a humidity controller (Ohmic Instruments Co, model EHC-100). Temperature was maintained between 20° and 30°C by two radiators. Both temperature and humidity measurements were made with a hygrothermometer (Extech instruments Model 45320).

In thirty-six 17.6 l pots, 50 wheat seeds were planted in a soil mixture of 50% autoclaved soil, 25% perlite, and 25% sand; the soil was obtained from the Agricultural Research, Development and Education Center at Colorado State University. Soil was brought to field capacity using one liter water and one liter modified Hoagland's nutrient solution containing Ca, N, K, Mg, P, Na and micronutrients (B, Mn, Zn, Cu, and Mo). Plants were watered two to three times a week and the N input varied between 100 and 200 g KNO_3 per 18 l solution.

A one percent ^{13}C sodium bicarbonate solution was added by an automated micropipetter (Hamilton Company, Reno, NE) to 10 M H_2SO_4 to maintain an average chamber CO_2 concentration of 350 ppm and a two percent isotopic enrichment. Chamber CO_2 was monitored by an infrared gas analyzer (LICOR model LI-800, Lincoln, NE).

Experimental Design

Four 200 g replicates of A- and C-horizon soils were mixed with either 0.26 g (1×) or 1.28 g (5×) ^{13}C wheat straw for four sampling dates (0, 0.5, 1.5 years). Samples were slowly wetted to field capacity, and allowed to equilibrate overnight in a refrigerator (4°C). The 0, 0.5, and 1.5 year samples were then placed into one large sealed chamber (to maintain humidity) at 25°C. The one quarter of the samples were placed into airtight 3.79 l glass jars and capped with lids containing septa for gas sampling. These samples were measured for total respiration every other day for the first month of incubation and monthly thereafter using an IRGA (LICOR model LI6252, Lincoln, NE).

Samples were destructively sampled, and then sieved and dried as done for field samples. We report results for the 1.5 year sample date only.

Carbon and ^{13}C Analysis

The ^{13}C –CO_2 signal was measured on the respired CO_2 using a Micromass VG Optima mass spectrometer (Micromass UK Ltd., Manchester, UK). Results were expressed as:

$$\delta^{13}C = \left[\frac{^{13}R_{sample} - {}^{13}R_{standard}}{^{13}R_{standard}} \right] * 1000$$

where $^{13}R = {}^{13}C/{}^{12}C$ and the standard is the international Pee Dee Belemnite. Residue-derived CO_2-^{13}C (Q_r) was calculated using the equation:

$$Q_t \times \delta_t = Q_r \times \delta_r + Q_s \times \delta_s + Q_b \times \delta_b$$

where Q_t, Q_r, Q_s, and Q_b are respired CO_2-C (mg C kg^{-1} soil) and δ_t, δ_r, δ_s, and δ_b = its isotopic composition (‰) from total, residue, soil, and blanks respectively.

Soil C and ^{13}C were determined on ground 1.5-year subsamples using a Carlo Erba NA 1500 CN analyzer (Carlo Erba, Milan, Italy) coupled with a Micromass VG isochrome-EA mass spectrometer (Micromass UK Ltd., Manchester, UK) (continuous flow measurement). Carbonates were removed prior to analysis by acid fumigation (Harris et al. 2001) modified to a half an hour fumigation for three gram samples. The proportion of residue-derived C stabilized in the soil (*f*) was calculated using the equation:

$$f = \frac{\delta_t - \delta_s}{\delta_r - \delta_s}$$

where $\delta_t = \delta^{13}C$ of the whole soil at time t (1.5), $\delta_s = \delta^{13}C$ of the original whole soil; $\delta_r = \delta^{13}C$ of the added residue (738.63 ‰). The quantity of residue-derived C stabilized in the soil was calculated as:

$$C_r = C_t * f$$

where C_t = total C content of the soil.

Statistical Analyses

The data were analyzed using the ANOVA procedure in SAS-STAT (SAS/STAT 1991). Within site, horizon or addition were the main factors in the model. Separation of means was tested using Tukey's significantly difference test with a $P < 0.05$.

Results

Expression of a C-accumulation Term

To examine C saturation using relatively short-term laboratory studies, we needed to account for differences in microbial activity and therefore microbial processed C input. In this case, greater microbial activity led to more C being metabolized and consequently a greater proportion of C entering the A-horizon compared to the C-horizon, especially in the 5× addition (Figure 2). The 5× residue addition provided more substrate to the microbial biomass than did the 1× addition and therefore more of the added C was decomposed in the 5× than the 1× addition (Figure 2). Consequently, total residue-derived C stabilized over 1.5 years is not only determined by the physicochemical characteristics of the soil, but also by differences in microbial processing rates between treatments in this experiment (Figure 3). We needed an expression of stabilized C that normalized for the amount of C processed with each treatment because analyzing the differences in C stabilization due to differences in native microbial communities in each site was not the focus of our study. Normalization allowed us to examine the stabilization potential between soil horizons and residue additions as determined by the physicochemical characteristics of the soil. We could correct for the total amount of C stabilized by accounting for differences in total respiration between treatments (Figure 4). Correcting for the total amount of C evolved would be confounding if there were a priming effect, i.e., an increase in soil respiration (CO_2) derived from soil (as opposed from residue) between the 1× and the 5× additions. However, there was no statistically
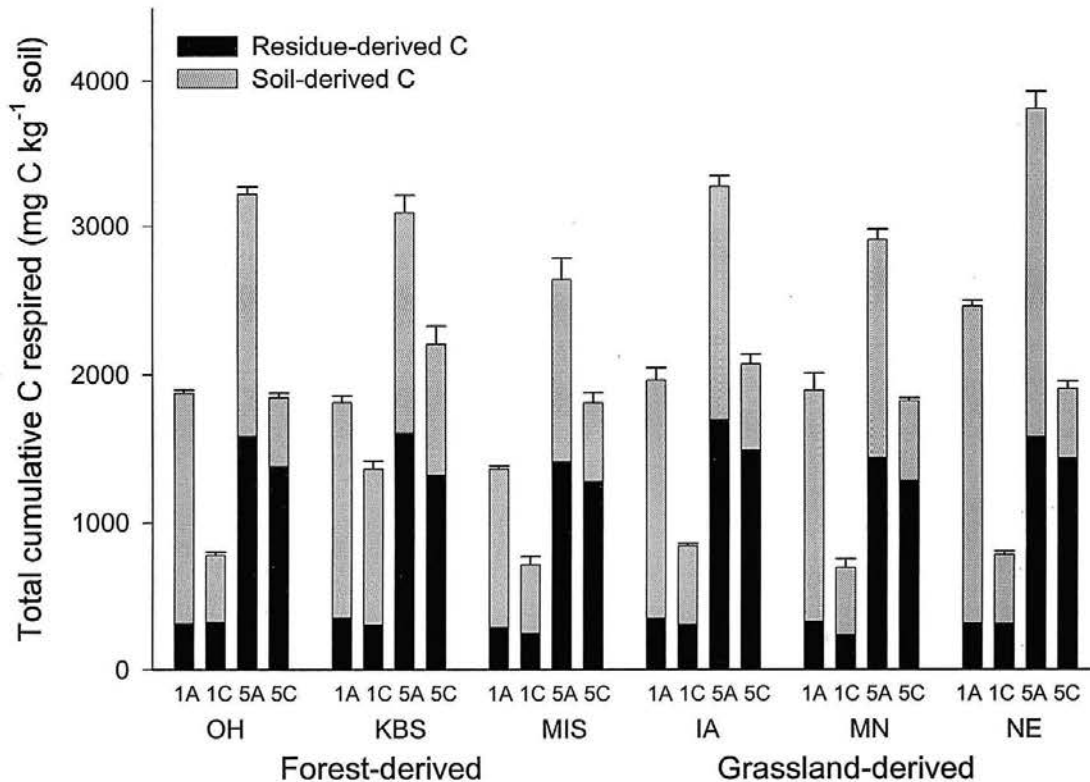
Figure 2: Soil-derived and residue-derived respiration comprising total respiration (mg C respired mg $^{-1}$ soil) for Sioux City, Iowa (IA), W.K. Kellogg Biological Station, Michigan (KBS), East Lansing, Michigan (MIS), Lamberton, Minnesota (MN), Mead, Nebraska (NE), and Wauseon, Ohio (OH) for the 1× addition to the A- and C-horizon (1A and 1C) and the 5× addition to the A- and C-horizon (5A and 5C) after at 1.5 years of incubation. Error bars represent standard errors of the means (n = 4).

significant difference (P < 0.05) between soil-derived C respired between additions in any of the soils, thereby precluding this possibly confounding effect (Figure 2).

A potential problem with normalizing by total C respired is that it could confound comparisons between horizons due to inherently greater C availability in the A-compared to the C-horizon. Indeed, soil-derived respiration comprised a greater proportion of total respiration (Figure 2) in the A- than the C- horizons. Therefore, using total C respired as a correction for stabilized residue-derived C incorrectly assumes that
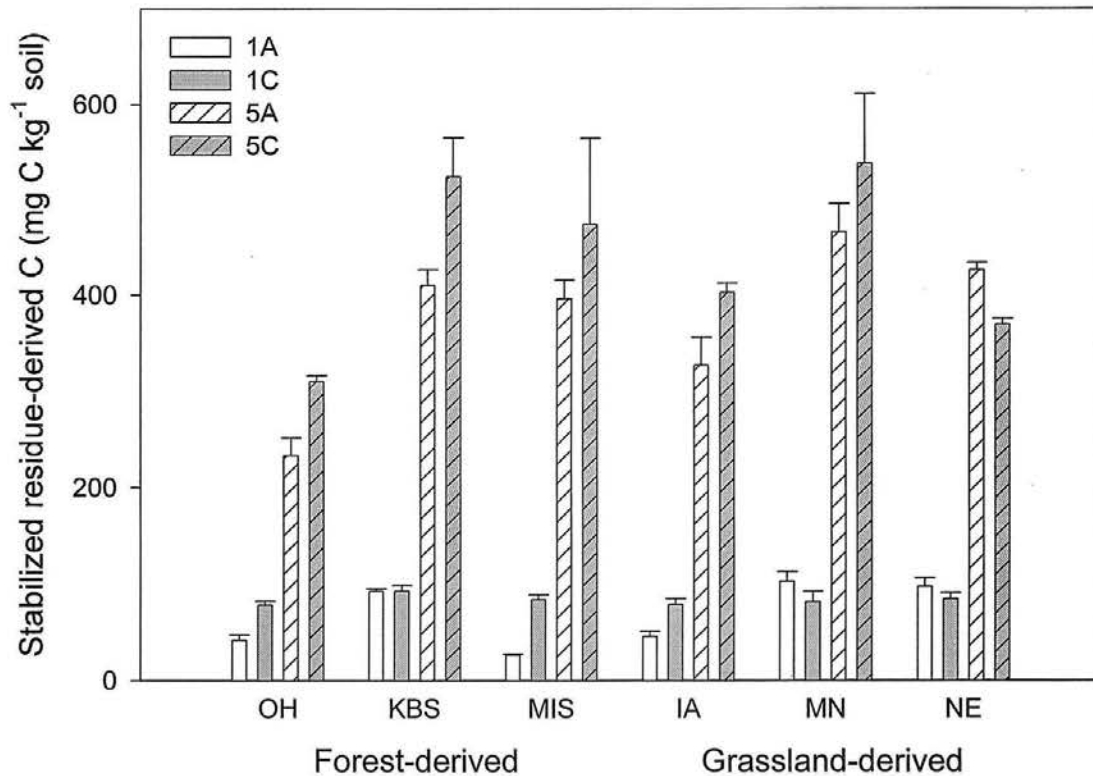
Figure 6 Figure 3: Total soil-stabilized C (mg C per kg^{-1} soil) for Sioux City, Iowa (IA), W.K. Kellogg Biological Station, Michigan (KBS), East Lansing, Michigan (MIS), Lamberton, Minnesota (MN), Mead, Nebraska (NE), and Wauseon, Ohio (OH) for the 1× addition to the A- and C-horizon (1A and 1C) and the 5× addition to the A- and C-horizon (5A and 5C). Error bars represent standard errors of the means (n = 4).

total C respired is an accurate indicator of microbial residue processing. Greater respiration in the A-horizon due to greater C availability over-corrected the amount of stabilized residue-derived C. Hence, we could only use the ^{13}C-derived respiration to correct for microbial processing and needed to express the data as residue-derived C stabilized corrected for the amount of added C that was processed, or stabilized residue-derived C/residue-derived respired C (Figure 5). Residue-derived respiration captures the differences between microbial processing of the 1× vs. 5× residue additions without

Figure 7 Figure 4: Stabilized residue-derived C (mg C (total mg C respired)$^{-1}$) for Sioux City, Iowa (IA), W.K. Kellogg Biological Station, Michigan (KBS), East Lansing, Michigan (MIS), Lamberton, Minnesota (MN), Mead, Nebraska (NE), and Wauseon, Ohio (OH) for the 1× addition to the A- and C-horizon (1A and 1C) and the 5× addition to the A- and C-horizon (5A and 5C). Error bars represent standard errors of the means (n = 4).

introducing the diluting factor of the soil-derived respiration in the A- versus C- horizon (Figure 2).

In summary, since there is no need to correct for priming and because residue-derived respiration effectively captures the variation in microbial processing of added residue between treatments, the unit we used to express our data is stabilized residue-derived soil C/residue-derived respiration (Figure 5).

Saturation deficit test

Generally, the C-horizon sequestered more residue-derived C compared to A-horizon in all sites except NE, suggesting that across the majority of our sites, soils with greater soil C saturation deficits sequestered greater amounts of added residue C after 1.5 years of incubation (Figure 5). In six of the twelve saturation deficit comparisons, this greater stabilization of added C in the C-horizon than the A-horizon was significant ($P < 0.05$). The two sandiest soils, IA and OH, had differences within both the 1× and 5× residue addition treatments, while two soils with greater silt and clay content, KBS and MIS, had statistically significant differences in only one addition rate (Figure 5).

Residue addition test

To test whether the 5× residue addition sequestered relatively less C than the 1× addition, we compared C stabilization of the A- and C-horizons within addition rates (i.e., (5C-5A)/(1C-1A)). Ratios less than one are indicative of C saturation.

Three of the six sites (IA, MIS, and OH) retained a greater proportion of residue-derived C between the C- and A- horizon of the 1× versus 5× residue addition (Figure 6). The soil C saturation concept predicted that as a soil approaches saturation, a 1× addition would sequester more added residue than the 5× addition with the same saturation deficit. Due to a limited stabilization capacity, the greater amounts of C input cannot be stabilized and are available for decomposition by microbes.

Data from these three sites indicate that C stabilization decreased as C input rate increased, even after correcting for the fact that more residue-derived C was processed in
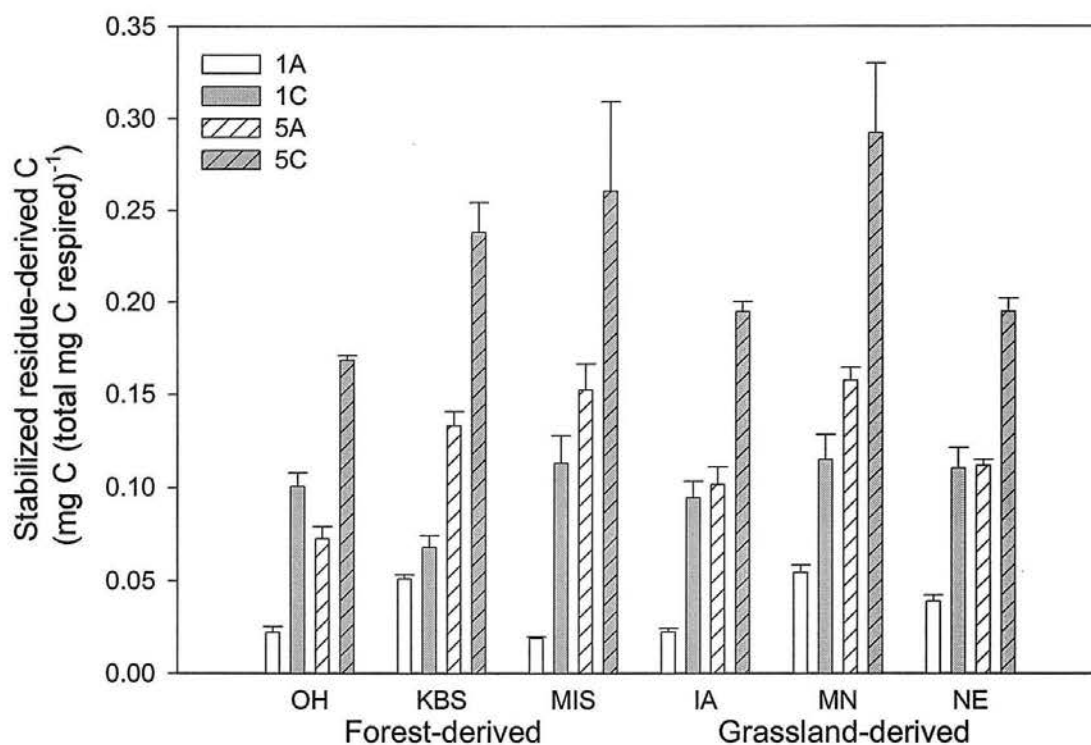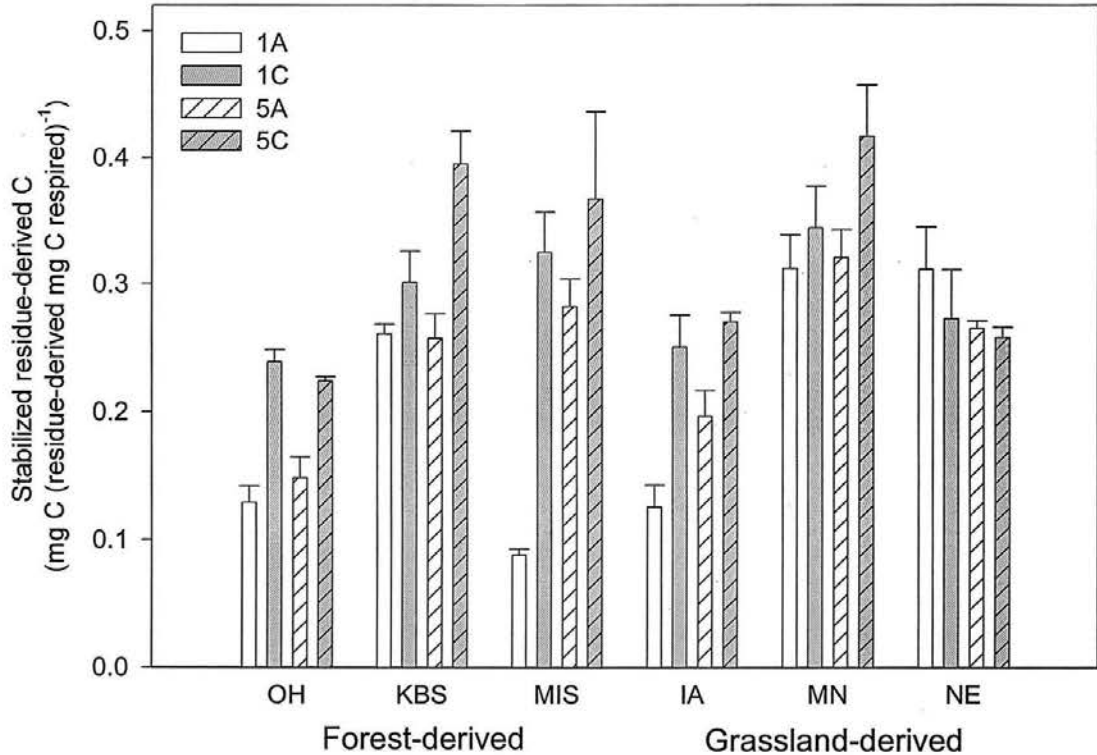
Figure 8 Figure 5: Stabilized residue-derived C (mg C mg^{-1} C respired) for Sioux City, Iowa (IA), W.K. Kellogg Biological Station, Michigan (KBS), East Lansing, Michigan (MIS), Lamberton, Minnesota (MN), Mead, Nebraska (NE), and Wauseon, Ohio (OH) for the 1× addition to the A- and C-horizon (1A and 1C) and the 5× addition to the A- and C-horizon (5A and 5C). Error bars represent standard errors of the means (n = 4).

the 5× addition. This data suggest that SOC accumulation behaved in accordance with the soil C saturation concept in these three sites. However, of the three remaining sites, MIS and KBS stabilized much greater amounts of added C in the 5× addition, even after correcting for the amount of residue-derived C respired and NE had a negative ratio, since its trend was opposite to what was hypothesized.
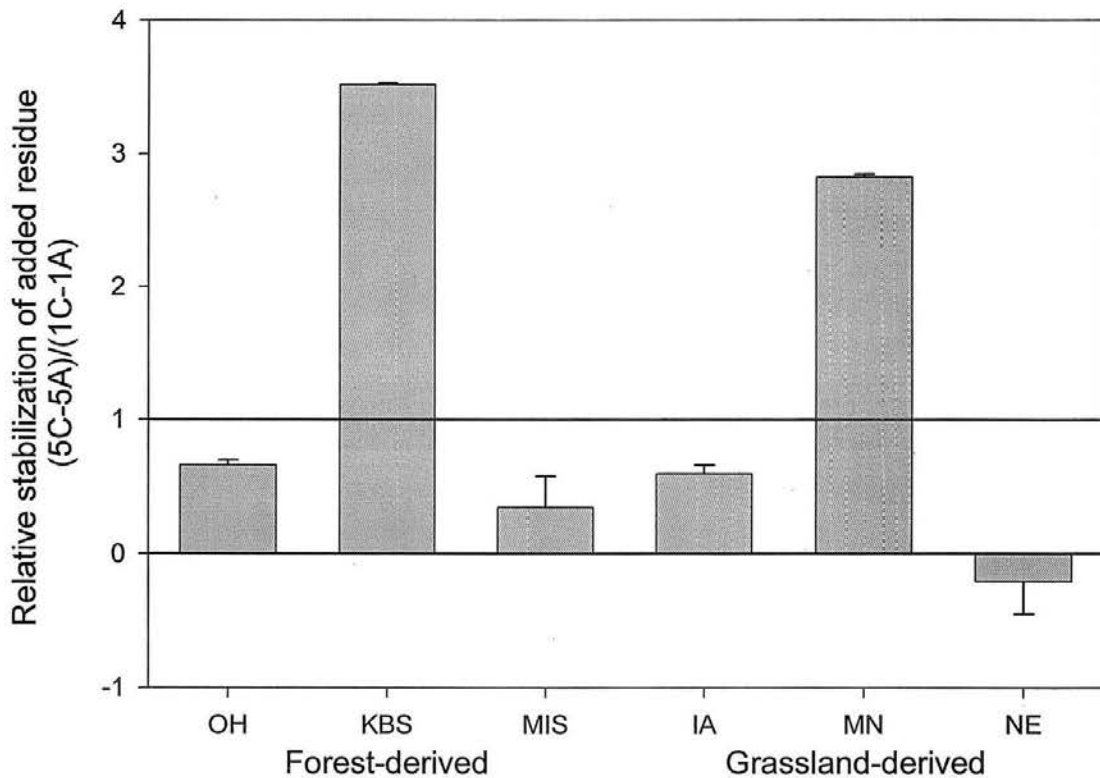
Figure 9 Figure 6: Relative stabilization of added residue (5C-5A)/(1C/1A) for Sioux City, Iowa (IA), W.K. Kellogg Biological Station, Michigan (KBS), East Lansing, Michigan (MIS), Lamberton, Minnesota (MN), Mead, Nebraska (NE), and Wauseon, Ohio (OH). Error bars represent standard errors of the means (n = 4).

Discussion

Our 1.5 year incubation data lend support to the hypotheses that stabilization of added C is greater in soils with a greater saturation deficit. The four sites that had significantly more C accumulation in the C- compared to the A-horizon within at least one addition level ranged in texture from sand to clay and were derived from both forest and grassland ecosystems. In this experiment, the effect of C saturation deficit appeared to be mediated by soil texture. Saturation deficit had the most significant effect on C stabilization in sandy soils, where both residue addition rates in IA and OH had

significantly more C stabilization in the C- compared to A-horizon. However, as silt plus clay content increased across sites, only one of the addition rates showed significant differences between the A- and C-horizons of KBS and MIS. Minnesota, with 60% silt plus clay, showed no significant differences between A- and C-horizons and Nebraska, which had the highest silt plus clay content of all the sites, showed no evidence of C saturation deficit influencing C stabilization. This is observation corresponds with data presented by Plante et al. (2005), who found that across two texture gradients in Ohio and Saskatchewan, the silt- and clay-associated C of the soil decreased as whole-soil silt plus clay content increased. They suggested that contrary to their hypothesis that silt and clay would be a good predictor of whole-soil C content, that the silt and clay content of the soil diluted the silt- and clay- associated C. These observations suggest that soils with a sandy texture are closer to their saturation level, presumably due to the small amount of silt and clay surfaces available for C stabilization. If this is the case, then adding C to the near-saturated sandy soil should produce little, if any additional C stabilization in the A-horizon. However, when the same amount of C is added to the C-horizon of the low-C soil, the greater saturation deficit should allow more C to be stabilized. This response was observed in the data from the IA and OH sites. Additionally, as the silt plus clay content of the soil increased, the difference between C stabilization in the C- and A- horizon lessened. If the silt and clay particles were further from their saturation level, which might be expected if the increased amount of clay led to less mineral surfaces loaded with C, then the same addition of C that elicited a C saturation response in a sandy soil may not have been sufficient to elicit the same response in a finer-textured soil.

This could also explain why, in three sites, soils further from their saturation limit did not accumulate a greater proportion of added C in the 1× compared to the 5× addition rate. Our 5× addition corresponds to a field addition rate of 2.3 Mg C ha^{-1} yr^{-1} and Stewart et al. (2006a) found that in the field, soils demonstrating C saturation dynamics within a site had C input rates of 4.4 Mg C ha^{-1} yr^{-1}. It is possible that our range of addition rates was not sufficiently broad to elicit C saturation-like responses and that SOC stabilization in these sites followed a linear response to C inputs as is the case on the low C-input end of the saturation curve (see Figure 1). One of our sites, NE, responded to added C in the manner opposite of what we hypothesized. Although there was an order of magnitude difference in C content between the A- and the C-horizon, there was no difference in the amount of added C stabilized after 1.5 years.

As C stabilization is limited in the short-term by microbial processing, it will be important to follow these incubations further to ascertain if these trends supporting the soil C saturation concept continue over time. From the 0.5-year sampling (data not shown) to the 1.5-year sampling, the number of sites showing greater C stabilization in the C- compared to the A-horizon increased from two to five out of six. Presumably, differences in microbial biomass and community influence the amount of C processed and due to the initial, faster processing of the added residue in the A- compared to the C-horizon, saturation dynamics are not well expressed. However, over time, the C-horizon processed a similar amount of added residue compared to the A-horizon (data not shown).

Observations of C saturation dynamics in the field were only apparent after 100 years of manure addition at Sanborn and more than 50 at Breton (Stewart et al. 2006a).

Although we expect these incubations to reach steady-state with their new C additions faster than field experiments due to constant temperature and moisture, there still should be some time required to establish true steady-state conditions in terms of C cycling.

Combined with the data compiled by Six et al. (2002) and Stewart et al. (2006a), this implicit test of C saturation lends support to the concept of soil C saturation. If soils from agroecosystems do behave according to the saturation concept, soils with low C contents and degraded lands may have the fastest rate and greatest potential to store added C, because they are further from their theoretical saturation level. Conversely, those soils with greater C content, would not provide much additional C stabilization if C inputs were increased.

References

Denef, K., Six, J., Merckx, R., Paustian, K., 2004. Carbon sequestration in microaggregates of no-tillage soils with different clay mineralogy. Soil Science Society of America Journal 68, 1935-1944.

Gee, G.W., Bauder, J.W., 1986. Particle size analysis. In: Klute, A. (Ed.), Methods of Soil Analysis, Part I. Physical and Mineralogical Methods, 2nd ed. American Society of Agronomy, Madison, WI, pp. 383-411.

Harris, D., Horwath, W.R., van Kessel, C., 2001. Acid fumigation of soils to remove carbonates prior to total organic carbon or carbon-13 isotopic analysis. Soil Science Society of America Journal 65, 1853-1856.

Kong, A.Y.Y., Six, J., Bryant, D.C., Denison, R.F., van Kessel, C., 2005. The relationship between carbon input, aggregation, and soil organic carbon stabilization in sustainable cropping systems. Soil Science Society of America Journal 69, 1078-1085.

Paustian, K., Collins, H.P., Paul, E.A., 1997. Management controls on soil carbon. In: Paul, E.A., Paustian, K., Cole, C.V. (Eds.), Soil Organic Matter in Temperate Agroecosystems: Long-Term Experiments in North America. CRC Press, New York, pp. 15-49.

Paustian, K., Six, J., Elliot, E.T., Hunt, H.W., 2000. Managment options for reducing CO_2 emissions from agricultural soils. Biogeochemistry 48, 147-163.

Plante, A.F., Conant, R.T., Stewart, C.E., Paustian, K., Six, J., 2005. Impact of soil texture on the distribution of soil organic matter in physical and chemical fractions. Canadian Journal of Soil Science. (in press).

Sherrod, L.A., Dunn, G., Peterson, G.A., Kolberg, R.L., 2002. Inorganic carbon analysis by modified pressure-calcimeter method. Soil Science Society of America Journal 66, 299-305.

Six, J., Elliot, E.T., Paustian, K., 2000. Soil macroaggregate turnover and microaggregate formation: a mechanism for C sequestration under no-tillage agriculture. Soil Biology and Biochemistry 32, 2099-2103.

Six, J., Conant, R.T., Paul, E.A., Paustian, K., 2002. Stabilization mechanisms of soil organic matter: Implications for C-saturation of soils. Plant and Soil 241, 155-176.

Stewart, C.E., Paustian, K., Conant, R.T., Plante, A.F., Six, J., 2006. Soil C saturation I: Concept, evidence, and evaluation. Biogeochemistry. (submitted).

Sumner, M.E., Miller, W.P., 1996. Cation exchange capacity and exchange coefficients. In: Sparks, D.L. (Ed.), Methods of Soil Analysis. Part 3. Chemical Methods. Soil Science Society of America, Inc., Madison, Wisconsin, pp. 1201-1229.

CHAPTER 5

SOIL CARBON SATURATION: IMPLICATIONS FOR MEASURABLE CARBON POOL DYNAMICS IN LONG-TERM INCUBATIONS

Abstract

The soil C saturation concept suggests a physicochemical limit to C accumulation with increasing steady-state C inputs based on inherent soil properties, such as soil texture and structure. This concept implies an ultimate soil C stabilization capacity comprised of four pools capable of C saturation: 1) non-protected, 2) physically- (microaggregate) protected, 3) chemically- (silt + clay) protected and 4) biochemically- (non-hydrolyzable) protected. Stabilization of C in each pool is dependent on C saturation deficit, or how far from its capacity to stabilize C, the soil is. To date, the role of soil C saturation deficit has only been tested indirectly by assuming total SOC content as a proxy, potentially introducing confounding factors of climate, management, soil texture, mineralogy and decomposition kinetics. Our objective was to experimentally test the concept of C saturation deficit and how it influences soil C stabilization in soil fractions corresponding to the theorized non-protected, physical, chemical and biochemical, C pools. More specifically, we examined the rate of ^{13}C- labeled residue stabilization in the A- versus C-horizon soils from six different sites with a broad range of SOC contents and physicochemical characteristics. We hypothesized that 1) the proportion of C stabilized

would be greater in soils with a larger compared to smaller C saturation deficit (i.e., the C- vs. A-horizon) and 2) the stabilization rate of added C would be greater if the amount of C input is smaller compared to the saturation deficit. At the majority of sites, protection of added residue in the microaggregate, chemically- and biochemically-protected pools was influenced by the soil's C saturation deficit, but in the non-protected C pool it was not. Based on these results, soils closer to their saturation limit will still accumulate C in non-protected pools while those further from saturation will preferentially sequester C in chemically-or aggregate- protected forms. To maximize the benefit of soil C storage as a potential CO_2 mitigation strategy, soil C saturation dynamics must be considered.

Keywords: carbon saturation, carbon sequestration, agroecosystems, particulate organic matter, soil aggregation

Introduction

Limits to C stabilization by clay surfaces have been well documented in isolated pure clays, which has been attributed to adsorption and desorption mechanisms (Harter & Stotzky 1971; Marshman & Marshall 1981). Saturation behavior with respect to C has also been observed in clay fractions of whole soils under differing management systems (Diekow et al. 2005) and through soil profiles (Roscoe et al. 2001). Hassink and Whitmore (1997) found that a model incorporating clay finite protective capacity determined by clay content, explained the most variance in whole soil C content between treatments of organic matter additions. This led them to suggest that C accumulation did

not necessarily depend only on the protective capacity (i.e. texture) of the soil, but the degree to which the protective capacity was already occupied by organic matter.

Several researchers have proposed that the capacity of the soil to sequester C is based on more than organic matter interactions with silt and clay, but attributable to aggregate protection and biochemical recalcitrance as well (see reviews by Six et al. 2002; Krull et al. 2003). Baldock and Skjemstad (2000) proposed that each mineral matrix had a unique capacity to stabilize organic C depending not only on the presence of mineral surfaces capable of adsorbing organic materials, but also the chemical nature of the soil mineral fraction, the presence of cations, and the architecture of the soil matrix. Carter (2002) proposed a conceptual model that included the silt and clay protective capacity, and a variable capacity related to C input, aggregate stability and macro-OM. As SOC concentration increased, C associated with clay and silt would reach the protective capacity of the soil and further C accumulation would occur in aggregate structures and macro-organic matter, as a function of soil type and C inputs (i.e. management) (Carter 2002).

The whole soil C saturation concept proposed by Six et al. (2002) is a function of the physically- or microaggregate-protected C pool, the chemically-or silt- and clay-protected C pool and a non-protected C pool, or non-occluded particulate organic matter (POM). However, they also hypothesized a fourth, biochemically-protected C pool. They suggested that each pool has a unique C saturation level and C accumulation within each pool would be dependent on its C saturation deficit. In their conceptual model, SOM is stabilized by chemical association through silt and clay, by physical protection due to microaggregation, and biochemical recalcitrance of the organic matter. The

130

chemical stabilization of SOM by silt and clay particles is limited by the amount of silt and clay particles in a soil as well as by the cation exchange capacity and specific surface area which is influenced by mineralogy. Physical occlusion of labile POM by microaggregates physically protects OM as well as reduces oxygen availability inhibiting microbial decomposition. This microaggregate protected pool is physically limited by texture, as silt and clay content dominates aggregate dynamics. Biochemical SOM protection occurs through the biochemical recalcitrance of its structure and is considered biologically unavailable. The non-protected C pool is limited by the steady-state balance of C inputs and decomposition and ultimately controlled by climate. Each of the conceptual pools could be isolated by a simple three-step fractionation procedure using physical, chemical, and density fraction methods. Theoretically, whole-soil C saturation comprises the cumulative behavior of these four soils C pools.

To determine if soil fractions exhibit C-saturation behavior, Stewart et al. (2006c) isolated the four theoretical C pools proposed by Six et al. (2002) from soils of eight long-term agroecosystem sites located across the US and Canada. They expressed total SOC content as the independent variable in their analysis due to treatment differences in decomposition across native, NT and CT systems which could confound comparisons within individual fractions (Stewart et al. 2006a). They then fit each fraction with models hypothesizing either linear or C-saturation dynamics and found that the C saturation model gave the best model fits for the chemical and biochemical pools in the majority of sites, and suggested that C saturation deficit influenced C stabilization in these pools. Their results support C saturation in chemically-, and some biochemically-protected C pools, and linear dynamics for the non-protected and microaggregate -protected pools.

In the present paper, our objective was to experimentally test if the C saturation deficit of soils influences soil C stabilization in measurable soil fractions corresponding to the conceptual chemical, physical, biochemical, and non-protected C pools proposed by Six et al. (2002). More specifically, we examined the rate of ^{13}C-labeled residue stabilization; for two rates of C additions in the A- versus C-horizon soils from six different sites with a broad range of SOC contents and physicochemical characteristics. We hypothesized that within soil fractions 1) the proportion of C stabilized would be greater in soils with a larger compared to smaller C saturation deficit (i.e., the C- vs. A-horizon) and 2) the relative stabilization rate of added C would be lower for the high of C input rate.

Materials & Methods

Rationale for experimental approach to test C saturation concept

To examine the influence of soil C saturation deficit on SOC accumulation, we needed a broad range of soils that varied in texture and saturation deficit, but where other factors affecting C dynamics (e.g. temperature and moisture) were similar. However, the controlling variables that produce the soil characteristics of interest also confound a field-based experiment to test the soil C saturation concept. Paramount is that field soil C contents are the result of the balance between C inputs (i.e., crop productivity) and C decomposition, both processes mediated by climate. Over the duration of a field study, the soil C saturation deficit is not only determined by differences in soil properties but is also affected by climatic variation across sites. Hence, field-level experiments have many confounding variables impeding the effect of C saturation deficit. Therefore, we chose to

directly test the influence of C saturation deficit and vary C inputs on C stabilization by using laboratory incubations, where both residue addition and decomposition factors could be controlled.

We chose six long-term agricultural research sites that were all cultivated under continuous corn for at least the last 15 years to minimize any effects of differing crop rotations (Table 1). We assumed the C content of the soils reflected steady-state C levels. Since we cannot compare C saturation deficits across sites due to confounding texture effects, we obtained low and high organic matter soils by sampling the A- and C-horizons at each site. The A- and C- horizons of our soils were similar in most major properties (e.g. clay content, pH, CEC); except for SOC content (Table 1). The sites we chose varied by up to an order of magnitude in SOC content between the A- and C- horizon. We added different amounts (i.e., 1× and 5× average annual C addition under field conditions) of ^{13}C-labelled wheat straw to both the A- and the C- horizons and were then able to trace the fate of added C within each soil.

Soil Sampling

We sampled A- (0-20 cm) and C-horizons (variable depths) from six long-term agricultural field experiments (Table 1) in the spring of 2001. These sites included three grassland-derived soils (Mead, NE; Wauseon, OH; and Lamberton, MN) and three forest-derived soils (Sioux City, IA; East Lansing, MI; and W.K. Kellogg Biological Station, MI). Samples were taken from soil pits dug to corresponding horizon depth. Soils were packaged to remain cool and uncompacted during transport to the laboratory. In the laboratory, large rocks, recognizable surface litter, and root material were removed, as

samples were gently broken by hand and passed through an 8-mm sieve. Soils were then air-dried, passed through a 2-mm sieve, and stored at room temperature.

Site		Texture (g 100g soil^{-1})			pH	Total Organic C†	δ^{13}C	Total N†	CEC ‡
		Sand	Clay	Silt					
Wauson, OH	A	85	7	8	5.7	1.1	-19.2	0.10	9.5
	C	90	7	3	6.4	0.1	-24.77	0.01	10.9
Kellogg Biological Station, MI	A	12	30	58	6.6	0.9	-23.32	0.10	23.5
	C	4	31	65	6.4	0.8	-22.22	0.07	23.1
Saginaw, MI	A	12	69	19	8.2	1.5	-21.64	0.18	36.6
	C	19	67	14	8.4	0.2	-24.22	0.05	37.7
Sioux City, IA	A	69	10	22	7.3	1.1	-19.25	0.10	15.4
	C	62	10	28	8.1	0.6	-24.01	0.04	17.2
Lamberton, MN	A	40	32	28	6.3	1.9	-15.98	0.19	28.6
	C	36	32	32	8.6	0.2	-23.57	0.03	37.3
Mead, NE	A	8	38	55	6.3	1.8	-14.57	0.20	25.6
	C	9	31	60	7.3	0.2	-20.76	0.04	28.7

† (g 100g soil^{-1})

‡ CEC, Cation exchange capacity (Meq 100 g^{-1})

Table 1: Sites and basic soil properties for long-term incubations.

Soil Analyses

All soils were analyzed for pH, texture, carbonates, field capacity, and total C and N content. Soil pH was determined in 2:1 water: soil ratio using a digital pH meter (Radiometer, Copenhagen). Soil texture was determined using a modified version of the standard hydrometer method without removal of carbonates or organic matter (Gee &

Bauder 1986) on a 30 g subsample dispersed with a 100 ml sodium-hexametaphosphate solution (5 g l^{-1}) for 18 hours. Total sand content was determined by sieving (53 μm) and clay content was measured by the two hour hydrometer method. Silt was determined by difference. Soil carbonates were determined by a modified pressure transducer method described by Sherrod et al. (2002).

Field capacity was determined on three replicates of 50 g, 2-mm sieved soil, wet slowly with 8 ml of deionized water in glass tubes covered with perforated parafilm and allowed to equilibrate overnight. A subsample from the middle of the tube was then weighed, dried overnight in a 105°C oven and weighed again. Field capacity was calculated using the equation:

Field Capacity (FC) = (wet weight – dry weight)/(dry weight)*100

Cation exchange capacity was determined by the Plant, Soil and Water Testing Laboratory, Colorado State University, Fort Collins, Colorado using the ammonium acetate method at a pH of 7 (Sumner & Miller 1996).

^{13}C Wheat Labeling

Spring wheat (*Triticum aestivum*, AC Teal, var awnless) was continuously labeled with ^{13}C in a 1.22 m x 1.37 m x 3.90 m airtight Plexiglas chamber. Air was mixed with two fans and humidity was maintained between 70% and 90% with a Frigidaire dehumidifier operated by a humidity controller (Ohmic Instruments Co, model EHC-100). Temperature was maintained between 20° and 30°C by two radiators. Both temperature and humidity measurements were made with a hygrothermometer (Extech instruments Model 45320).

In thirty-six 17.6 1 pots, 50 wheat seeds were planted in a soil mixture of 50% autoclaved soil, 25% perlite, and 25% sand; the soil was obtained from the Agricultural Research, Development and Education Center at Colorado State University. Soil was brought to field capacity using 1 L of water and 1 L of modified Hoagland's nutrient solution containing Ca, N, K, Mg, P, Na and micronutrients (B, Mn, Zn, Cu, and Mo). Plants were watered two to three times a week and the N input varied between 100 and 200 g KNO_3 per 18 L solution.

A 1% atom excess ^{13}C sodium bicarbonate solution was added by an automated micropipetter (Hamilton Company, Reno, NE) to 10 M H_2SO_4 to maintain an average chamber CO_2 concentration of 350 ppm and a 1% isotopic enrichment. Chamber CO_2 was monitored by an infrared gas analyzer (LICOR model LI-800, Lincoln, NE).

Experimental Design

Four 200 g replicates of A- and C-horizon soils were mixed with either 0.26 g (1× annual field return rate) or 1.28 g (5× annual field return rate) ^{13}C wheat straw. Samples were slowly wetted to field capacity, and allowed to equilibrate overnight in a refrigerator (4°C). The samples were placed into airtight 3.79 L glass jars and capped with lids containing septa for gas sampling. These samples were measured for total respiration every other day for the first month of incubation and monthly thereafter using an IRGA (LICOR model LI6252, Lincoln, NE). Samples were destructively sampled, and then sieved and dried as done for field samples.

Soil fractionation

Separation of the various C pools was accomplished by a combination of physical and chemical fractionation techniques in a simple three-step process (Figure 1) detailed by Plante et al. (2006b). The first step was the partial dispersion and physical fractionation of the soil to obtain three size fractions: > 250 μm (coarse non-protected particulate organic matter, **cPOM**), 53-250 μm (microaggregate fraction, **µagg**), and < 53 μm (easily dispersed silt and clay, **dSilt** and **dClay**). Physical fractionation was accomplished by fractionating air-dried 2 mm sieved soil in the microaggregate isolator described by Six et al. (2000). The microaggregate isolator dispersed the greater than 2 mm soil with 50 glass beads in running water over a 250 μm sieve so that microaggregates and finer particles were flushed through the 250 μm mesh screen. Material greater than 250 μm (cPOM) remained on the sieve. Microaggregates were collected on a 53 μm sieve that was subsequently wet sieved by hand for 50 strokes in 2 minutes (Elliott 1986) to separate the easily dispersed silt- and clay-sized fractions from the water-stable microaggregates. The resulting suspension was centrifuged to separate the easily dispersed silt- and clay-sized fractions. Fractions were dried in a 60°C oven and weighed.

The second step involved further fractionation of the microaggregate fraction isolated in the first step (Plante et al. 2006b). Density flotation with 1.85 g cm^{-3} sodium polytungstate (SPT) was used to isolate fine non-protected POM (**LF**). After removing the fine non-protected POM, the heavy fraction was dispersed overnight by shaking with 12 glass beads and passed through a 53 μm sieve, separating the
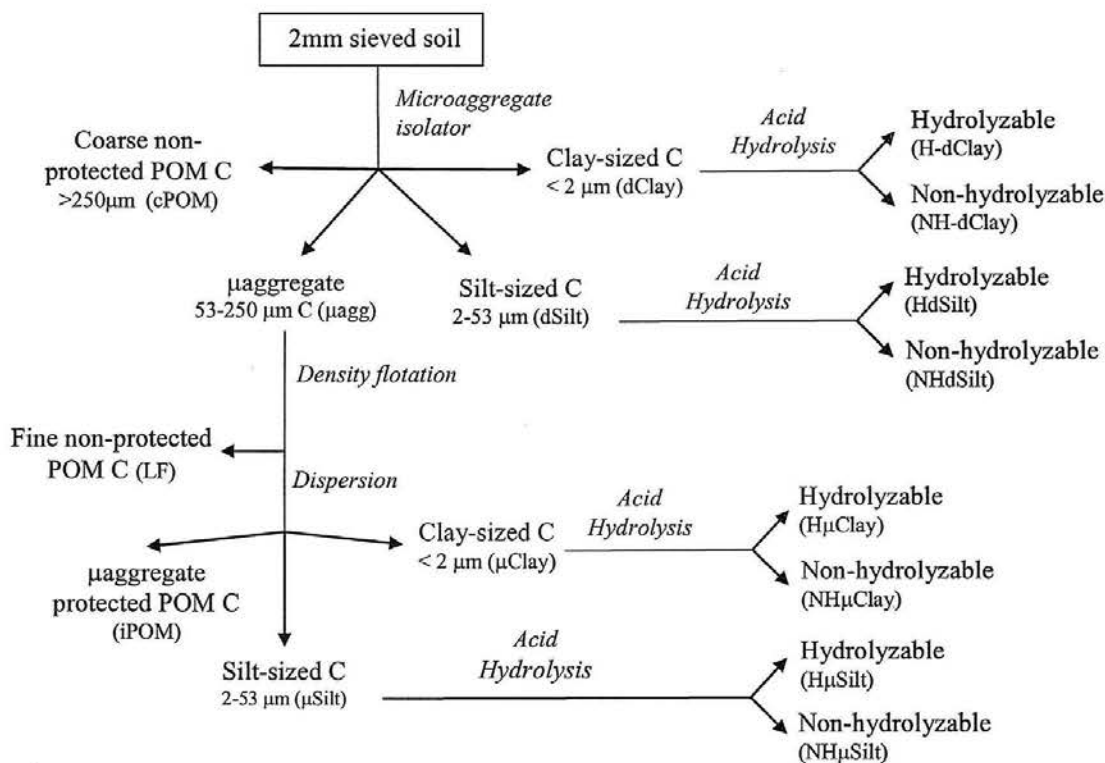
Figure 1: Soil fraction scheme to isolate the four hypothesized C pools; non-protected, physically-protected (microaggregate), the chemically-protected (silt + clay), and biochemically-protected pools. Modified from Six et al. (2002) to separate silt- and clay-associated C pools.

microaggregate protected POM (>53 μm in size, **iPOM**) and the microaggregate-derived silt- and clay-sized fractions (**μSilt** and **μClay**).

The third step involved the acid hydrolysis of each of the isolated silt- and clay-sized fractions. The silt- and clay-fractions from both the density floatation (μSilt and μClay) and the initial dispersion and physical fractionation (dSilt and dClay) were subjected to acid hydrolysis as described in Plante et al. (2006a). Acid hydrolysis consisted of refluxing at 95°C for 16 h in 25 ml of 6 M HCl. After refluxing, the suspension was filtered and washed with deionized water over a glass-fiber filter. Residues were oven-dried at 60°C, weighed and analyzed for organic C content. These

138

represented the non-hydrolyzable C fractions (**NH-dSilt, NH-dClay, NH-μSilt** and **NH-μClay**). The hydrolyzable C fractions (**H-dSilt, H-dClay, H-μSilt** and **H-μClay**) were determined by difference between the total organic C content of the fractions and the C contents of the non-hydrolyzable fractions.

This simple three-step process isolates a total of sixteen fractions of C, some of which are composites of others (e.g., μagg is composed of LF, iPOM, μSilt and μClay, and the latter two are each composed of hydrolyzable and non-hydrolyzable portions). This fractionation scheme is based on the assumed link between the isolated fractions and the protection mechanisms involved in the stabilization of organic C within that pool and is described in detail by Six et al. (2002). The non-protected C pool consists of the coarse POM fraction (cPOM) isolated during the first dispersion step, and the fine non-protected POM fraction (LF) isolated during the second fractionation step. The physically-protected C pool consists of the microaggregate (μagg) fraction as a whole and the POM occluded within it (iPOM). The chemically-protected pool corresponds to the hydrolyzable portion of the silt- and clay-sized fractions isolated during the initial dispersion (H-dSilt and H-dClay). Carbon is stabilized in these fractions through mineral-organic matter bindings, dictated by both texture and mineralogy of the soil. The biochemically-protected pool corresponds to the non-hydrolyzable C remaining in the silt and clay fractions after acid hydrolysis (NH-dSilt and NH-dClay).

Interactions between the biochemical and the physical protection mechanisms are captured by the microaggregate-derived non-hydrolyzable fraction (NH-μSilt and NH-μClay). Similarly, interactions between the chemical and the physical protection mechanisms are estimated by the hydrolyzable microaggregate-derived silt and clay

fractions (H-µSilt and H-µClay). The µSilt and µClay fractions represent a composite of the physical, biochemical and chemical protection mechanisms.

Carbon and ^{13}C Analysis

The ^{13}C-CO_2 signal was measured on the respired CO_2 of the 2.5 year samples using a Micromass VG Optima mass spectrometer (Micromass UK Ltd., Manchester, UK). Results were expressed as:

$$\delta^{13}C = \left[\frac{^{13}R_{sample} - {}^{13}R_{standard}}{^{13}R_{standard}} \right] *1000$$

where $^{13}R = {}^{13}C/^{12}C$ and the standard is the international Pee Dee Belemnite. Residue-derived CO_2 (Q_r) was calculated using the equation:

$$Q_t \times \delta_t = Q_r \times \delta_r + Q_s \times \delta_s + Q_b \times \delta_b$$

where Q_t, Q_r, Q_s, and Q_b are the respired CO_2-C (mg C kg^{-1} soil) and δ_t, δ_r, δ_s, and δ_b are the isotopic composition (‰) from total CO_2, residue-derived CO_2, soil CO_2, and blank CO_2 respectively.

Soil C and ^{13}C were determined on ground subsamples using a Carlo Erba NA 1500 CN analyzer (Carlo Erba, Milan, Italy) coupled with a Micromass VG isochrome-EA mass spectrometer (Micromass UK Ltd., Manchester, UK) (continuous flow measurement). Carbonates were removed prior to analysis by acid fumigation (Harris et al. 2001) modified to a half an hour fumigation for three milligram samples. The proportion of residue-derived C stabilized (*f*) in the whole soil and fractions were calculated using the equation:

$$f = \frac{\delta_t - \delta_s}{\delta_r - \delta_s}$$

where $\delta_t = \delta^{13}C$ of the whole soil or fraction at time t, $\delta_s = \delta^{13}C$ of the original whole soil or fraction; $\delta_r = \delta^{13}C$ of the added residue (738.63 ‰). The quantity of residue-derived C stabilized in the soil or fraction was calculated as:

$$C_r = C_t * f$$

where C_t = total C content of the whole soil or fraction.

Expression of a C-accumulation Term

To examine C saturation using relatively short-term laboratory studies, we needed to account for differences in microbial activity and therefore microbial processed C input. Between depths, greater microbial activity led to more residue being metabolized and consequently a greater proportion of C entering the A-horizon compared to the C-horizon, especially in the 5× addition (Stewart et al. 2006b). The 5× residue addition provided more substrate to the microbial biomass than did the 1× addition and therefore more of the added C was decomposed in the 5× than the 1× addition. Consequently, total residue-derived C stabilized over 2.5 years is not only determined by the physicochemical characteristics of the soil, but also by differences in microbial processing rates between treatments in this experiment. We needed an expression of stabilized C that normalized for the amount of C processed with each treatment because analyzing the differences in C stabilization due to differences in microbial activity in each site was not the focus of our study. Stewart et al. (2006b) found that there was no need to correct for priming in this experiment and because residue-derived respiration effectively captured the variation in microbial processing of added residue between

treatments, the unit we used to express our data is stabilized residue-derived soil C/residue-derived respiration (Stewart et al. 2006b).

Statistical Analyses

The data were analyzed using the ANOVA procedure in SAS-STAT (SAS Institute, Cary NC). Within site, horizon or addition were the main factors in the model. Separation of means was tested using Tukey's significantly difference test with a $P < 0.05$.

Results

After 2.5 years, the whole soil results of our incubation were mixed, with six of twelve comparisons stabilizing significantly more added C in the whole soil of the C-horizon soil versus the A-horizon soil supporting our hypothesis, but only one site having the opposite trend. Four of the significant comparisons were in the 1× addition rate (Table 2 and Figure 2) and two were in the 5× addition rate (Table 3). Additionally, two sites in the 1× and three sites in the 5× addition rate showed a trend of more added C stabilized in the C- than in the A-horizon soil.

The non-protected C pool (cPOM and LF fractions) tended to gain more residue-derived C in the A- compared to the C-horizon, except for the LF fraction of the 5× addition (Figure 2). In the cPOM fraction, only one site in the 1× addition rate accumulated significantly more C in the C-horizon and no sites in the 5× addition (Table 2 and 3, respectively). The majority of the sites in the 1× and 5× addition rates tended to

142

Table 2: Number out of six sites with differences in C accumulation between the A- and C-horizon for the 1× addition rate. Sum = the number of significant differences and trends. Individual site, horizon, addition, and fraction data may be found in Appendix 3.

Pool	Fraction	# of sites with C accumulation greater in C- than A-horizon			# of sites with C accumulation greater in A- than C-horizon		
		Significant	Trend	Sum	Trend	Significant	Sum
	Whole Soil	4	1	5	1	0	1
Non-protected	CPOM	1	0	1	4	1	5
	LF	0	2	2	0	4	4
Physical	μagg	3	2	5	1	0	1
	iPOM	0	2	2	0	4	4
Chemical	HdClay	5	1	6	0	0	0
	HdSilt	5	1	6	0	0	0
Biochemical	NHdClay	4	1	5	1	0	1
	NHdSilt	3	1	4	2	0	2
Biochemical × Chemical	dClay	5	1	6	0	0	0
	dSilt	5	1	6	0	0	0
Physical × Biochemical	NH-μClay	4	1	5	0	1	1
	NH-μSilt	3	1	4	2	0	2
Physical × Chemical	H-μClay	2	1	3	3	0	3
	H-μSilt	1	2	3	0	3	3
Physical × Biochemical × Chemical	μClay	3	1	4	2	0	2
	μSilt	1	2	3	1	2	3
Total number		49	22	71	16	15	31

Table 3: Number of sites with differences in C accumulation between the A- and C-horizon for the 5× addition rate. Sum = the number of significant differences and trends. Individual site, horizon, addition, and fraction data may be found in Appendix 3.

Pool	Fraction	# of sites with C accumulation greater in C- than A-horizon			# of sites with C accumulation greater in A- than C-horizon		
		Significant	Trend	Sum	Trend	Significant	Sum
	Whole Soil	2	3	5	1	0	1
Non-protected	CPOM	0	1	1	5	1	6
	LF	2	3	5	1	0	1
Physical	μagg	1	3	4	2	0	2
	iPOM	0	1	1	4	1	5
Chemical	HdClay	3	3	6	0	0	0
	HdSilt	5	1	6	0	0	0
Biochemical	NHdClay	3	3	6	0	0	0
	NHdSilt	5	1	6	0	0	0
Biochemical ×	dClay	3	3	6	0	0	0
Chemical	dSilt	5	1	6	0	0	0
Physical ×	NH-μClay	1	4	5	1	0	1
Biochemical	NH-μSilt	3	1	4	0	2	2
Physical ×	H-μClay	2	2	4	1	1	2
Chemical	H-μSilt	0	3	3	2	1	3
Physical × Biochemical ×	μClay	4	0	4	2	0	2
Chemical	μSilt	0	3	3	3	0	3
Total number		40	35	75	22	6	28
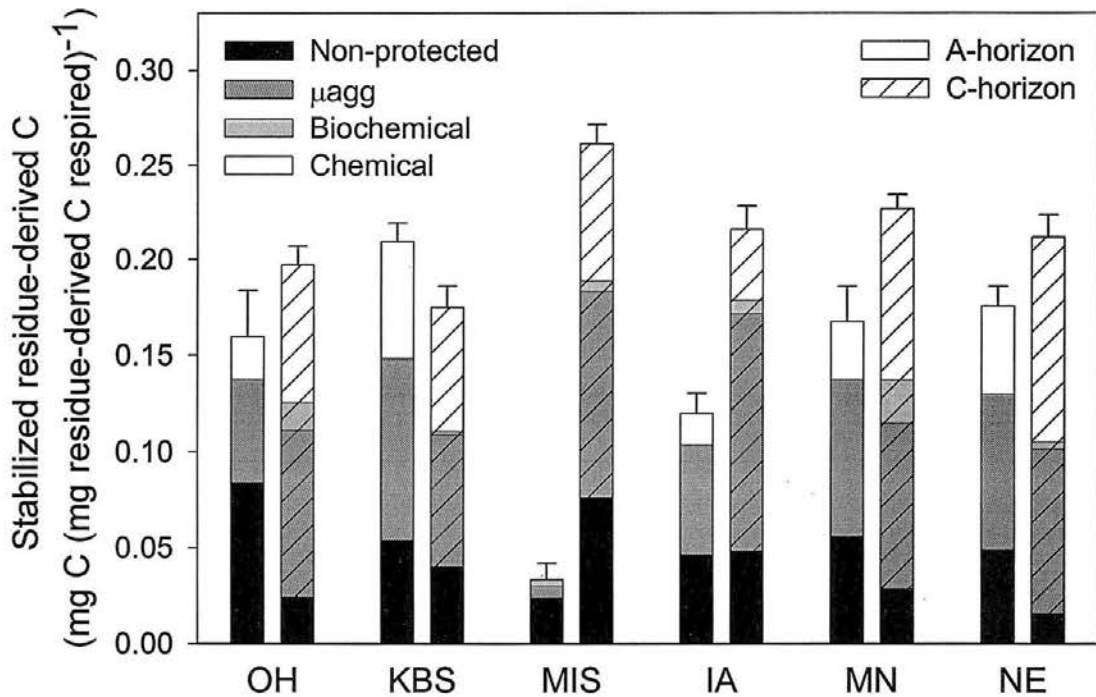
Figure 2: Stabilized residue-derived C (mg C (mg residue-derived C respired)$^{-1}$) in the four theorized C pools capable of C saturation for the A- and C-horizons with the 1× C addition rate. Non-protected are cPOM + LF, Physical is the µagg fraction, Biochemical=NH-dSilt + NH-dClay and Chemical = H-dSilt and H-dClay. Error bars represent standard errors of all fractions combined.

have greater relative amounts of added residue in the non-protected pool of the A-horizon of four and five sites, respectively. One site in both addition rates had significantly greater C accumulation in the A-horizon than C-horizon. Results in the LF fraction were mixed, with the 5× addition having a pattern of greater C accumulation in the C- horizon of most sites, whereas the majority of sites in the 1× addition had significantly greater C accumulation in the A-horizon.

In the physically-protected pool (µagg and iPOM fractions), there was a pattern of increased C stabilization in the C- versus A-horizon of the µagg fraction but not in the

iPOM fraction (Table 2 and 3). Half the sites in the 1× and one site in the 5× addition stored more C in the C-compared to the A-horizon. Another two, and three sites, respectively, tended to have more C accumulated in the C-horizon than the A- horizon in the 1× and 5× additions. Only one site in the 1× and two sites in the 5× addition had greater C accumulation in the A-horizon. However, the iPOM, had the opposite trend, with greater accumulation in the A- compared to C-horizon in both the 1× and 5× additions, although significant in only four comparisons (Table 2 and 3).
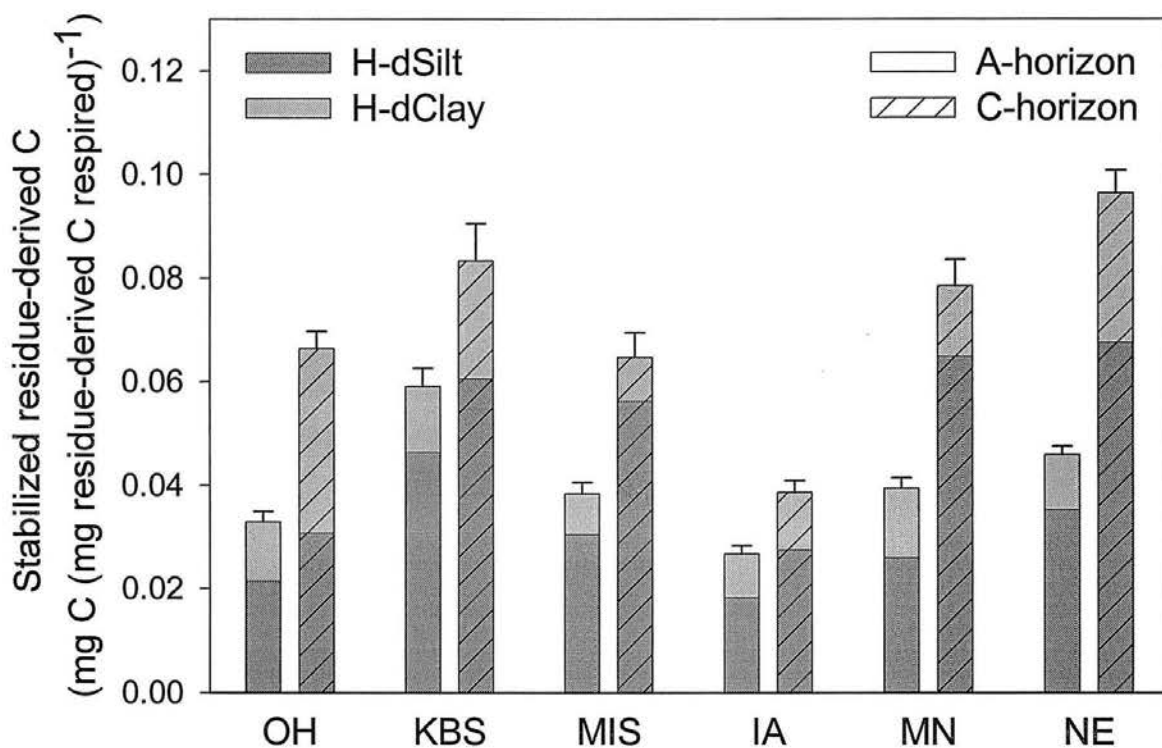
Figure 3: Stabilized residue-derived C (mg C (mg residue-derived C respired)[-1]) in the fractions (H-dSilt and H-dClay) comprising the chemical pool in the A- and C-horizons with the 5× C addition rate. Error bars represent standard errors of both fractions combined.

After 2.5 years, C accumulation in the chemically-protected pool (i.e. the sum of H-dSilt and H- dClay fractions) was significantly greater in the C-horizon compared to the A-horizon at five of the six sites in the 1× addition (data not shown) and in the 5× addition (Figure 3). All six sites sequestered more of the added residue in the chemically-protected pool of the C- horizon compared to the A-horizon, although not significant is some cases. Carbon accumulation was significantly greater in the C- compared to the A-horizon in H-dSilt fraction in five sites in both the 1× and 5× addition rates (Figure 3; Table 2 and 3). No site accumulated significantly more C in the A-horizon. The H-dClay fraction also had significantly more C accumulation in the C-horizon of five sites in the 1× and three sites in the 5× addition rate with no opposite trends observed (Tables 2 and 3). Additionally, the H-dSilt fraction stabilized significantly more of added C than the H-dClay fraction of the A- and C- horizons of both the 1× (data not shown) and 5× addition rates (Figure 3).

Generally, stabilization of residue-derived C in the biochemically- protected pool (i.e. the sum of NH-dSilt NH-dClay fractions) was small, ranging from 0.000 to 0.019 mg stabilized residue-derived C (mg respired residue-derived C)$^{-1}$) (Figure 4). In the total biochemically- protected pool (NH-dSilt + NH-dClay), we found that four and five sites in the 1× (data not shown) and 5× addition rates (Figure 4), respectively, stabilized more added C in the C- compared to the A-horizon. Three sites in the 1× and 5 sites in the 5× addition rate sequestered significantly more added C in the C- compared to the A-horizon of the NH-dSilt fraction, with only two sites in the 1× addition having the opposite trend (Table 2 and 3). In the NH-dClay fraction, four and three sites, in the 1×

and 5× addition rates, respectively, sequestered more C in the C- compared to the A-horizon. The only site with the opposite trend was in the 1× addition.

In the 1× addition, the C-horizon of two sites accumulated significantly more C in the NH-dSilt compared to NH-dClay, while three others had the opposite relationship (data not shown). The 5× addition showed similar results with five sites in both horizons stabilizing more C in the NH-dSilt than the NH-dClay fraction and three other sites showing the opposite trend (Figure 4).
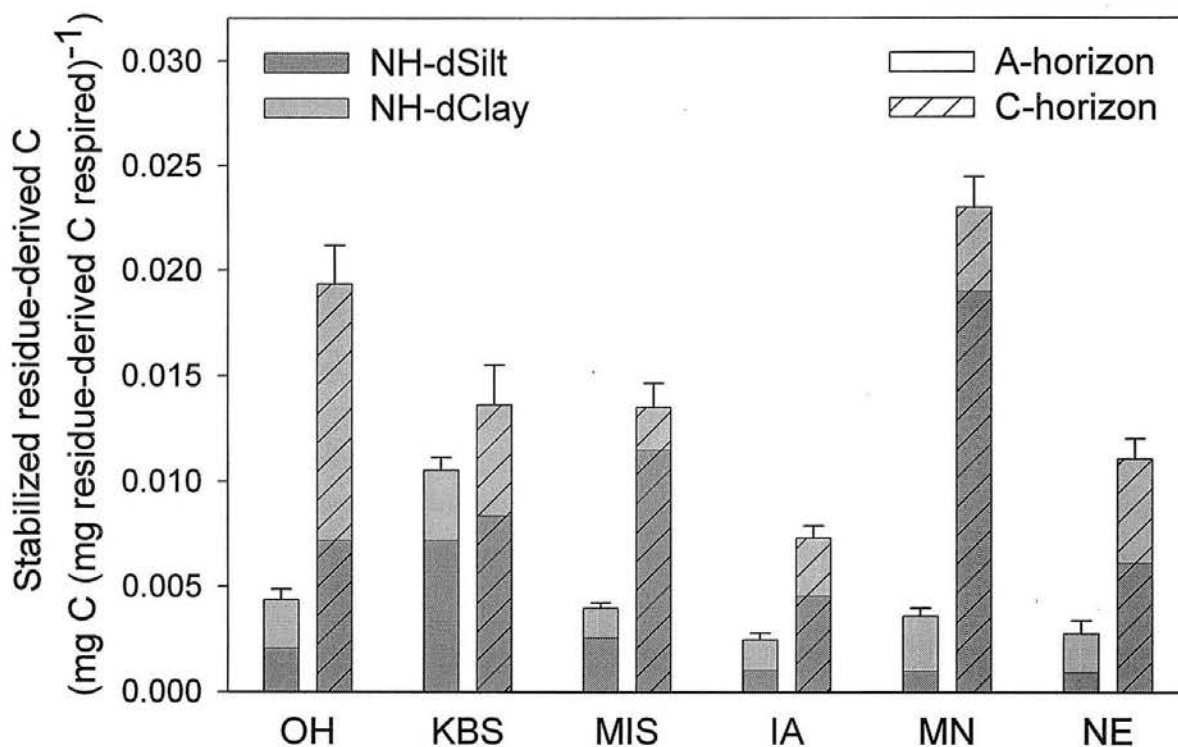
Figure 4: Stabilized residue-derived C (mg C (mg residue-derived C respired)$^{-1}$) in the biochemical pool (NH-dSilt and NH-dClay fractions) for the A- and C-horizons with the 5× C addition rate. Error bars represent standard errors of both fractions combined.

The behavior of the biochemical × chemical pool (dSilt and dClay fractions) was similar to that of the individual pools with the C-horizon accumulating significantly more added C than the A-horizon at the majority of sites. The dSilt fraction had significantly greater C accumulation in five sites with both the 1× and 5× addition rates The majority of the dClay fractions in the 5× addition and three sites in the 1× addition stabilized significantly more added C in the C compared to A-horizon. None of the sites had the opposite trend.

The fractions representing the interaction between the physical × biochemical pools (NH-μSilt and NH-μClay fraction) generally had greater C stabilization in the C-compared to the A-horizon. Three sites in the 1× and 5× addition rates had significantly greater C accumulation in the C- compared to the A-horizon, and two sites had a significant opposite relationship with the A-horizon sequestering more C than the C-horizon in the NH-μSilt fraction. Carbon stabilization in the NH-μClay fraction was quite different between the addition rates with the 1× having four sites and the 5× having only one site where the C-horizon sequestered more C than the A-horizon. However, the rest of the sites had a trend of more C accumulation in the C-horizon, and only one site showed the opposite relationship.

In contrast to the biochemically-protected pool, the physical × biochemical pool appeared to be dominated by the clay-associated C rather than silt-associated C. In both horizons and addition rates, NH-μClay sequestered greater amounts of added residue than the NH-μSilt fraction. Four sites in both the A- and C- horizons 5× addition (Figure 5) and three sites in the C-horizon of the 1× addition (data not shown) stabilized more C in the NH-μClay than the NH-μSilt fraction. When the two fractions were combined, four

sites in the 1× and three sites in the 5× addition (OH was excluded, as it had only 1

replicate) had more C stabilized in the C- compared to the A-horizon (Figure 5).
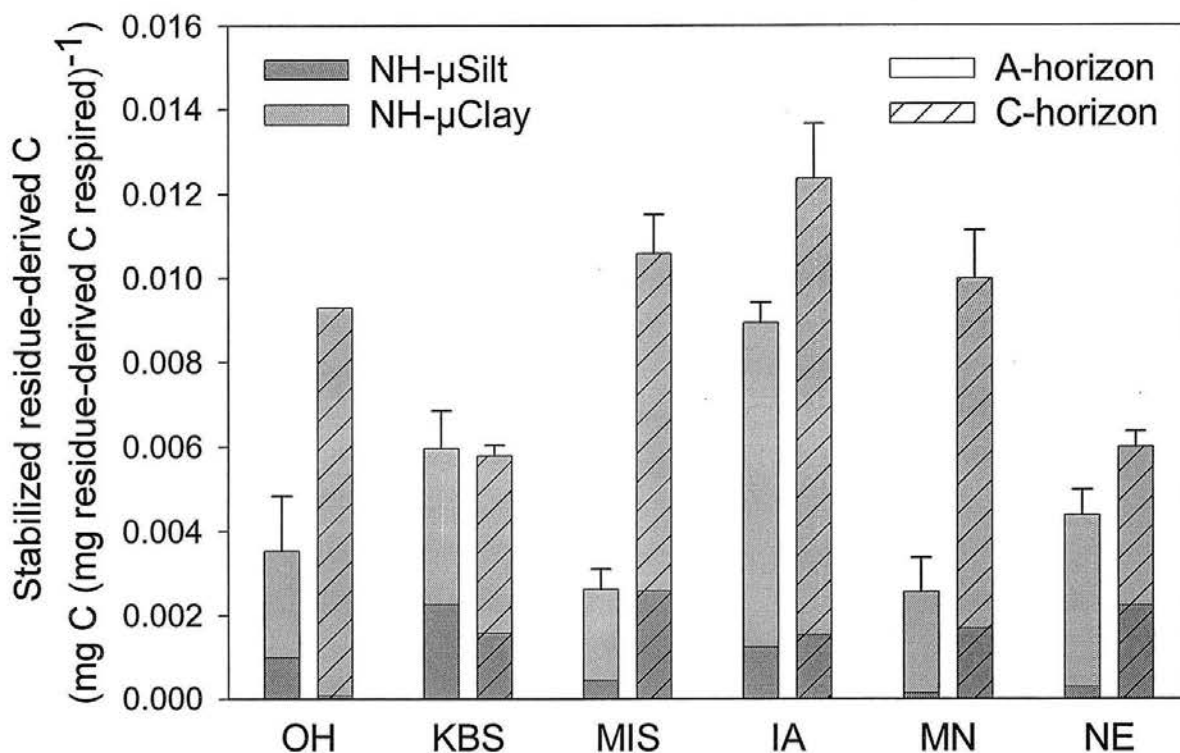
Figure 5: Stabilized residue-derived C (mg C (mg residue-derived C respired)$^{-1}$) in the biochemical × physical pools (NH-μSilt + NH-μClay fractions) for the A- and C-horizons with the 5× C addition rate. Error bars represent standard errors of both fractions combined. OH C-horizon has no error, as all replicates were combined due small sample size.

Carbon stabilization in the physical × chemical pool (H-μSilt and H-μClay fractions) had no clear results in either fraction. The H-μSilt of only one site in the 1× addition had significantly more C stabilized in the C- compared to the A-horizon and three sites demonstrated the opposite relationship. In the H-μClay fraction of two sites in both the 1× and 5× additions sequestered more added C in the C-compared to A-horizon,

but one site had the opposite significant relationship, and three sites, the opposite trend (Tables 2 and 3). There was also no clear pattern of either silt- or clay-C accumulation in the chemically-or biochemically-protected pools. Two sites (MN and NE) had no difference between H-μSilt and H-μClay, two (MIS and KBS) had greater C accumulation in H-μClay, and two (IA and OH) had greater C accumulation in H-μSilt. Perhaps not surprisingly, combining the H-μSilt and H-μClay yielded few significant differences between the C- and A- horizon in C accumulation, although there was a trend in the majority of sites in the 5× addition to have greater C accumulation in the C-compared to A-horizon (Figure 6).

In the pool representing the interactions of the physical × biochemical × chemical pools (μSilt and μClay fractions), the μClay fraction showed the strongest pattern with three and four sites in the 1× and 5× addition rate, respectively, having greater C accumulation in the C- compared to the A- horizon. Two sites in both additions had the reverse relationship. The μSilt had two sites in the 1× addition retaining greater amount of C in the A- than the C- horizon.

Discussion

Whole soil

After 2.5 years, stabilization of added ^{13}C in the whole soil was greater in the C-horizon compared to the A-horizon in the majority of our soils, suggesting soil C saturation deficit influenced the stabilization of new C across a wide range of textures (clay to sandy loam). The apparent influence of soil C saturation deficit on the whole soil C accumulation agrees with other studies that have investigated the concept of protective

151

capacity on SOC accumulation (Hassink 1996; Hassink 1997; Hassink et al. 1997; Carter et al. 2003; Jolivet et al. 2003). Whole soil C saturation deficit has been suggested as the mechanism behind diminishing C sequestration of no-till compared to conventional till treatments over increasing SOC contents in a compilation of paired long-term agroecosystem tillage treatments (Stewart et al. 2006a).
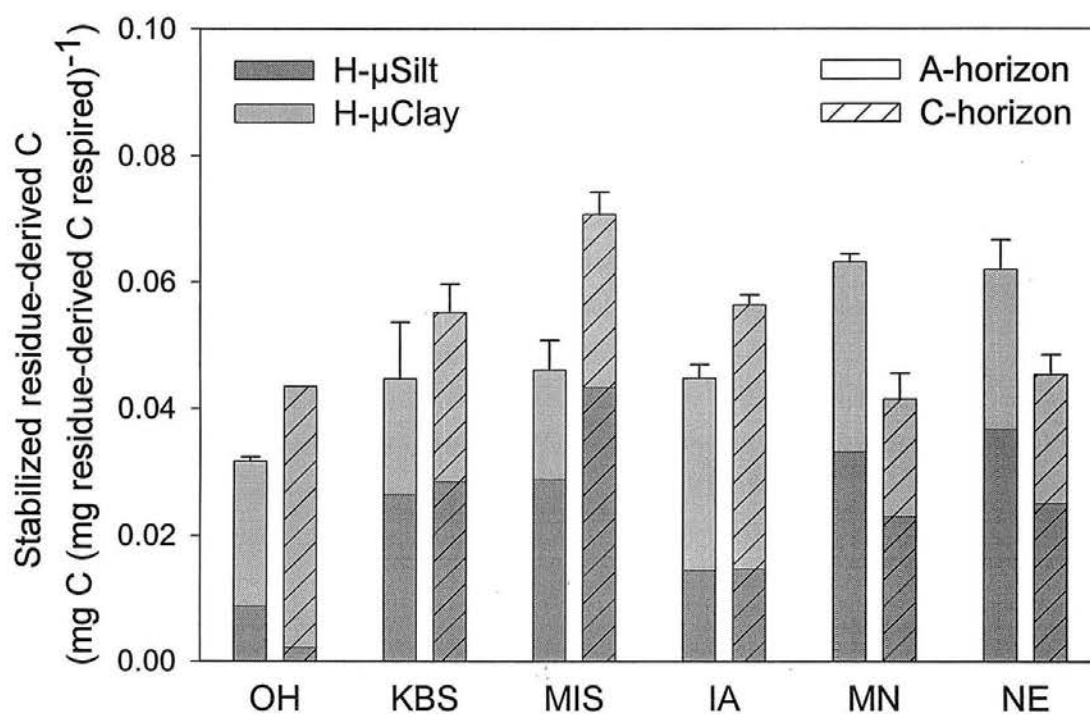
Figure 6: Stabilized residue-derived C (mg C (mg residue-derived C respired)[-1]) in the chemical × physical pools (H-μSilt and H-μClay fractions) for the A- and C-horizons with the 5× C addition rate. Error bars represent standard errors of both fractions combined.

Previous work on whole-soil C saturation capacity has focused on the influence of the protective (silt + clay) capacity of the soil (Hassink 1997; Carter et al. 2003), however, other mechanisms such as aggregation (Six et al. 2002), and biochemical

protection (Baldock & Skjemstad 2000; Six et al. 2002) may also influence the ultimate capacity of soils to protect C. We found that newly added C was predominantly sequestered in the microaggregate, chemical and non-protected C pool, although more than expected was stored in the biochemically-protected pool after 2.5 years.

Chemically-protected pools

Greater stabilization of residue-derived C in the C- compared to A-horizon in both the 1× and 5× addition treatments suggests a limit to the amount of C that could be bound to H-dSilt and H-dClay fractions. These results correspond to a large body of work supporting the influence of the protective capacity and the degree to which it is filled on soil C accumulation (Hassink 1997; Six et al. 2002; Carter et al. 2003).

In an analysis of ten field sites, Stewart et al. (2006c) found C accumulation in the H-dSilt and H-dClay fractions, as a function of total SOC content to be influenced by C saturation deficit. Across a number of field tillage treatments that produced differing SOC contents, H-dSilt and in most cases, the H-dClay fractions were best-fit with a C saturation model.

The C saturation limit to the chemically-protected pool is directly controlled by texture and mineralogy. Greater SOM protection in finer textured soils has been correlated to greater C content in the silt + clay fractions around the world with differing mineralogies (Carter et al. 1997; Hassink 1997; Six et al. 2002).

Physically-protected pools

The majority of μagg fractions (iPOM + μSilt + μClay) demonstrated trends consistent with the saturation hypothesis (C- > A-horizon) suggesting that saturation deficit influences physical protection mechanisms of SOC stabilization. Our results support those of the composite site analysis of Stewart et al. (2006c), who evaluated μagg C content over increasing whole SOC content and found that the majority of sites were better fit with a C-saturation compared to a linear model. However, at individual sites there was no evidence of C saturation in the μagg fraction.

Physical protection of POM by silt- and clay-sized particles prevents microbial access to the substrate as well as decreases oxygen diffusion and therefore microbial activity within aggregates. Although microaggregate protection has been proposed as the main process of POM C stabilization (Six et al. 2002), greater C stabilization in the C-horizon in the μagg fraction does not seem to be due to the physical protection of iPOM. The majority of iPOM fractions showed greater C accumulation in the A- compared to the C-horizon, indicating no support for saturation deficit influenced C stabilization. This result contrasts the work of Kolbl and Kogel-Knabner (2004), who found that as silt and clay content increased, occluded POM reached a maximum limit.

Saturation deficit driven C stabilization of the μagg fraction as a whole, is better explained by the interaction of the physical × biochemical × chemical pool (μSilt and μClay fractions) rather than the direct physical protection of iPOM. Between 45 and 65% of μagg C was stabilized in the mineral-associated fractions within the aggregates (μSilt + μClay), while between 4 to 40% was in the iPOM fraction. Stewart et al. (2006c) also found the majority of C to be associated with the μSilt and μClay fractions

(60 - 70%) and only 12 - 30% iPOM. Our data support that of Stewart et al. (2006a) suggesting that microaggregate-protection of C is conferred by the interaction of physical protection with chemical and biochemical pools rather than only the physical protection of iPOM.

Non-protected

Similar to the response of the iPOM fraction, accumulation of residue-derived C in the non-protected pools (cPOM and LF fractions) of A-horizon compared to the C-horizon soil showed no evidence of being influenced by C saturation deficit (Figure 2). Our data agree with that of Diekow et al. (2005) who also found no influence of saturation deficit (as a function of SOC content) on total POM fraction C. Diekow et al. (2005) found total POM content to increase exponentially as total SOC increased in the 0 - 2.5 cm depth (Mg ha^{-1}), while the data from the 2.5 - 7.5 cm depth (Mg ha^{-1}) was fit with a linear relationship. Stewart et al. (2006c) also fit a linear relationship between their cPOM and LF fractions and total SOC content in all eight sites they modeled.

Six et al. (2002) proposed that C saturation behavior of the non-protected C pool would be independent of the other protection mechanisms and would be purely the result of a balance between C input through plant production and the specific decomposition rate of the C components in the pool. Since the non-protected pool is primarily comprised of plant residues, fungal hyphae and spores, they suggested that controls on microbial activity such as soil temperature, moisture, substrate biodegradability and N availability would influence C storage in this pool. By experimentally controlling C input and decomposition factors (by the expression of our data), the differences in C

accumulation between horizons (within addition rate) should reflect the inherent ability of the soil to sequester C.

The observed greater C accumulation in the unprotected pools of the A-horizons may reflect the inability of C to be stored in silt and clay fractions because of their lower saturation deficits: if the silt and clay fractions are saturated, then the decomposition of POM C might be retarded because there is no sink for the C products derived from the POM decomposition. The latter is corroborated by Hassink et al. (1997) who found that when the protective capacity of the soil had been exceeded, C accumulated in the light and intermediate macroorganic matter fractions (> 20 µm). Carter et al. (2003) also found that C accumulation occurred only in the POM fraction with increasing C addition rates for sites near or at silt + clay capacity level. Kolbl and Kogel-Knabner (2004) found that although there was a limit to C protected as clay content increased, non-protected POM show no limit.

Biochemically-protected pools

The biochemical pools (NH-dSilt and NH-dClay) showed strong evidence of saturation in both the 1× and 5× additions with the C-horizon sequestering more residue-derived C than the A-horizon. These findings clarify the influence of saturation deficit on C accumulation in the biochemically-protected pool. Stewart et al. (2006c) found mixed results in this pool, with half their sites showing linear, and the other half, C saturation dynamics. Biochemical protection is acquired through condensation or complexation reactions or the inherent complex chemical nature of the plant material (Six et al. 2002). However, a portion of biochemically recalcitrant (i.e. charcoal) may not be a

direct function of C input, but a function of climatic variables such as fire interval. Our sites appear to be dominated by biochemically recalcitrant plant-derived material, as our biochemically-protected fractions show strong evidence of C saturation.

Plante et al. (2006a) noted a greater susceptibility of the clay- compared to the silt-sized fraction to hydrolyze which they attributed to differences in biochemical composition between the two fractions. Carbohydrate concentration of clays is greater than that of the silt-sized fractions (Guggenberger et al. 1994; Amelung et al. 1999; Kiem & Kogel-Knabner 2003) and could account for differences in hydrolyzability between the two fractions, suggesting that greater microbial alteration and carbohydrate concentration is associated with the clay-sized fraction. However, it is possible that silt-sized aggregates formed in the C-horizon apparently have the capacity to form stable complexes which resist degradation by acid hydrolysis as was seen by greater amounts of added residue C stabilized in the non-hydrolysable silt-sized fraction of the C-horizon soils than of the A-horizon soils.

Some authors suggest that SOC sequestration follows an order, based on the saturation of C pools (Hassink 1997; Carter 2002). The protective capacity is related to soil texture, and thus sandier soils have a lower and clayey soils have a higher protective capacity. Carbon content of clay fractions as a function of clay content of the soil have been found to be negative (Jolivet et al. 2003; Plante et al. 2006b) suggesting that the clay in sandy soils is closer to saturation than the clays in clayey soils. This conjecture is confirmed by several studies that have examined protective capacity and, across texture, found that soils with a lower silt + clay content tended to be saturated, while those with greater clay content still had potential to store more C (Hassink 1997; Carter et al. 2003).

Once the protective capacity is filled, further C accumulation occurs in the aggregate and POM fractions. Soils near or at their 'protective capacity' have been shown to be influenced by management, but not texture (Hassink 1997; Carter et al. 2003).

Conclusions

After 2.5 years, stabilization of residue-derived C in the whole soil was greater in the C-horizon compared to the A-horizon in the majority of our whole soils, supporting the concept of saturation deficit driven C stabilization. Greater C stabilization in the C-horizon of the whole soil generally occurred in the chemical, physical, and biochemical C pools. The non-protected pool showed little evidence for C saturation. Overall, this study corroborates the whole soil C saturation concept (Six et al. 2002; Stewart et al. 2006a) and the C saturation of different C fractions (Six et al. 2002; Stewart et al. 2006c). Soils far from their saturation limit (C-horizon) do accumulate C in the chemically-, and biochemically-protected pools faster than soils closer to their C saturation limit (A-horizon).

If soils from agroecosystems do behave according to the saturation concept, soils with low C contents and degraded lands may have the fastest rate and greatest potential to store added C, because they are further from their theoretical saturation level. Conversely, those soils with greater C content, would not provide much additional C stabilization if C inputs were increased. Soils close to their protective capacity of silt and clay will accumulate C in the aggregate and non-protected fractions. This C is inherently less stable and subject to increased decomposition due to changes in management. To maximize the benefit of soil C storage as a potential CO_2 mitigation strategy, soil C saturation dynamics of the whole soil and related fractions must be considered.

Acknowledgements

References

Amelung W, Flach KW & Zech W (1999) Lignin in particle-size fractions of native grassland soils as influenced by climate. Soil Sci Soc Am J 63: 1222-1228

Baldock JA & Skjemstad JO (2000) Role of the soil matrix and minerals in protecting natural organic materials against biological attack. Organic Geochemistry 31: 697-710

Carter MR (2002) Soil quality for sustainable land management: Organic matter and aggregation interactions that maintain soil functions. Agron J 94: 38-47

Carter MR, Angers DA, Gregorich EG & Bolinder MA (1997) Organic carbon and nitrogen stocks and storage profiles in cool, humid soils of eastern Canada. Can J Soil Sci 77: 205-210

Carter MR, Angers DA, Gregorich EG & Bolinder MA (2003) Characterizing organic matter retention for surface soils in eastern Canada using density and particle size fractions. Can J Soil Sci 83: 11-23

Diekow J, Mielniczuk J, Knicker H, Bayer C, Dick DP & Kogel-Knabner I (2005) Carbon and nitrogen stocks in physical fractions of a subtropical Acrisol as influenced by long-term no-till cropping systems and N fertilisation. Plant Soil 268: 319-328

Elliott ET (1986) Aggregate structure and carbon, nitrogen, and phosphorus in native and cultivated soils. Soil Sci Soc Am J 50: 627-633

Gee GW & Bauder JW (1986) Particle size analysis. In: Klute A (Ed) Methods of Soil Analysis, Part I. Physical and Mineralogical Methods, 2nd ed. pp 383-411). American Society of Agronomy, Madison, WI

Guggenberger G, Christensen BT & Zech W (1994) Land-Use Effects on the Composition of Organic-Matter in Particle-Size Separates of Soil .1. Lignin and Carbohydrate Signature. Eur J Soil Sci 45: 449-458

Harris D, Horwath WR & van Kessel C (2001) Acid fumigation of soils to remove carbonates prior to total organic carbon or carbon-13 isotopic analysis. Soil Sci Soc Am J 65: 1853-1856

Harter RD & Stotzky G (1971) Formation of Clay-Protein Complexes. Soil Science Society of America Proceedings 35: 383-388

Hassink J (1996) Preservation of plant residues in soils differing in unsaturated protective capacity. Soil Sci Soc Am J 60: 487-491

Hassink J (1997) The capacity of soils to preserve organic C and N by their association with clay and silt particles. Plant Soil 191: 77-87

Hassink J & Whitmore AP (1997) A model of the physical protection of organic matter in soils. Soil Sci Soc Am J 61: 131-139

Hassink J, Whitmore AP & Kubat J (1997) Size and density fractionation of soil organic matter and the physical capacity of soils to protect organic matter. Eur J Agron 7: 189-199

Jolivet C, Arrouays D, Leveque J, Andreux F & Chenu C (2003) Organic carbon dynamics in soil particle-size separates of sandy Spodosols when forest is cleared for maize cropping. Eur J Soil Sci 54: 257-268

Kiem R & Kogel-Knabner I (2003) Contribution of lignin and polysaccharides to the refractory carbon pool in C-depleted arable soils. Soil Biol Biochem 35: 101-118

Kolbl A & Kogel-Knabner I (2004) Content and composition of free and occluded particulate organic matter in a differently textured arable Cambisol as revealed by solid-state C-13 NMR spectroscopy. Journal of Plant Nutrition and Soil Science-Zeitschrift Fur Pflanzenernahrung Und Bodenkunde 167: 45-53

Krull ES, Baldock JA & Skjemstad JO (2003) Importance of mechanisms and processes of the stabilisation of soil organic matter for modeling carbon turnover. Funct Plant Biol 30: 207-222

Marshman NA & Marshall KC (1981) Bacterial-Growth on Proteins in the Presence of Clay-Minerals. Soil Biol Biochem 13: 127-134

Plante AF, Conant RT, Paul EA, Paustian K & Six J (2006a) Acid hydrolysis of easily dispersed and microaggregate-derived silt and clay-sized fractions to isolate resistant soil organic matter. Eur J Soil Sci: (in press)

Plante AF, Conant RT, Stewart CE, Paustian K & Six J (2006b) Impact of soil texture on the distribution of soil organic matter in physical and chemical fractions. Soil Sci Soc Am J 70: 287-296

Roscoe R, Buurman P, Velthorst EJ & Vasconcellos CA (2001) Soil organic matter dynamics in density and particle size fractions as revealed by the C-13/C-12 isotopic ratio in a Cerrado's oxisol. Geoderma 104: 185-202

Sherrod LA, Dunn G, Peterson GA & Kolberg RL (2002) Inorganic carbon analysis by modified pressure-calcimeter method. Soil Sci Soc Am J 66: 299-305

Six J, Conant RT, Paul EA & Paustian K (2002) Stabilization mechanisms of soil organic matter: Implications for C-saturation of soils. Plant Soil 241: 155-176

Six J, Elliot ET, Paustian K & J.W. D (1998) Aggregation and soil organic matter accumulation in cultivated and native grassland soils. Soil Sci Soc Am J 62: 1367-1377

Stewart CE, Paustian K, Conant RT, Plante AF & Six J (2006a) Soil C saturation I: Concept, evidence, and evaluation. Biogeochemistry: (in review)

Stewart CE, Paustian K, Conant RT, Plante AF & Six J (2006b) Soil C saturation III: Evaluation and corroboration by long-term incubations. Soil Biol Biochem: (in review)

Stewart CE, Plante AF, Paustian K & Six J (2006c) Soil C saturation II: Linking concept and measurable carbon pools. Biogeochemistry: (in prep)

Sumner ME & Miller WP (1996) Cation exchange capacity and exchange coefficients. In: Sparks DL (Ed) Methods of Soil Analysis. Part 3. Chemical Methods. pp 1201-1229). Soil Science Society of America, Inc., Madison, Wisconsin

Appendix 1 Linear and C-saturation model fits for the eight sites in Chapter 2.

Table 1: Results of linear and C-saturation model fits for the non-protected pool comprised of cPOM and LF. The C saturation model did not converge in some cases, and r^2 values were not calculated in these cases.

	cPOM				LF			
	Linear model		CSAT model		Linear model		CSAT model	
Site	p-value	r^2	p-value	r^2	p-value	r^2	p-value	r^2
AB	> 0.001	0.945	> 0.001	0.879	> 0.001	0.625	> 0.001	n/a
CO	> 0.001	0.856	> 0.001	0.617	0.004	0.244	> 0.001	n/a
GA	> 0.001	0.972	> 0.001	0.897	0.024	0.279	> 0.001	n/a
KY	> 0.001	0.875	> 0.001	0.842	0.002	0.347	> 0.001	0.307
OH	> 0.001	0.826	> 0.001	0.744	0.378	0.031	> 0.001	n/a
SC	> 0.001	0.605	> 0.001	0.563	0.084	0.135	> 0.001	0.186
SCO	> 0.001	0.952	> 0.001	0.040	0.067	0.144	> 0.001	0.058
SV	> 0.001	0.884	> 0.001	0.589	0.266	0.068	> 0.001	0.099

Table 2: Results of linear and C-saturation model fits for the µaggregate-protected pool comprised of µagg and iPOM.

	µagg				iPOM			
	Linear model		CSAT model		Linear model		CSAT model	
Site	p-value	r^2	p-value	r^2	p-value	r^2	p-value	r^2
AB	> 0.001	0.916	> 0.001	0.916	> 0.001	0.833	> 0.001	0.798
CO	> 0.001	0.955	> 0.001	0.950	> 0.001	0.873	> 0.001	0.777
GA	> 0.001	0.934	> 0.001	0.934	> 0.001	0.890	> 0.001	0.880
KY	> 0.001	0.981	> 0.001	0.968	> 0.001	0.828	> 0.001	0.822
OH	> 0.001	0.981	> 0.001	0.981	> 0.001	0.692	> 0.001	0.687
SC	> 0.001	0.929	> 0.001	0.924	> 0.001	0.928	> 0.001	0.768
SCO	> 0.001	0.961	> 0.001	0.958	> 0.001	0.798	> 0.001	0.197
SV	> 0.001	0.941	> 0.001	0.934	> 0.001	0.821	> 0.001	0.541

Table 3: Results of linear and C-saturation model fits for the chemical pool comprised of HdSilt and HdClay.

	H–dSilt				H-dClay			
	Linear model		**CSAT model**		**Linear model**		**CSAT model**	
Site	**p-value**	r^2	**p-value**	r^2	**p-value**	r^2	**p-value**	r^2
AB	> 0.001	0.831	> 0.001	0.861	> 0.001	0.826	> 0.001	0.859
CO	> 0.001	0.656	> 0.001	0.673	> 0.001	0.546	> 0.001	0.545
GA	> 0.001	0.865	> 0.001	0.858	> 0.001	0.902	> 0.001	0.857
KY	> 0.001	0.826	> 0.001	0.828	> 0.001	0.877	> 0.001	0.860
OH	> 0.001	0.938	> 0.001	0.954	> 0.001	0.960	> 0.001	0.969
SC	0.022	0.248	> 0.001	0.291	> 0.001	0.746	> 0.001	0.799
SCO	> 0.001	0.712	> 0.001	0.834	> 0.001	0.777	> 0.001	0.816
SV	0.389	0.044	> 0.001	0.089	0.229	0.079	> 0.001	0.083

Table 4: Results of linear and C-saturation model fits for the biochemical pool comprised of *NHdSilt* and NHdClay.

	NH-dSilt				NH-dClay			
	Linear model		CSAT model		Linear model		CSAT model	
Site	p-value	r^2	p-value	r^2	p-value	r^2	p-value	r^2
AB	> 0.001	0.733	> 0.001	0.781	> 0.001	0.733	> 0.001	0.858
CO	0.015	0.181	0.015	0.240	0.015	0.181	> 0.001	0.728
GA	> 0.001	0.942	> 0.001	0.917	> 0.001	0.942	> 0.001	0.802
KY	> 0.001	0.746	> 0.001	0.744	> 0.001	0.746	> 0.001	0.898
OH	> 0.001	0.921	> 0.001	0.918	> 0.001	0.921	> 0.001	0.940
SC	0.693	0.008	0.693	0.228	> 0.001	0.008	> 0.001	0.446
SCO	> 0.001	0.621	> 0.001	0.748	0.693	0.621	> 0.001	0.798
SV	> 0.001	0.598	> 0.001	0.517	0.229	0.598	> 0.001	0.067

Table 5: Results of linear and C-saturation model fits for the chemical × physical protected pool comprised of HμSilt and HμClay.

| | H–μSilt | | | | H-μClay | | | |
| | Linear model | | CSAT model | | Linear model | | CSAT model | |
Site	p-value	r^2	p-value	r^2	p-value	r^2	p-value	r^2
AB	> 0.001	0.844	> 0.001	0.850	> 0.001	0.800	> 0.001	0.801
CO	> 0.001	0.601	0.015	0.600	0.015	0.917	> 0.001	0.929
GA	> 0.001	0.679	> 0.001	0.674	> 0.001	0.566	> 0.001	0.524
KY	> 0.001	0.809	> 0.001	0.808	0.599	0.013	> 0.001	0.018
OH	> 0.001	0.570	> 0.001	0.619	> 0.001	0.806	> 0.001	0.801
SC	0.007	0.295	0.693	0.299	> 0.001	0.756	> 0.001	0.729
SCO	> 0.001	0.730	> 0.001	0.756	> 0.001	0.654	> 0.001	0.825
SV	0.677	0.010	> 0.001	0.020	0.606	0.015	> 0.001	0.013

Table 6: Results of linear and C-saturation model fits for the biochemical × physical - protected pool comprised of NHµSilt and NHµClay.

	NH̃-µSilt				NH-µClay			
	Linear model		CSAT model		Linear model		CSAT model	
Site	p-value	r^2	p-value	r^2	p-value	r^2	p-value	r^2
AB	> 0.001	0.923	> 0.001	0.934	> 0.001	0.872	> 0.001	0.862
CO	> 0.001	0.387	> 0.001	0.443	> 0.001	0.824	> 0.001	0.847
GA	0.276	0.079	> 0.001	0.185	> 0.001	0.811	> 0.001	0.797
KY	> 0.001	0.815	> 0.001	0.814	0.067	0.219	> 0.001	0.267
OH	> 0.001	0.876	> 0.001	0.876	> 0.001	0.864	> 0.001	0.853
SC	> 0.001	0.747	> 0.001	0.732	0.029	0.395	> 0.001	0.331
SCO	> 0.001	0.702	> 0.001	0.826	0.006	0.388	> 0.001	0.648
SV	0.145	0.114	> 0.001	0.087	0.103	0.141	> 0.001	0.129

Table 7: Results of linear and C-saturation model fits for the chemical × biochemical pool comprised of dSilt and dClay.

| | dSilt | | | | dClay | | | |
| | Linear model | | CSAT model | | Linear model | | CSAT model | |
Site	p-value	r^2	p-value	r^2	p-value	r^2	p-value	r^2
AB	> 0.001	0.826	> 0.001	0.870	> 0.001	0.902	> 0.001	0.935
CO	> 0.001	0.702	> 0.001	0.754	> 0.001	0.849	> 0.001	0.890
GA	> 0.001	0.953	> 0.001	0.918	> 0.001	0.876	> 0.001	0.849
KY	> 0.001	0.976	> 0.001	0.975	0.067	0.913	> 0.001	0.898
OH	> 0.001	0.971	> 0.001	0.971	> 0.001	0.977	> 0.001	0.972
SC	0.001	0.398	> 0.001	0.416	0.029	0.856	> 0.001	0.857
SCO	> 0.001	0.705	> 0.001	0.854	0.006	0.810	> 0.001	0.938
SV	0.006	0.355	> 0.001	0.402	0.222	0.082	> 0.001	0.098

Table 8: Results of linear and C-saturation model fits for the chemical × biochemical × physical pool comprised of μSilt and μClay.

| | μSilt | | | | μClay | | | |
| | Linear model | | CSAT model | | Linear model | | CSAT model | |
Site	p-value	r^2	p-value	r^2	p-value	r^2	p-value	r^2
AB	> 0.001	0.922	> 0.001	0.932	> 0.001	0.930	> 0.001	0.929
CO	> 0.001	0.793	> 0.001	0.338	> 0.001	0.913	> 0.001	0.931
GA	> 0.001	0.911	> 0.001	0.870	> 0.001	0.861	> 0.001	0.825
KY	> 0.001	0.939	> 0.001	0.938	0.082	0.131	> 0.001	0.175
OH	> 0.001	0.913	> 0.001	0.913	> 0.001	0.971	> 0.001	0.959
SC	0.001	0.630	> 0.001	0.622	0.029	0.684	> 0.001	0.642
SCO	> 0.001	0.775	> 0.001	0.870	0.006	0.513	> 0.001	0.753
SV	0.044	0.207	> 0.001	0.216	0.351	0.049	> 0.001	0.043

Appendix 2 C saturation model estimates for the eight sites in Chapter 2.

Table 1: Parameter estimates, error, and p-values for the C-saturation model fits of the dSilt fraction.

Site	C_{maxf} estimate	C_{maxf} error	C_{maxf} p-value	k_f estimate	k_f error	k_f p-value
AB	5.432	0.441	> 0.001	0.812	0.039	> 0.001
CO	1.754	0.165	> 0.001	0.574	0.056	> 0.001
GA	7.514	1.399	> 0.001	0.489	0.048	> 0.001
KY	5.250	0.498	> 0.001	1.084	0.039	> 0.001
OH	n/a	n/a	n/a	1.058	0.018	> 0.001
SC	3.187	0.671	> 0.001	0.556	0.152	0.001
SCO	5.341	0.350	> 0.001	0.469	0.044	> 0.001
SV	2.521	0.394	> 0.001	0.425	0.123	0.003

Table 2: Parameter estimates, error, and p-values for the C-saturation model fits of the dClay fraction.

Site	$C_{\mathrm{max}f}$ estimate	$C_{\mathrm{max}f}$ error	$C_{\mathrm{max}f}$ p-value	k_f estimate	k_f error	k_f p-value
AB	14.659	1.246	> 0.001	0.553	0.020	> 0.001
CO	5.424	0.467	> 0.001	0.297	0.018	> 0.001
GA	30.324	26.041	0.261	0.436	0.065	> 0.001
KY	6.208	0.600	> 0.001	0.424	0.031	> 0.001
OH	69.086	38.391	0.084	0.986	0.042	> 0.001
SC	9.396	1.160	> 0.001	0.342	0.033	> 0.001
SCO	10.890	0.506	> 0.001	0.271	0.016	> 0.001
SV	2.851	0.919	0.006	0.307	0.221	0.182

Table 3: Parameter estimates, error, and p-values for the C-saturation model fits of the µagg fraction.

Site	$C_{\mathrm{max}f}$ estimate	$C_{\mathrm{max}f}$ error	$C_{\mathrm{max}f}$ p-value	k_f estimate	k_f error	k_f p-value
AB	n/a	n/a	n/a	1.185	0.032	> 0.001
CO	n/a	n/a	n/a	1.015	0.020	> 0.001
GA	n/a	n/a	n/a	0.777	0.028	> 0.001
KY	n/a	n/a	n/a	0.721	0.010	> 0.001
OH	162.697	158.869	0.316	0.909	0.032	> 0.001
SC	n/a	n/a	n/a	1.172	0.029	> 0.001
SCO	61.231	34.897	0.093	1.041	0.057	> 0.001
SV	n/a	n/a	n/a	1.069	0.021	> 0.001

Table 4: Parameter estimates, error, and p-values for the C-saturation model fits of the LF fraction.

Site	C_{maxf} estimate	C_{maxf} error	C_{maxf} p-value	k_f estimate	k_f error	k_f p-value
AB	131.493	83.956	0.123	n/a	n/a	n/a
CO	n/a	n/a	n/a	n/a	n/a	n/a
GA	n/a	n/a	n/a	0.059	0.012	> 0.001
KY	20.831	1.035	> 0.001	-0.011	0.004	0.006
OH	71.465	17.195	> 0.001	n/a	n/a	n/a
SC	17.948	2.064	> 0.001	-0.023	0.010	0.035
SCO	16.849	1.501	> 0.001	-0.014	0.012	0.254
SV	16.898	2.377	> 0.001	-0.020	0.014	0.173

Table 5: Parameter estimates, error, and p-values for the C-saturation model fits of the μClay fraction.

Site	C_{maxf} estimate	C_{maxf} error	C_{maxf} p-value	k_f estimate	k_f error	k_f p-value
AB	145.409	132.270	0.277	0.686	0.033	> 0.001
CO	8.191	1.036	> 0.001	0.419	0.020	> 0.001
GA	37.495	37.776	0.336	0.378	0.062	> 0.001
KY	3.099	0.449	> 0.001	0.173	0.079	0.039
OH	19.080	3.393	> 0.001	0.893	0.044	> 0.001
SC	6.929	1.109	> 0.001	0.315	0.055	> 0.001
SCO	9.151	0.779	> 0.001	0.254	0.033	> 0.001
SV	2.093	0.681	0.007	0.267	0.297	0.381

Table 6: Parameter estimates, error, and p-values for the C-saturation model fits of the μSilt fraction.

Site	C_{maxf} estimate	C_{maxf} error	C_{maxf} p-value	k_f estimate	k_f error	k_f p-value
AB	20.617	3.858	> 0.001	0.975	0.040	> 0.001
CO	2.740	0.287	> 0.001	0.534	0.043	> 0.001
GA	17.745	8.920	0.065	0.424	0.054	> 0.001
KY	51.619	83.939	0.545	1.207	0.074	> 0.001
OH	36.553	15.341	0.025	0.752	0.057	> 0.001
SC	7.327	2.426	0.007	0.641	0.118	> 0.001
SCO	9.037	1.029	> 0.001	0.586	0.054	> 0.001
SV	3.127	0.526	> 0.001	0.230	0.104	0.040

Table 7: Parameter estimates, error, and p-values for the C-saturation model fits of the H-dSilt fraction.

Site	C_{maxf} estimate	C_{maxf} error	C_{maxf} p-value	k_f estimate	k_f error	k_f p-value
AB	2.062	0.178	> 0.001	2.265	0.112	> 0.001
CO	1.533	0.387	> 0.001	1.691	0.206	> 0.001
GA	2.375	0.316	> 0.001	0.730	0.091	> 0.001
KY	2.624	0.494	> 0.001	1.481	0.148	> 0.001
OH	10.343	2.468	> 0.001	2.123	0.112	> 0.001
SC	2.420	1.475	0.117	1.723	0.663	0.018
SCO	2.110	0.093	> 0.001	0.674	0.067	> 0.001
SV	1.276	0.357	0.002	0.546	0.428	0.219

Table 8: Parameter estimates, error, and p-values for the C-saturation model fits of the H-dClay fraction.

Site	C_{maxf} estimate	C_{maxf} error	C_{maxf} p-value	k_f estimate	k_f error	k_f p-value
AB	5.332	0.580	> 0.001	1.199	0.063	> 0.001
CO	2.526	0.518	> 0.001	0.573	0.091	> 0.001
GA	7.741	2.382	0.005	0.590	0.081	> 0.001
KY	3.722	0.367	> 0.001	0.596	0.052	> 0.001
OH	8.417	1.077	> 0.001	1.658	0.069	> 0.001
SC	5.798	1.274	> 0.001	0.831	0.099	> 0.001
SCO	4.874	0.378	> 0.001	0.536	0.058	> 0.001
SV	1.533	0.507	0.007	0.533	0.420	0.220

Table 9: Parameter estimates, error, and p-values for the C-saturation model fits of the H-μSilt fraction.

Site	C_{maxf} estimate	C_{maxf} error	C_{maxf} p-value	k_f estimate	k_f error	k_f p-value
AB	6.482	1.786	0.001	2.953	0.186	> 0.001
CO	2.309	1.004	0.029	1.743	0.254	> 0.001
GA	n/a	n/a	n/a	0.874	0.089	> 0.001
KY	78.598	726.302	0.915	2.396	0.280	> 0.001
OH	5.114	1.571	0.003	1.388	0.243	> 0.001
SC	2.753	1.297	0.046	1.185	0.426	0.011
SCO	3.560	0.642	0.000	1.649	0.222	> 0.001
SV	1.587	0.686	0.033	0.308	0.515	0.557

Table10: Parameter estimates, error, and p-values for the C-saturation model fits of the

H-μClay fraction.

Site	C_{maxf} estimate	C_{maxf} error	C_{maxf} p-value	k_f estimate	k_f error	k_f p-value
AB	16.904	5.541	0.004	1.162	0.063	> 0.001
CO	4.676	0.631	> 0.001	0.777	0.038	> 0.001
GA	4.463	1.289	0.003	0.358	0.103	0.003
KY	2.120	0.644	0.003	0.148	0.234	0.534
OH	6.618	1.910	0.002	1.675	0.191	> 0.001
SC	3.582	0.630	> 0.001	0.554	0.107	> 0.001
SCO	4.285	0.321	> 0.001	0.488	0.055	> 0.001
SV	1.152	0.434	0.016	0.297	0.612	0.633

Table11: Parameter estimates, error, and p-values for the C-saturation model fits of the NH-dSilt fraction.

Site	C_{maxf} estimate	C_{maxf} error	C_{maxf} p-value	k_f estimate	k_f error	k_f p-value
AB	3.374	0.369	> 0.001	1.265	0.083	> 0.001
CO	0.590	0.071	> 0.001	0.584	0.182	0.003
GA	9.783	5.793	0.111	1.275	0.139	> 0.001
KY	4.200	3.941	0.298	3.763	0.511	> 0.001
OH	n/a	n/a	n/a	1.787	0.056	> 0.001
SC	0.679	0.094	> 0.001	0.832	0.316	0.016
SCO	3.351	0.439	> 0.001	1.136	0.155	> 0.001
SV	1.475	0.373	0.001	1.536	0.363	0.001

Table12: Parameter estimates, error, and p-values for the C-saturation model fits of the NH-dClay fraction.

Site	C_{maxf} estimate	C_{maxf} error	C_{maxf} p-value	k_f estimate	k_f error	k_f p-value
AB	9.61	1.46	> 0.001	1.019	0.058	> 0.001
CO	2.90	0.47	> 0.001	0.613	0.065	> 0.001
GA	n/a	n/a	n/a	1.232	0.084	> 0.001
KY	2.61	0.35	> 0.001	1.417	0.105	> 0.001
OH	n/a	n/a	> 0.001	2.017	0.052	> 0.001
SC	3.80	0.83	> 0.001	0.522	0.134	0.001
SCO	6.00	0.59	> 0.001	0.542	0.063	> 0.001
SV	1.48	0.37	> 0.001	1.536	0.363	0.001

Table13: Parameter estimates, error, and p-values for the C-saturation model fits of the NH-μSilt fraction.

Site	C_{maxf} estimate	C_{maxf} error	C_{maxf} p-value	k_f estimate	k_f error	k_f p-value
AB	14.15	2.68	> 0.001	1.456	0.060	> 0.001
CO	1.13	0.17	> 0.001	0.667	0.129	> 0.001
GA	1.77	0.59	0.01	0.375	0.214	0.101
KY	14.84	25.92	0.57	2.431	0.276	> 0.001
OH	n/a	n/a	n/a	1.439	0.053	> 0.001
SC	5.04	1.82	0.01	1.356	0.194	> 0.001
SCO	5.52	0.72	> 0.001	0.910	0.099	> 0.001
SV	1.65	0.78	0.05	0.743	0.573	0.211

Table14: Parameter estimates, error, and p-values for the C-saturation model fits of the NH-μClay fraction.

Site	$C_{\text{max}f}$ estimate	$C_{\text{max}f}$ error	$C_{\text{max}f}$ p-value	k_f estimate	k_f error	k_f p-value
AB	n/a	n/a	n/a	1.492	0.049	> 0.001
CO	3.53	0.66	> 0.001	0.909	0.069	> 0.001
GA	n/a	n/a	n/a	0.934	0.073	> 0.001
KY	1.43	0.42	> 0.001	0.829	0.375	0.044
OH	15.76	9.54	0.11	1.889	0.190	> 0.001
SC	3.06	1.45	0.06	0.763	0.342	0.050
SCO	4.53	0.62	> 0.001	0.539	0.098	> 0.001
SV	0.97	0.30	> 0.001	1.014	0.623	0.121

Appendix 3 Stabilized residue-derived C (mg C (mg residue-derived C respired)$^{-1}$) and standard deviation for all sites and treatments from Chapter 4.

Table 1: Stabilized residue-derived C (mg C (mg residue-derived C respired)$^{-1}$) and standard deviation for fractions isolated by microaggregate isolation in the A- and C-horizons with the 1× and 5× C addition rates for all sites.

Site	Horizon (Addition)		cPOM	μagg	dSilt	dClay
OH	1	A	0.081 ± 0.045	0.053 ± 0.016	0.015 ± 0.005	0.007 ± 0.002
		C	0.022 ± 0.017	0.087 ± 0.006	0.040 ± 0.005	0.046 ± 0.004
	5	A	0.055 ± 0.031	0.084 ± 0.013	0.024 ± 0.005	0.014 ± 0.001
		C	0.033 ± 0.008	0.101 ± 0.019	0.038 ± 0.009	0.048 ± 0.005
KBS	1	A	0.047 ± 0.002	0.094 ± 0.018	0.048 ± 0.005	0.014 ± 0.002
		C	0.029 ± 0.017	0.069 ± 0.007	0.048 ± 0.010	0.018 ± 0.003
	5	A	0.052 ± 0.020	0.079 ± 0.019	0.054 ± 0.007	0.016 ± 0.002
		C	0.033 ± 0.016	0.096 ± 0.018	0.069 ± 0.017	0.029 ± 0.004
MIS	1	A	0.023 ± 0.014	0.006 ± 0.009	0.000 ± 0.000	0.002 ± 0.001
		C	0.069 ± 0.016	0.107 ± 0.010	0.069 ± 0.008	0.011 ± 0.001
	5	A	0.084 ± 0.046	0.084 ± 0.020	0.033 ± 0.004	0.009 ± 0.002
		C	0.067 ± 0.009	0.142 ± 0.018	0.068 ± 0.011	0.010 ± 0.002
IA	1	A	0.046 ± 0.010	0.057 ± 0.018	0.011 ± 0.002	0.005 ± 0.003
		C	0.041 ± 0.013	0.123 ± 0.020	0.031 ± 0.003	0.013 ± 0.002
	5	A	0.045 ± 0.005	0.086 ± 0.020	0.019 ± 0.003	0.010 ± 0.002
		C	0.061 ± 0.033	0.113 ± 0.015	0.032 ± 0.004	0.014 ± 0.003
MN	1	A	0.047 ± 0.021	0.081 ± 0.029	0.018 ± 0.005	0.012 ± 0.002
		C	0.021 ± 0.008	0.086 ± 0.009	0.088 ± 0.006	0.024 ± 0.003
	5	A	0.065 ± 0.019	0.101 ± 0.022	0.027 ± 0.003	0.016 ± 0.002

Table 1: Continued.

Site	Addition Horizon		cPOM	μagg	dSilt	dClay
		C	0.039 ± 0.038	0.085 ± 0.014	0.084 ± 0.012	0.018 ± 0.004
NE	1	A	0.035 ± 0.002	0.081 ± 0.015	0.032 ± 0.008	0.014 ± 0.002
		C	0.008 ± 0.010	0.086 ± 0.020	0.074 ± 0.006	0.036 ± 0.002
	5	A	0.079 ± 0.012	0.122 ± 0.021	0.036 ± 0.003	0.012 ± 0.002
		C	0.033 ± 0.004	0.091 ± 0.018	0.074 ± 0.008	0.034 ± 0.005

Table 2: Stabilized residue-derived C (mg C (mg residue-derived C respired)$^{-1}$) and standard deviation for fractions isolated by the density separation and iPOM dispersion in the A- and C-horizons with the 1× and 5× C addition rates for all sites. Replicates were combined for analysis of OH 1× C-horizon therefore, standard deviations are unavailable.

Site	Addition Horizon		LF	iPOM	μSilt	μClay
OH	1	A	0.003 ± 0.002	0.011 ± 0.006	0.007 ± 0.003	0.019 ± 0.005
		C	0.002 ± n/a	0.016 ± 0.003	0.008 ± 0.004	0.043 ± 0.009
	5	A	0.004 ± 0.002	0.014 ± 0.001	0.010 ± 0.001	0.027 ± 0.001
		C	0.006 ± 0.008	0.020 ± 0.008	0.005 ± 0.002	0.046 ± 0.003
KBS	1	A	0.007 ± 0.006	0.023 ± 0.006	0.028 ± 0.007	0.021 ± 0.011
		C	0.011 ± 0.009	0.025 ± 0.021	0.019 ± 0.002	0.020 ± 0.004
	5	A	0.008 ± 0.005	0.017 ± 0.003	0.029 ± 0.017	0.022 ± 0.004
		C	0.013 ± 0.005	0.012 ± 0.004	0.030 ± 0.009	0.031 ± 0.003
MIS	1	A	0.001 ± 0.001	0.017 ± 0.006	0.000 ± 0.000	0.000 ± 0.001
		C	0.008 ± 0.005	0.004 ± 0.004	0.034 ± 0.005	0.024 ± 0.005
	5	A	0.008 ± 0.003	0.020 ± 0.015	0.029 ± 0.009	0.019 ± 0.004
		C	0.049 ± 0.056	0.002 ± 0.003	0.046 ± 0.006	0.034 ± 0.001
IA	1	A	0.000 ± 0.001	0.064 ± 0.020	0.045 ± 0.008	0.033 ± 0.002
		C	0.008 ± 0.005	0.017 ± 0.005	0.017 ± 0.006	0.049 ± 0.003
	5	A	0.000 ± 0.001	0.035 ± 0.008	0.016 ± 0.003	0.039 ± 0.004
		C	0.008 ± 0.005	0.019 ± 0.015	0.016 ± 0.002	0.053 ± 0.005
MN	1	A	0.009 ± 0.007	0.015 ± 0.007	0.036 ± 0.007	0.025 ± 0.003
		C	0.008 ± 0.003	0.005 ± 0.001	0.032 ± 0.004	0.026 ± 0.006
	5	A	0.016 ± 0.005	0.022 ± 0.001	0.033 ± 0.001	0.032 ± 0.004
		C	0.008 ± 0.003	0.011 ± 0.006	0.025 ± 0.005	0.026 ± 0.004
NE	1	A	0.014 ± 0.011	0.017 ± 0.008	0.019 ± 0.007	0.034 ± 0.006
		C	0.008 ± 0.008	0.009 ± 0.002	0.014 ± 0.010	0.026 ± 0.009
	5	A	0.024 ± 0.014	0.020 ± 0.007	0.037 ± 0.007	0.029 ± 0.008
		C	0.020 ± 0.013	0.013 ± 0.002	0.027 ± 0.006	0.024 ± 0.003

Table 3: Stabilized residue-derived C (mg C (mg residue-derived C respired)$^{-1}$) and standard deviation for fractions by the acid hydrolysis procedure for the easily-dispersed silt and clay fractions in the A- and C-horizons with the 1× and 5× C addition rates for all sites.

Site	Addition	Horizon	NH-dSilt	NH-dClay	H-dSilt	H-dClay
OH	1	A	0.000 ± 0.000	0.000 ± 0.000	0.015 ± 0.005	0.007 ± 0.002
		C	0.005 ± 0.003	0.009 ± 0.001	0.035 ± 0.003	0.037 ± 0.003
	5	A	0.002 ± 0.001	0.002 ± 0.000	0.021 ± 0.004	0.012 ± 0.001
		C	0.007 ± 0.003	0.012 ± 0.003	0.031 ± 0.006	0.036 ± 0.003
KBS	1	A	0.000 ± 0.000	0.001 ± 0.001	0.048 ± 0.005	0.013 ± 0.002
		C	0.000 ± 0.000	0.002 ± 0.001	0.048 ± 0.010	0.016 ± 0.002
	5	A	0.007 ± 0.001	0.003 ± 0.000	0.046 ± 0.007	0.013 ± 0.001
		C	0.008 ± 0.003	0.005 ± 0.002	0.061 ± 0.014	0.023 ± 0.003
MIS	1	A	0.000 ± 0.000	0.003 ± 0.002	0.000 ± 0.000	0.001 ± 0.001
		C	0.004 ± 0.002	0.001 ± 0.000	0.063 ± 0.006	0.010 ± 0.001
	5	A	0.003 ± 0.000	0.001 ± 0.000	0.031 ± 0.004	0.008 ± 0.002
		C	0.012 ± 0.002	0.002 ± 0.000	0.056 ± 0.009	0.008 ± 0.002
IA	1	A	0.000 ± 0.000	0.000 ± 0.000	0.011 ± 0.002	0.005 ± 0.003
		C	0.005 ± 0.001	0.003 ± 0.001	0.027 ± 0.003	0.010 ± 0.001
	5	A	0.001 ± 0.001	0.001 ± 0.000	0.018 ± 0.003	0.008 ± 0.001
		C	0.005 ± 0.001	0.003 ± 0.001	0.028 ± 0.003	0.011 ± 0.004
MN	1	A	0.000 ± 0.000	0.000 ± 0.000	0.018 ± 0.005	0.012 ± 0.002
		C	0.017 ± 0.003	0.005 ± 0.001	0.071 ± 0.008	0.019 ± 0.002
	5	A	0.001 ± 0.001	0.003 ± 0.001	0.026 ± 0.003	0.013 ± 0.002
		C	0.019 ± 0.003	0.004 ± 0.001	0.065 ± 0.010	0.014 ± 0.002
NE	1	A	0.000 ± 0.000	0.000 ± 0.000	0.032 ± 0.008	0.014 ± 0.002
		C	0.000 ± 0.000	0.003 ± 0.001	0.074 ± 0.006	0.033 ± 0.002
	5	A	0.001 ± 0.001	0.002 ± 0.000	0.035 ± 0.003	0.011 ± 0.002
		C	0.006 ± 0.002	0.005 ± 0.001	0.068 ± 0.008	0.029 ± 0.004

Table 4: Stabilized residue-derived C (mg C (mg residue-derived C respired)$^{-1}$) and standard deviation for fractions by the acid hydrolysis procedure for the μagg associated silt and clay fractions in the A- and C-horizons with the 1× and 5× C addition rates for all sites. Replicates were combined for analysis of OH samples; therefore, standard deviations are unavailable.

Site	Addition Horizon		NH-μSilt	NH-μClay	H-μSilt	H-μClay
OH	1	A	0.0000± 0.0000	0.0000± 0.0000	0.0072± 0.0030	0.0200± 0.0061
		C	0.0007± n/a	0.0042± n/a	0.0027± n/a	0.0358± n/a
	5	A	0.0010± 0.0001	0.0025± 0.0026	0.0088± 0.0013	0.0230± n/a
		C	0.0001± n/a	0.0092± n/a	0.0022± n/a	0.0412± n/a
KBS	1	A	0.0000± 0.0000	0.0017± 0.0003	0.0283± 0.0065	0.0189± 0.0110
		C	0.0000± 0.0000	0.0007± 0.0005	0.0193± 0.0017	0.0196± 0.0035
	5	A	0.0023± 0.0008	0.0037± 0.0016	0.0265± 0.0176	0.0182± 0.0026
		C	0.0016± 0.0004	0.0042± 0.0003	0.0286± 0.0085	0.0266± 0.0030
MIS	1	A	0.0000± 0.0000	0.0000± 0.0000	0.0000± 0.0000	0.0003± 0.0005
		C	0.0006± 0.0005	0.0048± 0.0011	0.0335± 0.0044	0.0195± 0.0052
	5	A	0.0005± 0.0002	0.0022± 0.0010	0.0289± 0.0089	0.0172± 0.0030
		C	0.0026± 0.0010	0.0080± 0.0016	0.0434± 0.0067	0.0273± 0.0026
IA	1	A	0.0000± 0.0000	0.0000± 0.0000	0.0446± 0.0076	0.0328± 0.0019
		C	0.0029± 0.0016	0.0054± 0.0017	0.0139± 0.0049	0.0432± 0.0025
	5	A	0.0012± 0.0007	0.0077± 0.0006	0.0145± 0.0021	0.0303± 0.0037
		C	0.0015± 0.0006	0.0108± 0.0025	0.0147± 0.0016	0.0417± 0.0025
MN	1	A	0.0000± 0.0000	0.0000± 0.0000	0.0363± 0.0065	0.0249± 0.0046
		C	0.0006± 0.0007	0.0050± 0.0017	0.0316± 0.0047	0.0210± 0.0046
	5	A	0.0001± 0.0002	0.0024± 0.0016	0.0332± 0.0010	0.0300± 0.0023
		C	0.0017± 0.0003	0.0083± 0.0023	0.0230± 0.0051	0.0184± 0.0065
NE	1	A	0.0000± 0.0000	0.0000± 0.0000	0.0186± 0.0068	0.0340± 0.0062
		C	0.0009± 0.0004	0.0027± 0.0016	0.0134± 0.0106	0.0231± 0.0075
	5	A	0.0003± 0.0002	0.0041± 0.0012	0.0368± 0.0067	0.0252± 0.0067
		C	0.0022± 0.0004	0.0038± 0.0006	0.0250± 0.0058	0.0203± 0.0025